

**CCT-K5: Comparison of local realizations of the ITS-90  
between the silver point and 1700 °C  
using vacuum tungsten strip lamps  
as transfer standards**

Prepared by  
M.J. de Groot, E.W.M. van der Ham and R. Monshouwer  
NMi Van Swinden Laboratorium B.V.  
Delft  
the Netherlands

Key Comparison 5  
Protocol by P. Bloembergen (NMi VSL)  
Coordinated by R. Bosma (NMi VSL)  
with  
G. Machin (NPL), sub-coordinator

# Contents

ABSTRACT .....	6
INTRODUCTION .....	6
PARTICIPATING METROLOGY INSTITUTES .....	6
DEVICES USED IN THE COMPARISON .....	7
PARTICIPANT INSTRUMENTATION, TECHNIQUES AND OTHER DETAILS .....	11
RESULTS OF THE COMPARISON .....	14
Measurement results as send by the participants .....	14
Analysis of the measurement data .....	14
<i>Difference between loops 1 and 2 through the pilot and co-pilot data.</i> .....	16
<i>Link the loops through pilot reference temperatures.</i> .....	19
Calculating the KCRV .....	22
<i>Input data for the KCRV.</i> .....	22
<i>Calculation of KCRV values.</i> .....	22
<i>Calculating the uncertainties associated with the KCRV values</i> .....	23
<i>Median as representative value for the KCRV</i> .....	24
Determine difference of participants with respect to KCRV .....	25
<i>Intraloop comparisons</i> .....	26
<i>Interloop comparisons</i> .....	26
<i>Graphical representations</i> .....	26
APPENDICES .....	79
Appendix I. Protocol used in the comparison .....	79
Appendix II. Uncertainty budgets .....	93
<i>NMi-VSL</i> .....	94
<i>NPL</i> .....	95
<i>CSIRO</i> .....	97
<i>KRISS</i> .....	100
<i>NIM</i> .....	102
<i>NMC</i> .....	106
<i>NRLM</i> .....	107
<i>VNIIM</i> .....	111
<i>NIST</i> .....	112
<i>NRC</i> .....	114
<i>CENAM</i> .....	115
<i>INM</i> .....	117
<i>IMGC</i> .....	118
<i>PTB</i> .....	120
Appendix III. Comments by participants on key comparison reference values .....	123
<i>Comments by NMC</i> .....	123
<i>Comments by VNIIM</i> .....	123
<i>Comments by NPL</i> .....	124
<i>Comments by NRC</i> .....	124
<i>Comments by INM</i> .....	135
Appendix IV. Instrumentation and experimental details .....	136

## Contents - Tables

Table 1 The circulation scheme of the intercomparison.....	7
Table 2 Physical constitution of the lamp elements.....	8
Table 3 Appropriate uncertainty components for each scheme realizing ITS-90. ....	12
Table 4 Overview of traceability schemes.....	13
Table 5 Specific information on the fixed-point blackbody cavity configurations.....	13
Table 6 Schematic representations of the data handling throughout KCRV analysis .....	15
Table 7 The average difference between the pilot and co-pilot measurements.....	17
Table 8 An analysis of variance between different lamp measurements at 1000°C. ....	17
Table 9 An analysis of variance between different lamp measurements at 1500°C. ....	18
Table 10 Results from an analysis of variance on the $\Delta t_{t_{nom}}$ data.....	18
Table 11 Measurement results as send in by CSIRO .....	27
Table 12 Measurement results as send in by KRISS .....	27
Table 13 Measurement results as send in by NIM .....	28
Table 14 Measurement results as send in by NMC .....	28
Table 15 Measurement results as send in by NRLM .....	29
Table 16 Measurement results as send in by NPL (I) .....	29
Table 17 Measurement results as send in by VNIIM .....	30
Table 18 Measurement results as send in by VSL (first run, I) .....	30
Table 19 Measurement results as send in by VSL (second run, I) .....	31
Table 20 Measurement results as send in by VSL (third run, I).....	31
Table 21 Measurement results as send in by CENAM .....	32
Table 22 Measurement results as send in by IMGC .....	32
Table 23 Measurement results as send in by INM .....	33
Table 24 Measurement results as send in by NIST .....	33
Table 25 Measurement results as send in by NPL (first run, II) .....	34
Table 26 Measurement results as send in by NPL (second run, II) .....	34
Table 27 Measurement results as send in by NPL (third run, II) .....	35
Table 28 Measurement results as send in by NRC .....	35
Table 29 Measurement results as send in by PTB .....	36
Table 30 Measurement results as send in by VSL (II) .....	36
Table 31 Differences between participants within loop at $T_{nom}=961^\circ\text{C}$ .....	37
Table 32 Differences between participants within loop at $T_{nom}=1000^\circ\text{C}$ .....	38
Table 33 Differences between participants within loop at $T_{nom}=1064^\circ\text{C}$ .....	39
Table 34 Differences between participants within loop at $T_{nom}=1084^\circ\text{C}$ .....	40
Table 35 Differences between participants within loop at $T_{nom}=1100^\circ\text{C}$ .....	41
Table 36 Differences between participants within loop at $T_{nom}=1200^\circ\text{C}$ .....	42
Table 37 Differences between participants within loop at $T_{nom}=1300^\circ\text{C}$ .....	43
Table 38 Differences between participants within loop at $T_{nom}=1400^\circ\text{C}$ .....	44
Table 39 Differences between participants within loop at $T_{nom}=1500^\circ\text{C}$ .....	45
Table 40 Differences between participants within loop at $T_{nom}=1600^\circ\text{C}$ .....	46
Table 41 Differences between participants within loop at $T_{nom}=1700^\circ\text{C}$ .....	47
Table 42 Differences between participants between loops at $T_{nom}=961^\circ\text{C}$ .....	48
Table 43 Differences between participants between loops at $T_{nom}=1000^\circ\text{C}$ .....	49
Table 44 Differences between participants between loops at $T_{nom}=1064^\circ\text{C}$ .....	50
Table 45 Differences between participants between loops at $T_{nom}=1084^\circ\text{C}$ .....	51
Table 46 Differences between participants between loops at $T_{nom}=1100^\circ\text{C}$ .....	52
Table 47 Differences between participants between loops at $T_{nom}=1200^\circ\text{C}$ .....	53
Table 48 Differences between participants between loops at $T_{nom}=1300^\circ\text{C}$ .....	54
Table 49 Differences between participants between loops at $T_{nom}=1400^\circ\text{C}$ .....	55
Table 50 Differences between participants between loops at $T_{nom}=1500^\circ\text{C}$ .....	56
Table 51 Differences between participants between loops at $T_{nom}=1600^\circ\text{C}$ .....	57

Table 52 Differences between participants between loops at $T_{\text{nom}}=1700^{\circ}\text{C}$ .....	58
--	----

## Contents - Figures

Figure 1 Schematic overview of the intercomparison sequence. ....	6
Figure 2 The GEC high-stability vacuum tungsten-strip lamp in side and front view. ....	8
Figure 3 The measured resistances of lamps C-564 (left) and C-681 (right) ....	9
Figure 4 The measured resistances of lamps C-860 (left) and C-864 (right) ....	10
Figure 5 A Youden plot analysis of the resistance at $20^{\circ}\text{C}$ of the lamps .....	10
Figure 6 A schematic of the comparison.....	14
Figure 7 The temperature differences $\Delta t(k, t_{\text{nom}})$ between the pilot and co-pilot.....	16
Figure 8 The average differences between the pilot and co-pilot.....	19
Figure 9 Differences with respect to the pilot reference temperature $t_{\text{prt}}(k, 960^{\circ}\text{C})$ .....	20
Figure 10 Comparison of different KCRV values for the nominal temperatures.....	23
Figure 11 The uncertainties ( $k=1$ ) as associated to alternatives for the KCRV .....	24
Figure 12 Loop 1, difference from KCRV for participant VSL1 (C564, C681).....	59
Figure 13 Loop 1, difference from KCRV for participant VSL2 .....	60
Figure 14 Loop 1, difference from KCRV for participant VSL3 .....	61
Figure 15 Loop 1, difference from KCRV for participant NPL1 .....	62
Figure 16 Loop 1, difference from KCRV for participant CSIRO.....	63
Figure 17 Loop 1, difference from KCRV for participant KRISS .....	64
Figure 18 Loop 1, difference from KCRV for participant NIM.....	65
Figure 19 Loop 1, difference from KCRV for participant NMC.....	66
Figure 20 Loop 1, difference from KCRV for participant NRLM.....	67
Figure 21 Loop 1, difference from KCRV for participant VNIIM.....	68
Figure 22 Loop 1, difference from KCRV for participant NPL1 (C860, C864) .....	69
Figure 23 Loop 1, difference from KCRV for participant NPL2 .....	70
Figure 24 Loop 1, difference from KCRV for participant NPL3.....	71
Figure 25 Loop 1, difference from KCRV for participant VSL1 .....	72
Figure 26 Loop 1, difference from KCRV for participant NIST.....	73
Figure 27 Loop 1, difference from KCRV for participant NRC.....	74
Figure 28 Loop 1, difference from KCRV for participant CENAM.....	75
Figure 29 Loop 1, difference from KCRV for participant INM.....	76
Figure 30 Loop 1, difference from KCRV for participant IMGC.....	77
Figure 31 Loop 1, difference from KCRV for participant PTB.....	78

## Abstract

This is a report to the Comité Consultatif de Thermométrie (CCT) on Key Comparison 5, i.e., Comparison of local realizations of the ITS-90 between silver point and 1700 °C using vacuum tungsten strip lamps as transfer standards. The differences in local realizations in this range of the ITS-90 and the uncertainties of those differences are given for the 14 national metrology institutes participating in the comparison.

## Introduction

The CCT decided during its 19<sup>th</sup> session in September 1996 to undertake an international comparison of the local realizations of the ITS-90 above the silver point. High-stability tungsten strip lamps would be used as transfer standards between the participating national metrology institutes.

The coordinating institute for this comparison was NMI-VSL. Given the large number of participants, two lamp sets were used for simultaneous comparisons in two loops to shorten the measurement time significantly (see Fig. 1). One sub-coordinating institute, the National Physical Laboratory (NPL) of the United Kingdom, was involved to support this measurement scheme. All measurement results of the NPL and NMI-VSL were used to link both sets of intercomparisons and to monitor drift in the lamp standards employed.

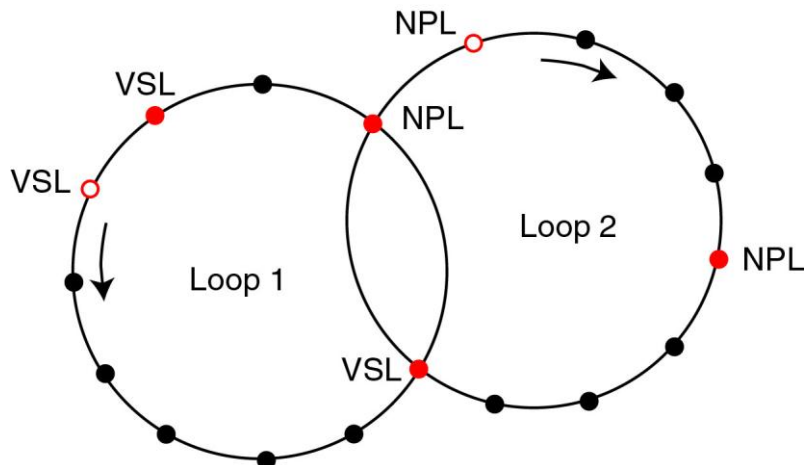


**Figure 1** Schematic overview of the intercomparison sequence. The participants, indicated by the dots, were divided into two groups with each group having individualist own set of two transfer standard lamps. In order to link the loops the pilot institutes (red dots) transferred their scale on both sets as indicated. The open dot and arrow indicates the start of the intercomparison and transfer of the set of lamps to the successive participant respectively.

This report provides an analysis of the obtained results, including differences in local realizations and the uncertainties of those differences for the 14 national metrology institutes participating in the comparison. The instructions to the participants are given in the protocol of Appendix I. The comparison started in May 1997 and ended in July 1999.

## Participating metrology institutes

The national metrology institutes from four RMOs participated in the comparison and were divided in two groups; APMP and COOMET (loop I) and EUROMET with SIM (loop II). The circulation scheme is presented in Table 1. A schematic representation is given in Fig.1. The piloting and drift monitoring institutes were NMI-VSL and NPL for group I and group II,

respectively. Each loop employed a set of two transfer standards. The lamp set of loop 1, lamps C564 and C681, was used in the agreed Euromet extension, project 412.

**Table 1** The circulation scheme of the intercomparison. In total 14 NMIs from four RMOs took part in the comparison. Participants from APMP and COOMET were in loop 1, piloted by NMi-VSL, whereas loop 2 consisted of EUROMET and SIM participants and piloted by NPL.

Loop I Lamp set C564 and C681		Loop II Lamp set C860 and C864	
Country	Participant	Country	Participant
The Netherlands	NMi-VSL	United Kingdom	NPL
Australia	CSIRO	United States of America	NIST
South Korea	KRISS	Canada	NRC
China	NIM	Mexico	CENAM
Singapore	NMC	United Kingdom	NPL
Japan	NRLM	France	INM
The Netherlands	NMi-VSL	Italy	IMGC
United Kingdom	NPL	The Netherlands	NMi-VSL
Russia	VNIIM	Germany	PTB
The Netherlands	NMi-VSL	United Kingdom	NPL

For the various institutes, the persons involved in the comparisons were:

NMi-VSL	P. Bloembergen, R. Bosma, E. W. M. van der Ham M. J. de Groot and R. Monshouwer
NPL	H.C. McEvoy and K. M. Raven
CSIRO	M. Ballico
KRISS	S.N. Park
NIM	Y. Zundong and D. Yuning
NMC	W. Li
NRLM	T. Fujihara, H. Sakate, A. Ono and F. Sakuma
VNIIM	M.S. Matveyev and A.I. Pokhodun
NIST	C. Gibson
NRC	C.K. Ma
CENAM	P. Vera, H. Rodríguez and J. Valencia
INM	B. Rougié, G. Bonnier and G. Negro
IMGC	T. Ricolfi and M. Battuello
PTB	J. Hartmann and J. Fischer

## Devices used in the comparison

Two sets of two GEC high-stability vacuum tungsten-strip lamps were used as transfer standards during the comparison (see Fig. 2). The first set was supplied by the NMi-VSL; the NPL supplied the second set of lamps. The lamps selected by VSL are denoted C564 and C681; lamp C680 was used as a spare lamp. Similarly, the selected lamps from NPL are denoted by C860, C864 and C840. To check proper operation of the lamp, each participant was asked to perform initial tests to check for drift or damage of the lamps after receipt. None of the participants reported abnormal drifts during the comparison and the spare lamps C680 and C840 were not used.



**Figure 2** The GEC high-stability vacuum tungsten-strip lamp in side and front view.

A set of two lamps was mounted in a metal case and was hand carried to each participating institute. Each strip lamp was supplied with a water-cooled base and a clear marking of the polarity of the current connectors. To monitor possible changes in the physical constitution of the lamp element, possibly induced during transport, the room-temperature resistance  $R_{\text{amb}}$  was also monitored along with ambient temperature  $T_{\text{amb}}$  measured with a calibrated PRT inserted in the lamp base. The reported values are presented in Table 2.

**Table 2** During the intercomparison the physical constitution of the lamp elements was monitored by measuring the room-temperature resistance  $R_{\text{amb}}$  at ambient temperature  $T_{\text{amb}}$ . The values as measured by each participant are given below.

Participant	Date	Loop I			
		C564		C681	
		$R_{\text{amb}}$ (mΩ)	$T_{\text{amb}}$ (°C)	$R_{\text{amb}}$ (mΩ)	$T_{\text{amb}}$ (°C)
NMi-VSL	05/97	40.076	22.11	34.197	22.08
	05/97	40.075	21.54	34.120	21.60
CSIRO	09/97	40.200	22.71	34.314	22.78
	09/97	40.207	22.77	34.247	22.35
KRISS	10/97	40.538	24.54	34.735	25.21
	12/97	40.487	24.59	34.697	25.39
NIM	-	-	-	-	-
	02/98	39.849	20.80	33.987	20.53
NMC	03/98	40.268	22.98	34.331	22.97
	03/98	40.222	22.94	34.345	22.97
NRLM	05/98	40.298	23.21	34.341	22.83
	05/98	40.149	22.34	34.368	22.88
NMi-VSL	07/98	40.338	23.67	34.434	23.59
	07/98	40.383	23.88	34.405	23.65
NPL	10/98	39.841	20.52	34.010	20.58
	10/98	39.833	20.67	34.044	21.04
VNIIM	03/99	39.860	21.1	34.055	21.1
	05/99	39.878	20.8	34.062	20.9
NMi-VSL	-	-	-	-	-
	06/99	40.303	23.59	34.567	23.83
<b>Loop II</b>					
Participant	Date	C860		C864	

		$R_{\text{amb}}$ (mΩ)	$T_{\text{amb}}$ (°C)	$R_{\text{amb}}$ (mΩ)	$T_{\text{amb}}$ (°C)
NPL	07/97	39.923	21.9	41.684	22.0
	08/97	40.234	24.5	42.805	28.5
NIST	11/97	39.863	21.49	41.574	21.15
	11/97	39.789	21.08	41.600	21.11
NRC	02/98	40.110	22.91	41.946	23.00
	-	-	-	-	-
CENAM	03/98	40.049	23.32	41.995	24.18
	05/98	40.156	23.76	41.537	24.52
NPL	06/98	39.966	22.0	41.780	22.2
	06/98	40.130	23.0	41.843	22.8
INM	09/98	40.233	22.5	42.002	22.5
	-	-	-	-	-
IMGC	11/98	40.100	23.01	41.855	23.00
	11/98	40.083	23.00	41.864	23.03
NMi-VSL	12/98	40.069	22.81	41.855	22.87
	12/98	40.084	22.96	41.780	22.63
PTB	01/99	40.210	23.6	41.837	23.4
	03/99	40.164	22.75	41.904	22.55
NPL	04/99	39.736	21.0	41.513	20.9
	05/99	39.969	22.3	41.671	22.0

To analyze this dataset one has to correct for the temperature dependence of Tungsten. A linear model for each lamp was used to calculate the measured resistance  $R$  back to a temperature of  $20^{\circ}\text{C}$  ( $R_{T=20^{\circ}\text{C}}$ ). A Taylor expansion of the Tungsten resistivity as a function of temperature  $t$  shows higher order terms being at least three orders of magnitude smaller than the linear term. The latter was confirmed by analysis of literature data from two different sources. The dataset for each lamp was used to determine the coefficients  $a_0$  and  $a_1$  from a fit to the relation  $R = a_0 + a_1(t-20)$ , where  $a_0 = R_{T=20^{\circ}\text{C}}$ . The results, the measured resistance of the lamp at  $20^{\circ}\text{C}$  as a function of time, are shown in Figs 3 and 4 for loop I and loop II, respectively.

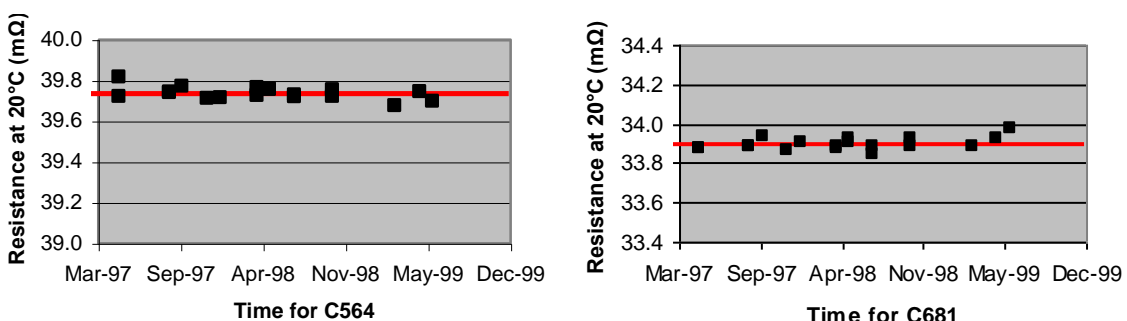


**Figure 3** The measured resistances of lamps C-564 (left) and C-681 (right) as a function of the simultaneously measured ambient temperature at the base of each lamp. Each point corresponds to an individual measurement by the participant either before or after the scale transfer measurements. A horizontal line, referring to  $R_{T=20^{\circ}\text{C}}$  as found from the fit, is added as a guide-to-the-eye.

From these results, one may conclude that there is no significant drift in the measured resistance that may indicate that the artefacts have changed with time. Scatter around the value  $R_{T=20^{\circ}\text{C}}$  as found from each fit might indicate that lamp set I was more stable than lamp set II. This is

clearly shown in the Youden plot of Fig. 5 where the results within each set are plotted against each other.

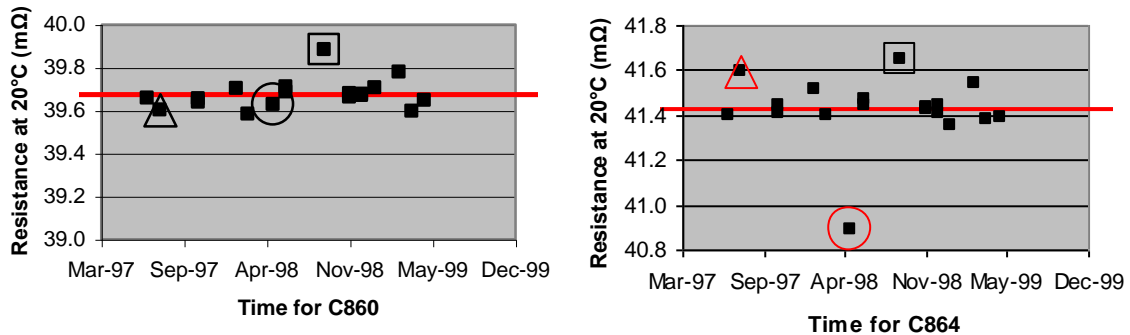


**Figure 4** The measured resistances of lamps C-860 (left) and C-864 (right) as a function of the simultaneously measured ambient temperature at the base of each lamp. Each point corresponds to an individual measurement by the participant either before or after the scale transfer measurements. A horizontal line, referring to  $R_{T=20^\circ\text{C}}$  as found from the fit, is added as a guide-to-the-eye. Three points in time are marked as indicated in the text.

In the Youden plot for loop I less scatter is shown around the centre of gravity than in loop II. Also, three points can be identified as marked with special symbols that might indicate resistance / ambient temperature measurement errors in lamp C864. The resistance measurement as indicated with a square deviates similarly for both artefacts and might indicate a systematic measurement error.

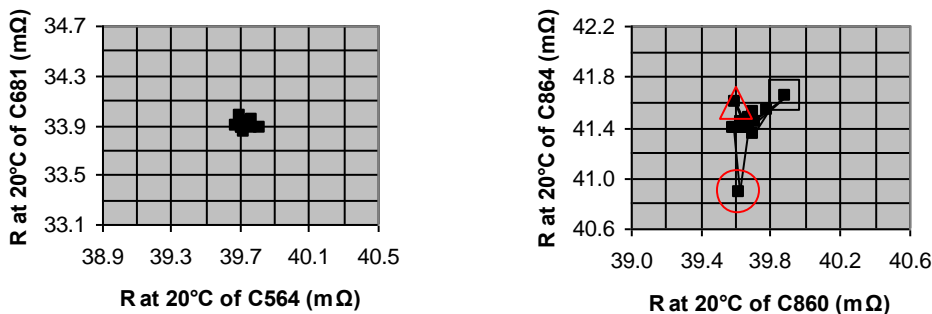


**Figure 5** A Youden plot analysis of the resistance at 20°C of the lamps of loop I (left) and loop II (right). Each point corresponds to 4-wire measurements performed either before or after the scale transfer onto the set of transfer lamps. The points are connected as a function of time. Clearly, the set of lamps from loop I appears more stable than the set of loop II. Three points are marked as indicated in the text.

Each participant was asked to study the interaction of the lamp with the calibration facility, i.e., lamp orientation with respect to the pyrometer/comparator. The relative change in photothermal signal due to spatial and angular displacement was determined. Some participants reported interreflection effects between the lamp window and the calibration facility. However, as these effects were found well outside the acceptance angle of the devices employed, these effects were of no influence on the measurement results. Similarly, the spatial displacement measurements as reported by all participants showed no anomalies.

In an attempt to follow the physical condition of the set of transfer standards, the ambient resistance of the Tungsten filament was measured on receipt and just before sending the artefacts to the next participants (see also the previous section). Furthermore, the lamps were subjected to a test to ensure proper operation. After registration of the radiance temperature at a specific current setting ( $\approx 1100$  °C), the lamp was set to the maximum current for a period of one hour. When operated again at the specified current, the radiance temperature should not deviate more than 50 mK.

By measuring in the direction of increasing current only, after having restabilized the lamp, as indicated above, hysteresis effects could be avoided. Furthermore, minimum equilibration times were specified in the protocol varying from 30 to 15 minutes, depending on the specific temperature range.

The measurements of the participating institutes had to be corrected to a reference condition as stated in the Protocol. In summary, the most important reference conditions are:

- a. The orientation of the strip,
- b. A base temperature of 20 °C,
- c. A wavelength of 650 nm,
- d. A set of eleven defined current settings (related to each lamp).

Given the properties of each specific lamp, corrections to reference conditions had to be made by each participant. These corrections were related to the orientation of the strip, the lamp base temperature, and the set of eleven defined current settings. Instructions were given in the measurement protocol (see Appendix). Other corrections as will be outlined later, were related to the participant instrumentation and include the target-size and size-of-source characteristics of the radiation thermometer employed, the effective central wavelength, etc.

## Participant instrumentation, techniques and other details

In the context of traceability, eleven participants used a calibrated radiation thermometer to transpose the scale directly onto the set of transfer lamps. Three participants, NIST (USA), VNIIM (Russia) and PTB (Germany), transposed the scale by comparison of the artefact with a known reference lamp. Basically, three different operational schemes can be devised for maintaining the ITS-90. The working group for radiation thermometry of the CCT investigated this issue in more detail [1]:

### Scheme 1:

- the fixed-point calibration is transferred to a reference tungsten strip lamp; this implies the determination of a current value on the lamp corresponding to a radiance temperature equal to the fixed-point temperature;
- a series of temperatures  $T_{90}$  are established and maintained on the lamp by measurement of radiance ratios; if necessary, the radiance ratios are adjusted for the non-linearity of the thermometer; this leads to the availability of a series of current and radiance temperature values; a polynomial interpolation equation can be calculated to relate temperature to current in a continuous way

### Scheme 2:

- the fixed-point calibration is transferred to a reference tungsten strip lamp;
- temperatures  $T_{90}$  of any source are determined according to the defining equation of the ITS-90 by measuring the signal ratios between the source at  $T_{90}$  and the reference lamp at the fixed-point temperature; if necessary, the signal ratios are adjusted for the non-linearity of the thermometer.

### Scheme 3:

- the fixed-point calibration is maintained on the thermometer. The output signal is assumed to be representative of  $T_{90}(X)$ ;

- a series of temperatures  $T_{90}$  are established as a function of the output signals of the thermometer. Signal ratios with respect to  $T_{90}(X)$  are calculated and, if necessary, adjusted for the non-linearity of the thermometer.

The three schemes for the realisation and maintenance of the ITS-90 give rise to different uncertainty budgets but with many common uncertainty components. Table 2 associates with each scheme the appropriate uncertainty components by filling a grey cell. The dark grey cells refer to higher temperatures not relevant to this intercomparison [1].

**Table 3** Appropriate uncertainty components for each scheme realizing the ITS-90. The cells in grey indicate the relevant uncertainty components whereas the dominating contributions are indicated in red.

Source of uncertainty		Scheme 1	Scheme 2	Scheme 3
<b>Fixed-point calibration</b>	Impurities			
	Emissivity			
	Temperature drop			
	Plateau identification			
	Repeatability			
<b>Spectral responsivity</b>	Wavelength			
	Reference detector			
	Scattering, Polarisation			
	Repeatability of calibration			
	Drift			
	Out-of-band-transmittance			
<b>Output signal</b>	Interpolation and Integration			
	SSE			
	Non-linearity			
	Drift			
	Ambient conditions			
<b>Lamp</b>	Gain ratios			
	Repeatability			
	Current			
	Drift, Stability			
	Base and ambient temperature			
	Positioning			
	Polynomial fit			

The radiation thermometers employed in the comparison, either absolutely calibrated or used as a comparator, also influence the comparison data due to differences in the target-size, the size-of-source characteristic, and the effective central wavelength. Table 4 presents an overview of the specific schemes and specifications of the radiation thermometers used. Again, detailed information, as presented by each participant, is given in Appendix IV.

**Table 4** Overview of traceability schemes and the characteristic properties of the radiation thermometers used; traceability scheme, target distance, the F-number, central wavelength, the full-width half-maximum of the interference filter, type of imaging system and the spectral methodology.

Participant	Scheme	Target distance (mm)	Target size (mm)	F	$\lambda_c$ (nm)	FWHM (nm)	Optics	Spectral method
NMi-VSL	3	500	0.75	9	661	10	Lens	Integral
NPL	1	1200	0.75	11	665	22	Mirror	$\lambda_{\text{eff}}$
CSIRO	3	600	0.6	10	650	10	Lens	Integral
KRISS	3	500	0.8	10	650	10	Lens	Integral
NIM	3	720	0.75	15	660	11.8	Lens	$\lambda_{\text{eff}}$
NMC	3	500	0.85	10.4	649	10	Lens	$\lambda_{\text{eff}}$
NRLM	3	250	0.5	6	650.3	14.7	Lens	$\lambda_{\text{eff}}$
VNIIM	1	330	0.7x0.7	12	656.3	4.5	Lens	$\lambda_{\text{eff}}$
NIST	2	640	0.6x0.8	13	655.3	5	Lens	$\lambda_{\text{eff}}$
NRC	3	508	0.6	10.6	650	10	Lens	$\lambda_{\text{eff}}$
CENAM	3	630	0.7	15.8	650	10	Lens	$\lambda_{\text{eff}}$
INM	3	550	0.5	12	650	3.2	Mirror	$\lambda_{\text{eff}}$
IMGC	3	600	1	12	655	11	Lens	$\lambda_{\text{eff}}$
PTB	1	1220	0.5	12	655	11	Miror	$\lambda_{\text{eff}}$

**Table 5** Specific information on the fixed-point blackbody cavity configuration as employed by each participant.

Participant	Fixed point	Purity	Emissivity
VSL	Ag	6N	0.999 994
NPL	Ag, Au	6N	0.999 98
CSIRO	Au	5N	0.999 95
KRISS	Cu	5N	0.999 95
NIM	Ag	5N	0.999 92
NMC	Ag	5N	0.999 9
NRLM	Ag, Cu	5N	0.999
VNIIM	Ag, Au, Cu	4N	0.999 4
NIST	Au	5N	0.999 9
NRC	Cu	5N	0.999 97
CENAM	Ag	6N	0.999 97
INM	Cu	4N	0.999 4
IMGC	Ag	6N	0.999 94
PTB	Au	5N	0.999 96

# Results of the comparison

## Measurement results as sent by the participants

The measurement results as sent by the participants are presented in Tables 8 through 27 per loop and in alphabetic order. The uncertainties,  $u(t)$ , are specified for  $k=1$ . Three participants performed additional measurements at 950 nm; these measurements are not used in the context of this key comparison and were therefore reported in the TEMPMEKO 2001 proceedings (T. Ricolfi et al., *Comparison of local realizations of the ITS-90 between 920 °C and 1590 °C at 950 nm using vacuum tungsten strip lamps as transfer standards*, in Proceedings Tempmeko 2001, B. Fellmuth, J. Seidel and G. Scholz eds., pp. 839-844, VDE Verlag GMBH (Berlin Offenbach) 2002).

## Analysis of the measurement data

The main issue to solve in this comparison is to identify the linkage mechanism between two sets of measurements preformed on four lamps: The link can be only realized through the pilot institutes of each loop as they are the only participants that measured all four lamps. A schematic representation is given below based on the figure presented earlier (see Fig. 1). The pilot and co-pilot data of both sets of transfer lamps is used to this purpose, as represented by the red open circles in Fig.6.

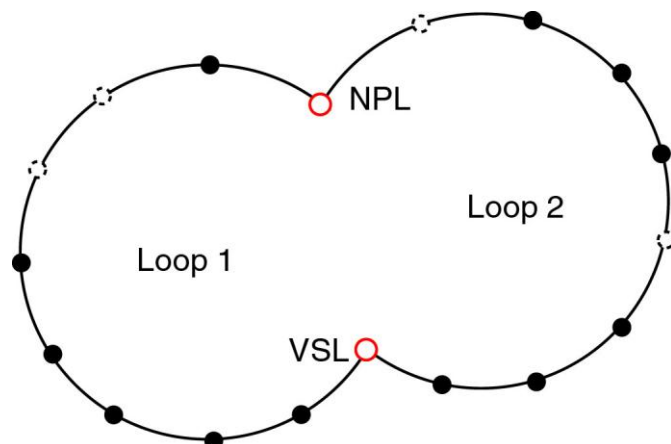
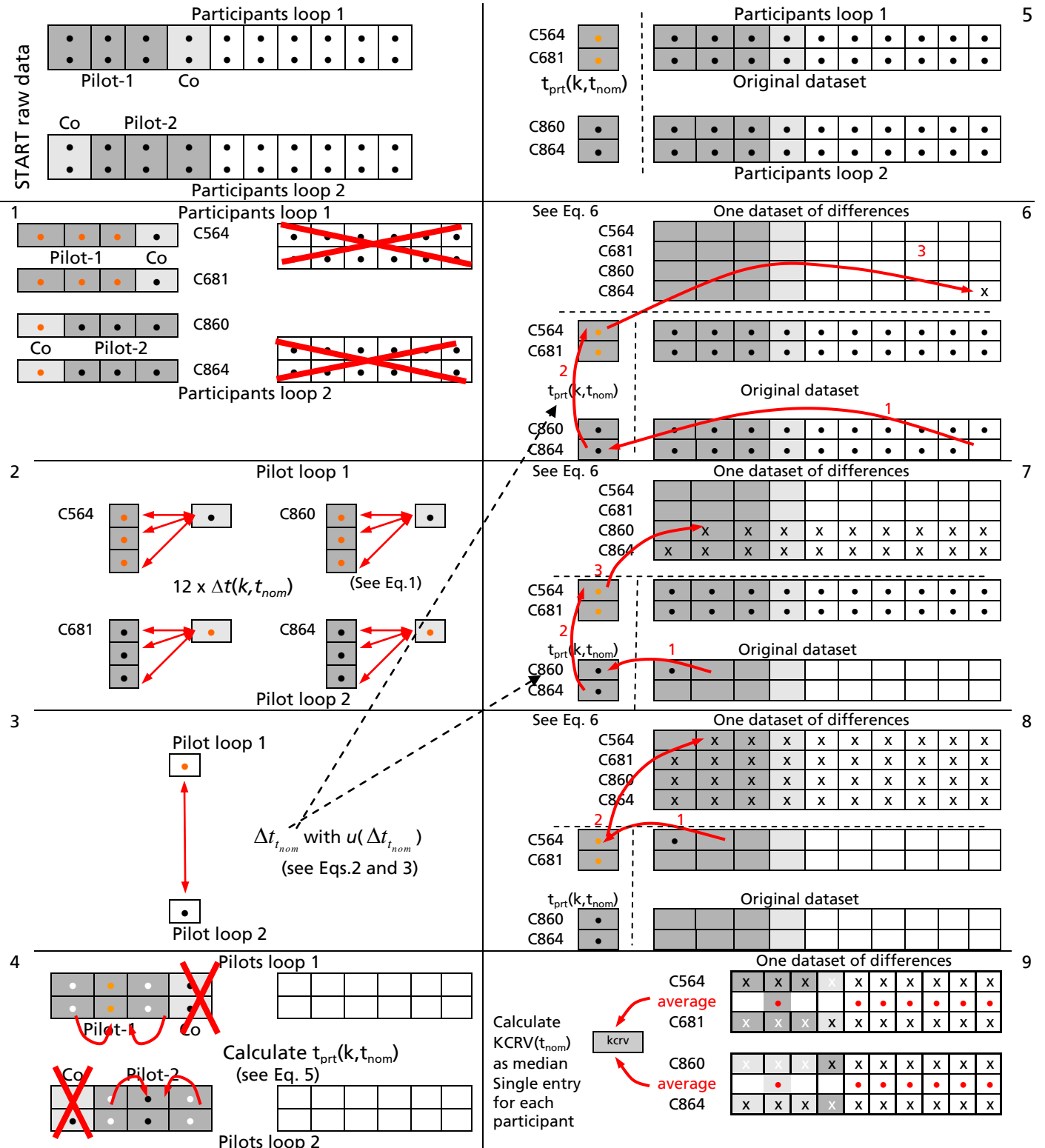


**Figure 6** A schematic of the comparison; loops 1 and 2 are connected through the pilots, indicated by the red open dots. All measurements of the pilot and co-pilot were used to link the loops (see also Fig.1).

The data analysis is presented as a two-step process: First, the link between the loops is investigated and determined. Subsequently the full data set is analyzed, several KCRV values are evaluated, and finally the chosen KCRV is implemented to generate the matrix of equivalence to map the degree of equivalence among the participants. The calculation was performed using Wolfram Mathematica software, combining symbolic algebra with the use of rational numbers where possible, rendering infinite precision. To ensure high precision, 20 significant digits were used when rounding off numbers. To validate the calculations in Mathematica, the entire analysis was repeated at one single temperature with conventional double precision arithmetic using software on an Octave programming platform.

**Table 6** Schematic representations of the data handling throughout KCRV analysis in 8 scenes; From 2 loops (scene 1) to determined difference (scene 2-3). From determination of the reference temperature per lamp (scene 4) to establishment of one dataset of differences on lamps (scene 5-7). Finally the median for each lamp is calculated, forming the KCRV (scene 8).



## Difference between loops 1 and 2 through the pilot and co-pilot data

Table 6 presents an overview of the mathematical steps that were taken to link the loops. The only participants that measured both sets of lamps were the pilot and co-pilot of each loop; that is, VSL with NPL for loop 1 and NPL with VSL for loop 2, respectively. For each of the four lamps, and for each lamp current, the pilot of the loop performed three measurements during the intercomparison, whereas the co-pilot performed one measurement (see Fig. 1). These measurements result in, at eleven nominal temperatures  $t_{nom}$ , a set of twelve differences in measured temperatures between the pilot and co-pilot for each lamp  $k$ . These four sets of temperature differences  $\Delta t(k, t_{nom})$  are given by the expression

$$\Delta t(k, t_{nom})_i = t_{pilot,i} - t_{copilot} \quad i \in \{1,2,3\} \quad k \in \{1,2,3,4\} \quad (1)$$

Without any data “massage” these differences are calculated using Eq.1 and presented versus the nominal temperatures in Fig. 7. The legend refers to the specific lamp and the associated pilot within that loop.

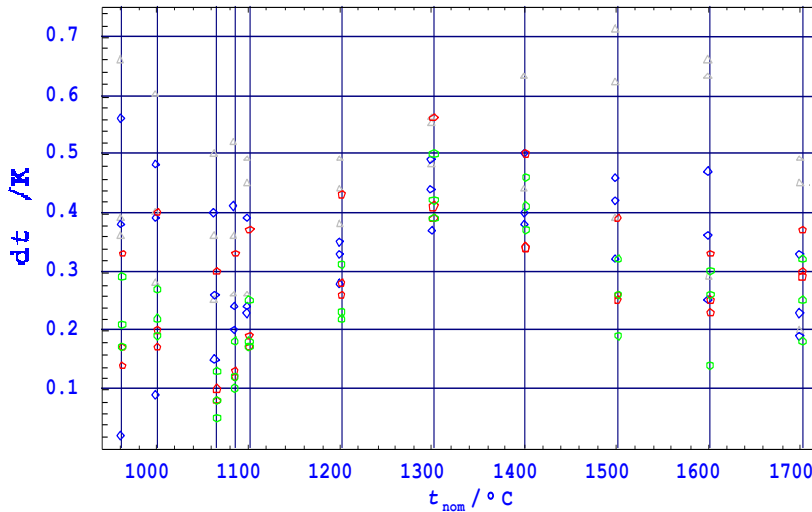


**Figure 7** The temperature differences  $\Delta t(k, t_{nom})$  between the pilot and co-pilot as a function of the nominal temperature for all four lamps.

At each nominal temperature, an average temperature difference  $\Delta t_{t_{nom}}$  is calculated, that is the average difference between the pilot and co-pilot, using

$$\Delta t_{t_{nom}} = \frac{1}{12} \sum_{i=1}^3 \sum_{k=1}^4 \Delta t(k, t_{nom})_i, \quad (2)$$

where  $\Delta t(k, t_{nom})_i$  is the  $i^{th}$  temperature difference at  $t_{nom}$  on lamp  $k$  as calculated from Eq.1. The calculated loop-pilot differences  $\Delta t_{t_{nom}}$  are given in Table 7.

The uncertainty in the average temperature difference  $\Delta t_{t_{nom}}$  is related to the standard deviation of the mean (std) as

$$u(\Delta t_{t_{nom}}) = \frac{1}{\sqrt{n-1}} std(\Delta t(k, t_{nom})_i) \quad i \in \{1,2,3\} \quad k \in \{1,2,3,4\}, \quad (3)$$

where  $n$  is the number of independent measurements.

**Table 7** The average difference  $\Delta t_{t_{nom}}$  and  $u(\Delta t_{t_{nom}})$  between the pilot and co-pilot measurements for 11 nominal temperatures  $t_{nom}$ . Each average value is based on 12 temperature differences, that is, three calculated differences on four individual lamps.

$t_{nom} / ^\circ C$	$\Delta t_{t_{nom}} / ^\circ C$	$u(\Delta t_{t_{nom}}) / ^\circ C (k=1)$
960	0.31	0.10
1000	0.31	0.09
1065	0.22	0.08
1085	0.25	0.08
1100	0.28	0.07
1200	0.33	0.05
1300	0.46	0.04
1400	0.45	0.06
1500	0.38	0.09
1600	0.35	0.09
1700	0.30	0.06

The graphical representation of the differences  $\Delta t(k, t_{nom})$  of Fig. 7 suggests that the differences on the transfer lamps originate from separate populations. For instance, the temperature differences for the C860 lamp are significantly higher than the differences for the other lamps. The latter consequently influences the effective degrees of freedom  $n$  in Eq.3. If all measurements originate from one population, i.e. independent, then the degrees of freedom is 11 ( $n=12-1$ ). If the measurements were from four distinct populations, then the degrees of freedom would be equal to 3 ( $n=4-1$ ).

For a more quantitative analysis of the correlation at each nominal temperature between the different lamp measurements, an analysis of variance was performed on the data. Two nominal temperatures in the analysis of variance, which turn out to be the extremes, are presented in Table 8 and 9 as examples. For comparison, the mean and associated standard deviation are added to the tables for lamps 1 through 4 and the full population.

**Table 8** An analysis of variance between different lamp measurements as performed for the nominal temperature  $t_{nom} = 1000^\circ C$ . For this nominal temperature the highest probability was found.

$t_{nom} = 1000^\circ C$	n	$\Sigma(\dots)^2 / K^2$	Avg((...) <sup>2</sup> ) / K <sup>2</sup>	F-ratio	Probability value
Model	3	0.0704	0.023	1.103	0.402
Error	8	0.1702	0.021		
Total	11	0.2406			
	$\Delta t_{t_{nom}} / ^\circ C$	Std( $\Delta t(k, t_{nom})_i$ ) / $^\circ C$			
All lamps	0.3075	0.1479			
Lamp 1	0.2567	0.1250			
Lamp 2	0.2267	0.0404			
Lamp 3	0.4267	0.1617			
Lamp 4	0.3200	0.2042			

**Table 9** An analysis of variance between different lamp measurements as performed for the nominal temperature  $t_{\text{nom}} = 1500^\circ\text{C}$ . For this nominal temperature the lowest probability was found.

$t_{\text{nom}} = 1500^\circ\text{C}$	n	$\Sigma(\dots)^2 / \text{K}^2$	$\text{Avg}((\dots)^2) / \text{K}^2$	F-ratio	Probability value
Model	3	0.1781	0.0594	5.552	0.023
Error	8	0.0855	0.0107		
Total	11	0.2636			
	$\Delta t_{t_{\text{nom}}} / ^\circ\text{C}$	$\text{Std}(\Delta t(k, t_{\text{nom}})_i) / ^\circ\text{C}$			
All lamps	0.3825	0.1548			
Lamp 1	0.3000	0.0781			
Lamp 2	0.2567	0.0651			
Lamp 3	0.5733	0.1650			
Lamp 4	0.4000	0.0721			

The result of the analysis does not confirm that the data from the four lamps originates from one single population ( $n=11$ ). On the other hand, the alternative hypothesis  $n=3$  has too large a probability. Table 10 provides the probability values found for all 11 nominal temperatures  $t_{\text{nom}}$ . An average probability of  $0.17 \pm 0.14$  is found which is larger than the lower limit of 0.05.

**Table 10** Results from an analysis of variance on the  $\Delta t_{t_{\text{nom}}}$  data for all given nominal temperatures  $t_{\text{nom}}$ . A detailed overview of the analysis is presented for the extremes (\*) in Tables 8 and 9.

$t_{\text{nom}} / ^\circ\text{C}$	Probability value
961	0.2984
1000*	0.4026
1064	0.0556
1084	0.0910
1100	0.1448
1200	0.0393
1300	0.3079
1400	0.1086
1500*	0.0235
1600	0.0835
1700	0.3435
	$0.17 \pm 0.14$

Setting the probability limit to 0.95, one has to conclude from the analysis of variances that one has to be conservative in the degrees of freedom and set n to 3. Consequently, the uncertainties  $u(\Delta t_{t_{\text{nom}}})$  from Table 7 related to the average pilot-loop difference  $\Delta t_{t_{\text{nom}}}$  is determined from Eq.3 with  $n=3$ . The average difference between the loops is determined through the pilot and co-pilot data and presented in Table 7. A continuous expression is needed to link the participants from one loop to the other and vice versa. To this purpose, a spline-fit is generated using the dataset  $[\Delta t_{t_{\text{nom}}}, u(\Delta t_{t_{\text{nom}}})]$  of Table 7. The result is presented in Fig.8.

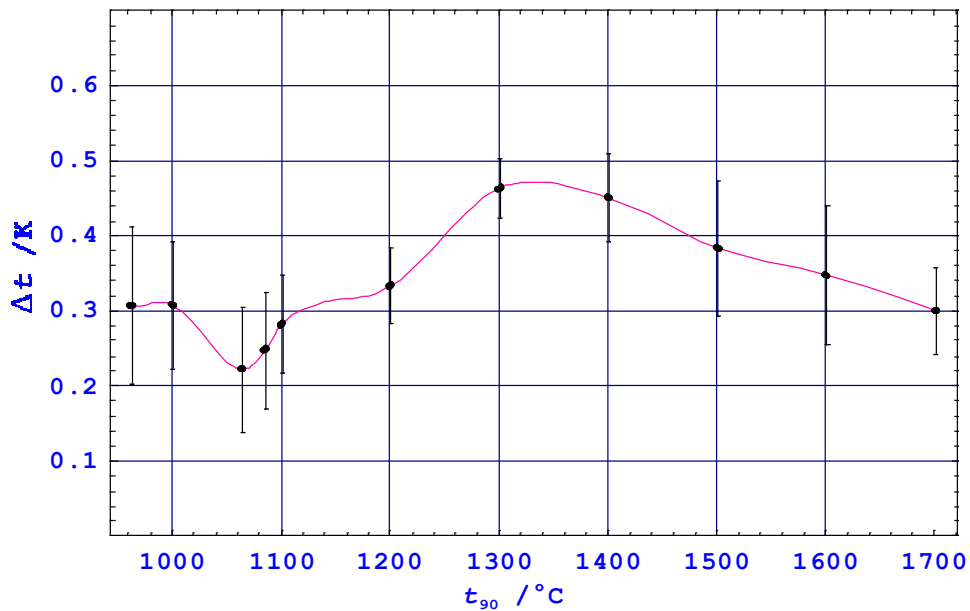


**Figure 8** The average differences  $\Delta t_{t_{nom}}$  and  $u(\Delta t_{t_{nom}})$  between the pilot and co-pilot measurements versus the nominal temperature (see Table 7). The dots and error bars represent the average and uncertainty, respectively. The spline represented by the red solid line is calculated on the basis of these points.

### Link the loops through the pilot reference temperatures

The average difference  $\Delta t_{t_{nom}}$  between the loops is determined through all pilot and co-pilot data. To establish the link through the average difference, a representative reference within each set of lamp data is needed. At a given nominal temperature, the participant data on a given lamp will be linked to the participant data on another lamp through the pilot reference temperatures for each lamp. In order to find the representative pilot reference temperature  $t_{prt}(k, t_{nom})$ , four different schemes are used to calculate  $t_{prt}(k, t_{nom})$  on each lamp  $k$  at each nominal temperature  $t_{nom}$ . For each lamp, four measurements are available; three from the pilot within the loop and one from the pilot of the other loop (the co-pilot). The following pilot reference temperatures were calculated:

- Pilot Mean based only on the three pilot entries within the loop,
- Pilot weighted Weighted mean based only on the three pilot entries within the loop,
- Pilot and co-pilot ( $t_{prt\_All}$ ) Mean based on both the co-pilot and the three pilot entries within the loop and
- Pilot and co-pilot weighted ( $t_{weight,prt\_All}$ ) Weighted mean based on both the co-pilot and the three pilot entries within the loop.

The first two nominees were calculated using conventional methods. The other two were calculated according to Eq. 4. To include the measurement of the co-pilot in the mean and weighted mean respectively, the co-pilot data is corrected for the loop difference (Eq. 2) for each nominal temperature and lamp.

$$\begin{aligned}
t_{prt\_ALL}(k, t_{nom}) &= \frac{1}{4} \left( \sum_{i=1}^3 t(k, t_{nom})_i^p + (t(k, t_{nom})^c \pm \Delta t(k, t_{nom})) \right) \\
t_{weight, prt\_ALL}(k, t_{nom}) &= \frac{\sum_{i=1}^3 \left( \frac{t(k, t_{nom})_i^p}{u(t(k, t_{nom})_i^p)} \right)^2 + \left( \frac{(t(k, t_{nom})^c \pm \Delta t(k, t_{nom}))}{u(t(k, t_{nom})^c)} \right)^2}{\sum_{i=1}^3 \left( \frac{1}{u(t(k, t_{nom})_i^p)} \right)^2 + \left( \frac{1}{u(t(k, t_{nom})^c)} \right)^2} \quad (4)
\end{aligned}$$

The superscript p denotes the pilot within the loop, c the co-pilot. The pilot differences  $\Delta t(k, t_{nom})$  are defined as described by Eq. 2. Note that the role of pilot and co-pilot are interchanged from loop 1 and loop 2. Consequently, in loop 1 the + sign should be chosen, for loop 2 the - sign. The uncertainties used in calculating the weighted mean originate from the pilot and co-pilot entries. As the correlation is unknown, correlation effects are ignored.

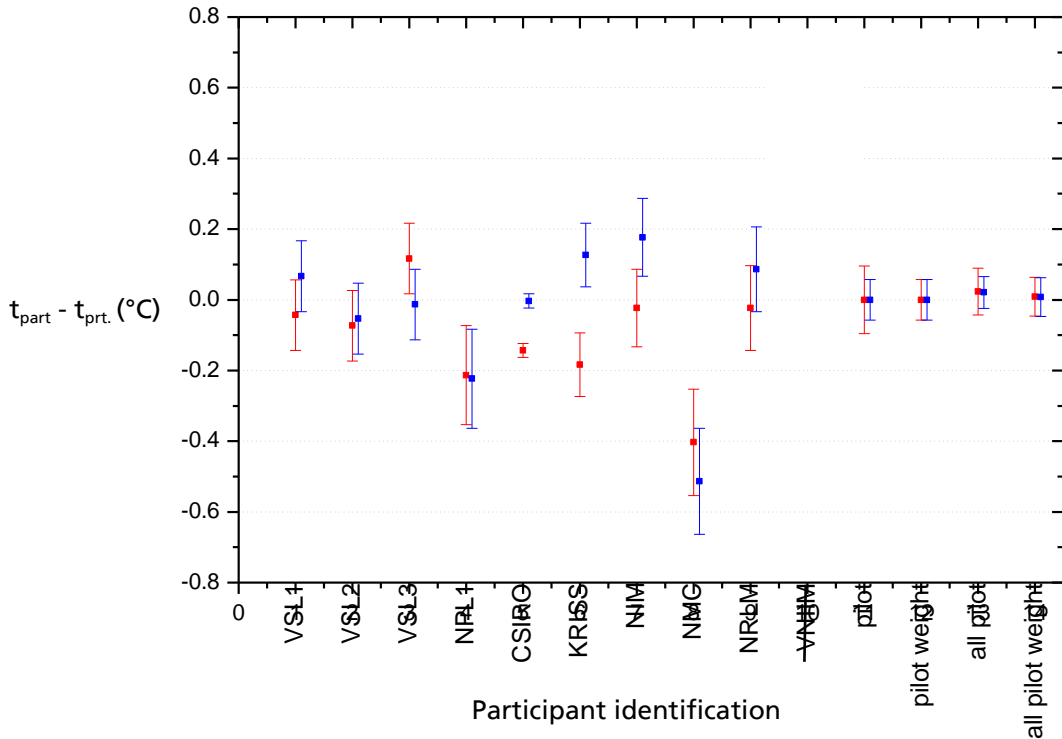


**Figure 9** Differences with respect to the pilot reference temperature  $t_{prt}(k, 960^\circ\text{C})$  of the participants in loop 1 at  $960^\circ\text{C}$ . The blue and red dots refer to lamp C681 and C564, respectively. The pilot mean is chosen for  $t_{prt}$ . For clarity, all options for  $t_{prt}$  are also plotted. Uncertainties are stated for  $k = 1$ , as given by the participants. The

Figure 9 presents a typical example of participant differences with respect to a pilot reference temperature. Here the pilot mean is taken as the reference  $t_{prt}(k, t_{nom})$ . The four options for  $t_{prt}$  are added to the participants of loop 1. Note that inclusion of the co-pilot in the calculation for  $t_{prt}$  shifts its value slightly upwards due to the relatively large loop difference  $\Delta t_{t_{nom}}$  ( $\Delta t_{960^\circ\text{C}} = 0.31^\circ\text{C}$ ). Similar plots can be generated for both loops and for each nominal temperature.

A choice had to be made regarding how  $t_{prt}(k, t_{nom})$  would be determined for each lamp  $k$  and each nominal temperature  $t_{nom}$ . As the correlation is unknown between the pilot entries, the weighted mean is not preferred. When all  $t_{prt}$ 's are analyzed for the pilot-mean and all-pilot-mean at the nominal temperatures, a maximum difference of 0.05°C is found. Since this difference is negligible compared to the total uncertainty, and as the system is clearer to understand, it was decided to neglect the co-pilot data in the calculation of  $t_{prt}(k, t_{nom})$ :

$$t_{prt}(k, t_{nom}) = \frac{1}{3} \left( \sum_{i=1}^3 t(k, t_{nom})_i^p \right). \quad (5)$$

With the pilot reference temperature defined for all  $k$  and  $t_{nom}$ , the differences  $\delta t_i(k, t_{nom})$  between the participant data  $t_i(k, t_{nom})$  and  $t_{prt}$  can be calculated and, in addition, corrected for the loop difference when needed (see Table 6, scene 5 through 7). By this mechanism, the loops are linked and one dataset of lamp differences is realized for the determination of the KCRV. In formulae, the dataset is described by

$$\begin{aligned} \delta t_i(k, t_{nom}) &\equiv t_i(k, t_{nom}) - t_{prt}(k, t_{nom}), & k = C564, C681 \\ \delta t_i(k, t_{nom}) &\equiv t_i(k, t_{nom}) - t_{prt}(k, t_{nom}) + \Delta t_{t_{nom}}, & k = C860, C864. \end{aligned} \quad (6)$$

## Calculating the KCRV

### Input data for the KCRV

The KCRV is calculated on the basis of a single contribution from each institute for each nominal temperature, if the participant contributes data at that specific current. Some measurements were not included in the KCRV calculation due to problems with the measurement system. This is described in more detail in the annex. Not incorporated in the calculation of the KCRV are:

VNIIM	Data entries below 1064 °C
NRC	All data
INM	Data entries from lamp C860

The comparison started before the MRA was defined and before the guidelines for key comparisons were issued. Not all participants received proper warning of anomalous data before draft-A was issued. Discussions during the 21<sup>st</sup> meeting of the CCT led to the conclusion that the identified data would not be used for the KCRV evaluation, but would be compared with the other data and with the KCRV in this report. Meanwhile, NRC has participated in a bilateral comparison with PTB, the results of which are reported in the proceedings of TEMPMEKO 2004 (see J. Hartmann, R. Thomas, C.K. Ma, A.G. Steele and K.D. Hill, *Bilateral comparison of the local realizations of the ITS-90 between the Silver-point and 1700 °C using vacuum Tungsten-strip lamps as transfer standards between NRC and PTB*, Proceedings of TEMPMEKO 2004, Cavtat-Dubrovnik Croatia, 2005).

To avoid unequal weighting of the data, averages for each participant were calculated with respect to the difference from the pilot reference temperatures. For each nominal temperature, there are eight such differences for the pilots. For INM, only the data from lamp C864 were used. For all other institutes, the averages of the deviations for the two lamps were taken for each nominal temperature, basically taking the average of the  $\delta t_i(k, t_{nom})$  of Eq. 5:

$$\delta t_i(t_{nom}) = \frac{1}{n} \sum_{k=1}^n \delta t_i(k, t_{nom}), \quad (7)$$

where, apart from exceptions mentioned above, n=2 or n=8 for participants and pilots, respectively. The uncertainty associated with this average  $\delta t$  is identical to that of a single entry  $\delta t_i$ . As, for all participants, the uncertainty does not depend on the lamp number but on the nominal temperature instead, this assumption is valid, given that there is no knowledge available regarding correlation effects.

### Calculation of KCRV values

For the calculation of the KCRV, the following alternatives were considered:

- *Arithmetic mean*: tends to be sensitive to outlying points;
- *Median*: less sensitive to outliers compared to the arithmetic mean;
- *Weighted mean*: sensitive to the points that have small uncertainty.

For the purpose of calculating the weighted mean, the uncertainty of the average temperature difference between the loops  $u(\Delta t_{t_{nom}})$ , see Eq. 3, is added in quadrature to the uncertainty of the participant  $u(\delta t_i(t_{nom}))$  at each nominal temperature:

$$u'(\delta t_i) = \sqrt{u(\delta t_i)^2 + u(\Delta t_{t_{nom}})^2} \quad (8)$$

The stability of the transfer standards (lamps) is evaluated along with the reproducibility of the pilot measurements during the comparison on each lamp. This reproducibility is estimated by

the uncertainty of the average temperature difference between the loops  $u(\Delta t_{t_{nom}})$ . The latter has only significant influence on the data of CSIRO as  $u(\delta t_{CSIRO}) < u(\Delta t_{t_{nom}})$ .

Figure 10 shows the results of the KCRV calculation. As the KCRVs are, in this comparison, based on differences between lamps/loops (Eq. 6) due to linkage of the loops, one has to compare the differences for the three options. Hence, the deviation of the median and weighted mean from the arithmetic mean as a function of the nominal temperature is plotted in Fig.10.

Clearly, the median and the weighted mean are systematically lower than the arithmetic mean. Since the median is less sensitive to outliers, the deviation suggests that the dataset has a significant proportion of outliers. The median and weighted mean show a similar trend, suggesting that these outliers are associated with relatively large uncertainties.

To make a conclusive argument for choosing between the mean, the weighted mean, or the median as the KCRV, the uncertainties associated with these KCRVs were calculated and analyzed.

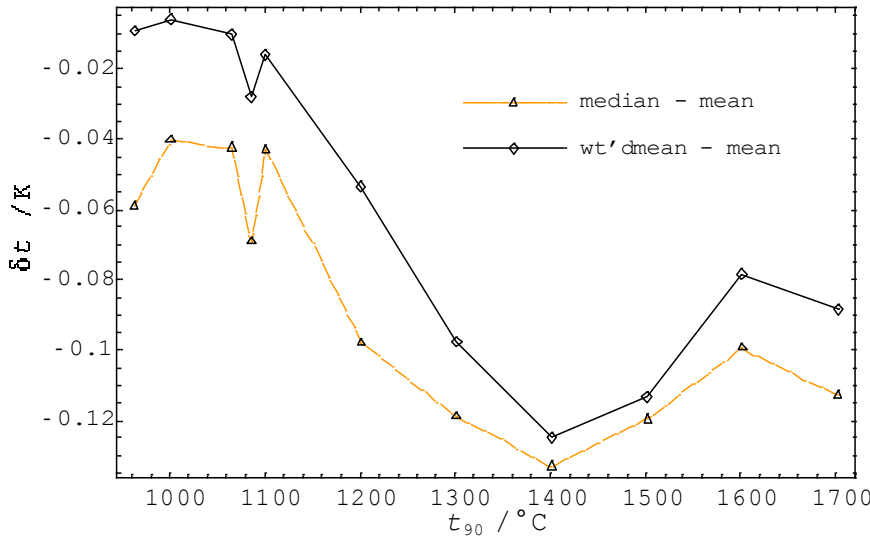


**Figure 10** Comparison of different KCRV values for the nominal temperatures, that is, the mean, median and weighted mean. Here the mean-based KCRV is taken as the reference, with the differences  $\text{KCRV}_{\text{median}} - \text{KCRV}_{\text{mean}}$  and  $\text{KCRV}_{\text{weighted mean}} - \text{KCRV}_{\text{mean}}$  shown as a function of the nominal temperature.

## Calculating the uncertainties associated with the KCRV values

To determine the uncertainties associated with the mean, weighted mean and median KCRV candidates, the following relations were used at each nominal temperature  $t_{\text{nom}}$ .

### Arithmetic mean KCRV

- Simple mean of the uncertainties

$$u_{s\_mean} = \frac{1}{N} \sum_{i=1}^N u_i$$

- Quadratic mean of the uncertainties

$$u_{q\_mean} = \sqrt{\frac{1}{N} \sum_{i=1}^N u_i^2}$$

- Standard deviation of the differences  $\delta t_i$

### Weighted mean KCRV

- Weighted mean of the uncertainties

$$u_{w\_mean} = \sqrt{\frac{1}{\sum_{i=1}^N \frac{1}{u_i^2}}}$$

### Median KCRV

- Uncertainty related to median using

$$u_{median} = \frac{1.858}{\sqrt{N-1}} \text{median}(|\delta t_i - m|),$$

where  $m$  is the median of the population

The uncertainties of the three KCRV candidates are calculated accordingly and presented in Fig. 10 as function of the nominal temperatures. Analyzing the five different models, one sees that, except for the case of the simple mean, the uncertainties are less than the average standard deviation of the differences  $\delta t_i$ . In particular, the weighted mean clearly underestimates the deviations in the data, being significantly smaller than the standard deviation of the differences. The Birge-ratio criterion indicates that the median and the arithmetic mean of the differences  $\delta t(t_{nom})$  are suitable choices for the KCRV.

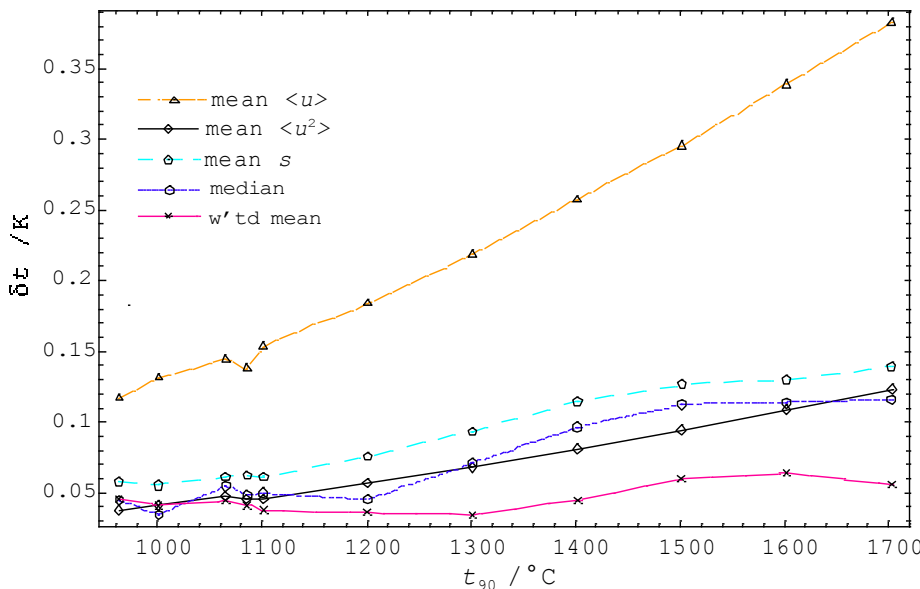


**Figure 11** The uncertainties ( $k=1$ ) associated with the alternatives for the KCRV

### Median as the representative value for the KCRV

Combining the results of the data and uncertainty analyses, one may conclude the median is the best choice to represent the KCRV. That is, the median is less sensitive to outliers and also the Birge-ratio criterion holds for the associated uncertainty. On the basis of the median, one may summarize the determination of the KCRV value at each nominal temperature as:

Determine per lamp the 'Pilot – Copilot' difference

$$\Delta t(k, t_{nom})_i = t_{pilot,i} - t_{copilot} \quad i \in \{1,2,3\} \quad k \in \{1,2,3,4\}$$

4 lamps, 3 differences per lamp, 11 nominal temperatures

Determine the average 'Pilot – Copilot' difference

$$\Delta t_{t_{nom}} = \frac{1}{12} \sum_{i=1}^3 \sum_{k=1}^4 \Delta t(k, t_{nom})_i$$

11 nominal temperatures

Determine uncertainty of the 'Pilot – Copilot' difference

$$u(\Delta t_{t_{nom}}) = \frac{1}{\sqrt{2}} \text{std}(\Delta t(k, t_{nom})_i) \quad i \in \{1,2,3\} \quad k \in \{1,2,3,4\}$$

11 nominal temperatures

Determine reference pilot temperature per lamp

$$\Delta t_{t_{nom}} = \frac{1}{3} \left( \sum_{i=1}^3 t(k, t_{nom})_i^p \right)$$

4 lamps, 11 nominal temperatures

Link the loops through 'Pilot – Copilot' difference and reference pilot temperature

$$\delta t_i(k, t_{nom}) \equiv t_i(k, t_{nom}) - t_{prt}(k, t_{nom}), \quad k = C564, C681$$

$$\delta t_i(k, t_{nom}) \equiv t_i(k, t_{nom}) - t_{prt}(k, t_{nom}) + \Delta t_{t_{nom}}, \quad k = C860, C864$$

1 dataset of differences with all participant entries

Determine KCRV from dataset of differences

$$\overline{\delta t(t_{nom})}_i = \frac{1}{n} \sum_{k=1}^n \delta t_i(k, t_{nom}), \quad n = 8, \text{ pilots}$$

$$n = 2, \text{ participants}$$

$$KCRV(t_{nom}) = \text{median}(\overline{\delta t(t_{nom})}_i)$$

11 nominal temperatures

Determine uncertainty KCRV from dataset of differences

$$u_{\text{median}}(KCRV(t_{nom})) = \frac{1.858}{\sqrt{10}} \text{median}(|\overline{\delta t(t_{nom})}_i - KCRV(t_{nom})|),$$

11 nominal temperatures

The expression for  $u_{\text{median}}(KCRV(t_{nom}))$  is based on the paper from J. W. Müller, *Possible Advantages of a Robust Evaluation of Comparisons*. (J. Res. Natl. Stand. Technol. 105 (2000) page 551-555). A schematic representation of this exercise is given in Table 6.

**Determine difference of participants with respect to KCRV**

Based on the calculated KCRV, one can determine the differences from the participant entries with respect to the KCRV and, together with the KCRV, the difference between two participants. The KCRV is global, that is, one set of values as a function of the nominal temperature, without a lamp- or loop-dependence. The set of differences per participant  $\delta t_i(k, t_{nom})$ , however, is still specified either from loop 1 or from loop 2. The latter is important when calculating the uncertainty associated with the difference between two participants as

one as to take the uncertainty of the loop difference,  $u(\Delta t_{t_{nom}})$ , into account as well. Based on this argument, one can distinguish interloop and intraloop intercomparisons. Three values are calculated and presented in the cross-reference tables; that is, in the  $nm^{\text{th}}$ -cell one finds from participant  $n$  to participant  $m$ :

A. The difference between participants:

$$\text{Intra-loop} \quad \Delta t_{nm}(k, t_{nom}) = \delta t_n(k, t_{nom}) - \delta t_m(k, t_{nom})$$

$$\text{Inter-loop} \quad \Delta t_{nm}(k, t_{nom}) = \delta t_n(k, t_{nom}) - \delta t_m(k, t_{nom}) \mp \Delta t_{t_{nom}}$$

The  $\pm$ -sign relates to either adding or subtracting the difference depending of participant  $n$  being in either loop 1 or loop 2, respectively. Note that, in this case, a total of 4 combinations can be made since both participants have measured 2 lamps.

B. The combined uncertainty,  $k=2$ :

$$\text{Intra-loop} \quad U(\Delta t_{nm}(t_{nom})) = 2\sqrt{u_n^2(t_{nom}) + u_m^2(t_{nom})}$$

$$\text{Inter-loop} \quad U(\Delta t_{nm}(t_{nom})) = 2\sqrt{u_n^2(t_{nom}) + u_m^2(t_{nom}) + u^2(\Delta t_{t_{nom}})}$$

C. The QDE<sub>95</sub> value

$$QDE_{95}(k, t_{nom}) = |\Delta t_{nm}(k, t_{nom})| + \left\{ 1.645 + 0.3295 \exp\left(\frac{-4.05|\Delta t_{nm}(k, t_{nom})|}{U(\Delta t_{nm}(k, t_{nom}))}\right) \right\} u(\Delta t_{nm}(k, t_{nom}))$$

## Intraloop comparisons

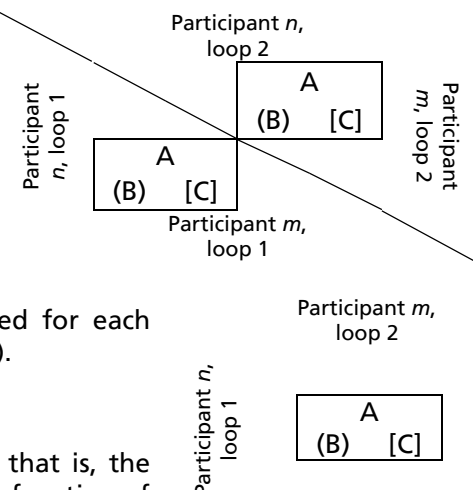
The components A, B and C *within a loop* are presented for each nominal temperature in Tables 31 through 41 (page 36 - 46). The lower left triangle of the table refers to loop 1 whereas the components A, B, and C of loop 2 are presented in the upper right triangle.

## Interloop comparisons

The components A, B and C *between loops* are presented for each nominal temperature in Tables 42 through 52 (page 47 - 57).

## Graphical representations

Figures 12 through 31 (page 58 - 77) present the results; that is, the difference of each participant with respect to the KCRV as a function of the nominal temperature. The uncertainty bars are for  $k=2$  and the temperature span on the Y-axis is set to 4°C, a value that is 4 times the largest uncertainty specified by a participant.



The results as sent by the participants are presented in the next 20 sets of tables. Each table in a set presents the results from an average of two successive runs. An exception is the set of participant CSIRO, where only one data set was available.

**Table 11** Measurement results as sent in by CSIRO

Lamp C564  
Laboratory CSIRO

I / A	t / °C	u(t) / °C
4.480	963.95	0.02
4.721	1002.00	0.02
5.169	1066.17	0.02
5.322	1086.57	0.02
5.441	1102.01	0.02
6.272	1201.92	0.02
7.194	1302.03	0.02
8.189	1402.40	0.02
9.242	1502.67	0.03
10.347	1602.98	0.03
11.502	1703.51	0.04

Lamp C681  
Laboratory CSIRO

I / A	t / °C	u(t) / °C
5.508	963.48	0.02
5.822	1001.78	0.02
6.399	1066.16	0.02
6.594	1086.55	0.02
6.745	1101.96	0.02
7.795	1202.09	0.02
8.948	1302.43	0.02
10.183	1402.82	0.02
11.487	1503.20	0.03
12.851	1603.25	0.03
14.273	1703.34	0.04

**Table 12** Measurement results as sent in by KRISS

Lamp C564  
Laboratory KRISS

I / A	t / °C	u(t) / °C
4.480	963.91	0.09
4.721	1001.98	0.09
5.169	1066.15	0.10
5.322	1086.56	0.08
5.441	1102.00	0.10
6.272	1201.91	0.12
7.194	1301.98	0.14
8.189	1402.32	0.16
9.242	1502.60	0.19
10.347	1602.91	0.21
11.502	1703.41	0.25

Lamp C681  
Laboratory KRISS

I / A	t / °C	u(t) / °C
5.508	963.61	0.09
5.822	1001.87	0.09
6.399	1066.27	0.10
6.594	1086.64	0.08
6.745	1102.01	0.10
7.795	1202.15	0.12
8.948	1302.52	0.14
10.183	1402.92	0.16
11.487	1503.21	0.19
12.851	1603.27	0.21
14.273	1703.38	0.25

**Table 13** Measurement results as sent in by NIM

Lamp C564  
Laboratory NIM

I / A	t / °C	u(t) / °C
4.480	964.07	0.11
4.721	1002.10	0.12
5.441	1102.11	0.14
6.272	1201.92	0.16
7.194	1302.03	0.18
8.189	1402.38	0.21
9.242	1502.67	0.24
10.347	1602.96	0.27
11.502	1703.48	0.31

Lamp C681  
Laboratory NIM

I / A	t / °C	u(t) / °C
5.508	963.66	0.11
5.822	1001.97	0.12
6.745	1102.20	0.14
7.795	1202.31	0.16
8.948	1302.71	0.18
10.183	1403.14	0.21
11.487	1503.51	0.24
12.851	1603.64	0.27
14.273	1703.81	0.31

**Table 14** Measurement results as sent in by NMC

Lamp C564  
Laboratory NMC

I / A	t / °C	u(t) / °C
4.480	963.69	0.15
4.721	1001.68	0.15
5.169	1065.83	0.16
5.322	1086.18	0.16
5.441	1101.60	0.16
6.272	1201.41	0.18
7.194	1301.40	0.21
8.189	1401.65	0.23
9.242	1501.82	0.26
10.347	1601.97	0.30
11.502	1702.32	0.34

Lamp C681  
Laboratory NMC

I / A	t / °C	u(t) / °C
5.508	962.97	0.15
5.822	1001.21	0.15
6.399	1065.50	0.16
6.594	1085.84	0.16
6.745	1101.24	0.16
7.795	1201.24	0.18
8.948	1301.47	0.21
10.183	1401.71	0.23
11.487	1501.83	0.26
12.851	1601.89	0.30
14.273	1701.69	0.34

**Table 15** Measurement results as sent in by NRLM

Lamp C564  
Laboratory NRLM

I / A	t / °C	u(t) / °C
4.480	964.07	0.12
4.721	1002.13	0.12
5.169	1066.31	0.13
5.322	1086.72	0.13
5.441	1102.16	0.13
6.272	1202.10	0.15
7.194	1302.25	0.18
8.189	1402.66	0.21
9.242	1502.99	0.24
10.347	1603.36	0.27
11.502	1703.93	0.31

Lamp C681  
Laboratory NRLM

I / A	t / °C	u(t) / °C
5.508	963.57	0.12
5.822	1001.87	0.12
6.399	1066.22	0.13
6.594	1086.62	0.13
6.745	1102.04	0.13
7.795	1202.25	0.15
8.948	1302.63	0.18
10.183	1403.09	0.21
11.487	1503.47	0.24
12.851	1603.65	0.27
14.273	1703.77	0.31

**Table 16** Measurement results as sent in by NPL (I)

Lamp C564  
Laboratory NPL1

I / A	t / °C	u(t) / °C
4.480	963.88	0.14
4.721	1001.88	0.14
5.169	1066.11	0.15
5.322	1086.47	0.15
5.441	1101.85	0.16
6.272	1201.63	0.20
7.194	1301.58	0.23
8.189	1401.98	0.28
9.242	1502.33	0.32
10.347	1602.62	0.37
11.502	1703.02	0.41

Lamp C681  
Laboratory NPL1

I / A	t / °C	u(t) / °C
5.508	963.26	0.14
5.822	1001.54	0.14
6.399	1066.00	0.15
6.594	1086.34	0.15
6.745	1101.67	0.16
7.795	1201.73	0.20
8.948	1301.88	0.23
10.183	1402.26	0.28
11.487	1502.69	0.32
12.851	1602.75	0.37
14.273	1702.76	0.41

**Table 17** Measurement results as sent in by VNIIM

Lamp C564  
Laboratory VNIIM

I / A	t / °C	u(t) / °C
4.480	964.66	0.16
4.721	1002.57	0.16
5.169	1066.33	0.16
5.322	1086.66	0.19
5.441	1101.96	0.21
6.272	1201.59	0.34
7.194	1301.51	0.47
8.189	1401.69	0.60
9.242	1502.16	0.73
10.347	1602.90	0.86
11.502	1703.93	0.99

Lamp C681  
Laboratory VNIIM

I / A	t / °C	u(t) / °C
5.508	964.07	0.16
5.822	1001.99	0.16
6.399	1065.89	0.16
6.594	1086.28	0.19
6.745	1101.64	0.21
7.795	1201.58	0.34
8.948	1301.63	0.47
10.183	1401.68	0.60
11.487	1501.77	0.73
12.851	1602.07	0.86
14.273	1702.93	0.99

**Table 18** Measurement results as sent in by VSL (first run, I)

Lamp C564  
Laboratory VSL1

I / A	t / °C	u(t) / °C
4.480	964.05	0.10
4.721	1002.08	0.10
5.169	1066.21	0.11
5.322	1086.60	0.11
5.441	1102.04	0.11
6.272	1201.91	0.12
7.194	1301.99	0.14
8.189	1402.32	0.16
9.242	1502.58	0.17
10.347	1602.85	0.19
11.502	1703.31	0.21

Lamp C681  
Laboratory VSL1

I / A	t / °C	u(t) / °C
5.508	963.55	0.10
5.822	1001.81	0.10
6.399	1066.13	0.11
6.594	1086.52	0.11
6.745	1101.92	0.11
7.795	1202.04	0.12
8.948	1302.38	0.14
10.183	1402.72	0.16
11.487	1503.01	0.17
12.851	1603.05	0.19
14.273	1703.01	0.21

**Table 19** Measurement results as sent in by VSL (second run, I)

Lamp C564  
Laboratory VSL2

I / A	t / °C	u(t) / °C
4.480	964.02	0.10
4.721	1002.05	0.10
5.169	1066.19	0.11
5.322	1086.59	0.11
5.441	1102.02	0.11
6.272	1201.89	0.12
7.194	1301.97	0.14
8.189	1402.32	0.16
9.242	1502.59	0.17
10.347	1602.87	0.19
11.502	1703.32	0.21

Lamp C681  
Laboratory VSL2

I / A	t / °C	u(t) / °C
5.508	963.43	0.10
5.822	1001.73	0.10
6.399	1066.05	0.11
6.594	1086.44	0.11
6.745	1101.84	0.11
7.795	1201.96	0.12
8.948	1302.30	0.14
10.183	1402.67	0.16
11.487	1502.95	0.17
12.851	1603.01	0.19
14.273	1703.08	0.21

**Table 20** Measurement results as sent in by VSL (third run, I)

Lamp C564  
Laboratory VSL3

I / A	t / °C	u(t) / °C
4.480	964.21	0.10
4.721	1002.28	0.10
5.169	1066.41	0.11
5.322	1086.80	0.11
5.441	1102.22	0.11
6.272	1202.06	0.12
7.194	1302.14	0.14
8.189	1402.48	0.16
9.242	1502.72	0.17
10.347	1602.95	0.19
11.502	1703.39	0.21

Lamp C681  
Laboratory VSL3

I / A	t / °C	u(t) / °C
5.508	963.47	0.10
5.822	1001.76	0.10
6.399	1066.08	0.11
6.594	1086.46	0.11
6.745	1101.85	0.11
7.795	1201.95	0.12
8.948	1302.27	0.14
10.183	1402.63	0.16
11.487	1502.88	0.17
12.851	1602.89	0.19
14.273	1702.94	0.21

**Table 21** Measurement results as sent in by CENAM

Lamp C860  
Laboratory CENAM

I / A	t / °C	u(t) / °C
5.072	962.26	0.21
5.380	1000.29	0.22
5.944	1064.44	0.25
6.141	1085.52	0.26
6.284	1100.50	0.26
7.298	1200.56	0.31
8.398	1300.67	0.37
9.570	1400.72	0.44
10.805	1500.87	0.50
12.099	1600.88	0.60
13.446	1700.73	0.65

Lamp C864  
Laboratory CENAM

I / A	t / °C	u(t) / °C
4.933	962.30	0.21
5.236	1000.28	0.22
5.788	1064.35	0.25
5.980	1085.40	0.26
6.120	1100.44	0.26
7.107	1200.49	0.31
8.177	1300.59	0.37
9.314	1400.62	0.44
10.513	1500.71	0.50
11.767	1600.72	0.60
13.074	1700.65	0.65

**Table 22** Measurement results as sent in by IMGC

Lamp C860  
Laboratory IMGC

I / A	t / °C	u(t) / °C
5.072	962.36	0.07
5.380	1000.41	0.08
5.944	1064.52	0.08
6.141	1085.61	0.09
6.284	1100.60	0.09
7.298	1200.67	0.10
8.398	1300.81	0.12
9.570	1400.96	0.14
10.805	1501.04	0.16
12.099	1601.08	0.18
13.446	1700.97	0.21

Lamp C864  
Laboratory IMGC

I / A	t / °C	u(t) / °C
4.933	962.24	0.07
5.236	1000.28	0.08
5.788	1064.32	0.08
5.980	1085.36	0.09
6.120	1100.40	0.09
7.107	1200.47	0.10
8.177	1300.67	0.12
9.314	1400.71	0.14
10.513	1500.83	0.16
11.767	1600.78	0.18
13.074	1700.76	0.21

**Table 23** Measurement results as sent in by INM

Lamp C860  
Laboratory INM

I / A	t / °C	u(t) / °C
5.072	961.71	0.13
5.380	999.75	0.14
5.944	1063.82	0.16
6.141	1084.92	0.16
6.284	1099.90	0.17
7.298	1199.95	0.19
8.398	1299.88	0.22
9.570	1400.01	0.26
10.805	1499.92	0.30
12.099	1599.90	0.34
13.446	1699.71	0.38

Lamp C864  
Laboratory INM

I / A	t / °C	u(t) / °C
4.933	962.08	0.13
5.236	1000.11	0.14
5.788	1064.13	0.16
5.980	1085.19	0.16
6.120	1100.26	0.17
7.107	1200.24	0.19
8.177	1300.49	0.22
9.314	1400.41	0.26
10.513	1500.50	0.30
11.767	1600.48	0.34
13.074	1700.40	0.38

**Table 24** Measurement results as sent in by NIST

Lamp C860  
Laboratory NIST

I / A	t / °C	u(t) / °C
5.380	1000.46	0.24
5.944	1064.43	0.26
6.284	1100.76	0.27
7.298	1200.85	0.31
8.398	1300.95	0.35
9.570	1401.17	0.39
10.805	1501.31	0.44
12.099	1601.60	0.49
13.446	1701.53	0.55

Lamp C864  
Laboratory NIST

I / A	t / °C	u(t) / °C
5.236	1000.31	0.24
5.788	1064.42	0.26
6.120	1100.51	0.27
7.107	1200.56	0.31
8.177	1300.73	0.35
9.314	1400.79	0.39
10.513	1500.94	0.44
11.767	1601.19	0.49
13.074	1701.19	0.55

**Table 25** Measurement results as sent in by NPL (first run, II)

Lamp C860  
Laboratory NPL1

I / A	t / °C	u(t) / °C
5.072	962.00	0.14
5.380	1000.12	0.14
5.944	1064.11	0.15
6.141	1085.21	0.15
6.284	1100.10	0.16
7.298	1200.19	0.20
8.398	1300.18	0.23
9.570	1400.25	0.28
10.805	1500.24	0.32
12.099	1600.30	0.37
13.446	1700.29	0.41

Lamp C864  
Laboratory NPL1

I / A	t / °C	u(t) / °C
4.933	962.13	0.14
5.236	1000.12	0.14
5.788	1064.11	0.15
5.980	1085.11	0.15
6.120	1100.11	0.16
7.107	1200.10	0.20
8.177	1300.18	0.23
9.314	1400.17	0.28
10.513	1500.24	0.32
11.767	1600.23	0.37
13.074	1700.30	0.41

**Table 26** Measurement results as sent in by NPL (second run, II)

Lamp C860  
Laboratory NPL2

I / A	t / °C	u(t) / °C
5.072	961.70	0.14
5.380	999.80	0.14
5.944	1063.97	0.15
6.141	1085.05	0.15
6.284	1100.06	0.16
7.298	1200.14	0.20
8.398	1300.17	0.23
9.570	1400.25	0.28
10.805	1500.33	0.32
12.099	1600.33	0.37
13.446	1700.33	0.41

Lamp C864  
Laboratory NPL2

I / A	t / °C	u(t) / °C
4.933	961.59	0.14
5.236	999.73	0.14
5.788	1063.86	0.15
5.980	1084.90	0.15
6.120	1099.95	0.16
7.107	1200.03	0.20
8.177	1300.11	0.23
9.314	1400.07	0.28
10.513	1500.20	0.32
11.767	1600.12	0.37
13.074	1700.20	0.41

**Table 27** Measurement results as sent in by NPL (third run, II)

Lamp C860  
Laboratory NPL3

I / A	t / °C	u(t) / °C
5.072	961.97	0.14
5.380	1000.00	0.14
5.944	1064.22	0.15
6.141	1085.31	0.15
6.284	1100.29	0.16
7.298	1200.25	0.20
8.398	1300.25	0.23
9.570	1400.44	0.28
10.805	1500.56	0.32
12.099	1600.67	0.37
13.446	1700.58	0.41

Lamp C864  
Laboratory NPL3

I / A	t / °C	u(t) / °C
4.933	961.77	0.14
5.236	999.82	0.14
5.788	1064.00	0.15
5.980	1085.07	0.15
6.120	1100.10	0.16
7.107	1200.05	0.20
8.177	1300.06	0.23
9.314	1400.19	0.28
10.513	1500.34	0.32
11.767	1600.34	0.37
13.074	1700.34	0.41

**Table 28** Measurement results as sent in by NRC

Lamp C860  
Laboratory NRC

I / A	t / °C	u(t) / °C
5.072	962.48	0.12
5.380	1000.49	0.12
5.944	1064.48	0.13
6.141	1085.55	0.14
6.284	1100.51	0.14
7.298	1200.46	0.16
8.398	1300.46	0.19
9.570	1399.98	0.22
10.805	1499.87	0.25
12.099	1599.68	0.28
13.446	1699.29	0.32

Lamp C864  
Laboratory NRC

I / A	t / °C	u(t) / °C
4.933	962.52	0.12
5.236	1000.48	0.12
5.788	1064.40	0.13
5.980	1085.42	0.14
6.120	1100.44	0.14
7.107	1200.35	0.16
8.177	1300.52	0.19
9.314	1400.00	0.22
10.513	1500.01	0.25
11.767	1599.89	0.28
13.074	1699.75	0.32

**Table 29** Measurement results as sent in by PTB

Lamp C860  
Laboratory PTB

I / A	t / °C	u(t) / °C
5.07	962.34	0.15
5.38	1000.28	0.16
5.94	1064.35	0.17
6.14	1085.50	0.17
6.28	1100.46	0.18
7.30	1200.62	0.19
8.40	1300.75	0.21
9.57	1400.80	0.24
10.81	1500.88	0.26
12.10	1600.98	0.29
13.45	1700.87	0.32

Lamp C864  
Laboratory PTB

I / A	t / °C	u(t) / °C
4.93	962.14	0.15
5.24	1000.08	0.16
5.79	1064.14	0.17
5.98	1085.22	0.17
6.12	1100.27	0.18
7.11	1200.49	0.19
8.18	1300.65	0.21
9.31	1400.64	0.24
10.51	1500.65	0.26
11.77	1600.63	0.29
13.07	1700.65	0.32

**Table 30** Measurement results as sent in by VSL (II)

Lamp C860  
Laboratory VSL1

I / A	t / °C	u(t) / °C
5.072	962.36	0.10
5.380	1000.40	0.10
5.944	1064.47	0.11
6.141	1085.57	0.11
6.284	1100.55	0.11
7.298	1200.63	0.12
8.398	1300.73	0.14
9.570	1400.88	0.16
10.805	1500.95	0.17
12.099	1600.96	0.19
13.446	1700.78	0.21

Lamp C864  
Laboratory VSL1

I / A	t / °C	u(t) / °C
4.933	962.15	0.10
5.236	1000.21	0.10
5.788	1064.26	0.11
5.980	1085.31	0.11
6.120	1100.34	0.11
7.107	1200.38	0.12
8.177	1300.55	0.14
9.314	1400.57	0.16
10.513	1500.66	0.17
11.767	1600.59	0.19
13.074	1700.53	0.21

Table 31 : Differences between participants within each loop at nominal temperature 961°C.

Given in each cell is the difference (top) the associated uncertainty (k=2) (round brackets) and the QDE [square brackets].

The sign of the difference with KCRV is defined as: 'column participant - KCRV'.

The sign of the difference between participants is defined as: 'row participant - column participant'.

Loop 1 : Lower left corner of the matrix.

Loop 2 : Upper right corner of the matrix.

	KCRV	NPL1	NPL2	NPL3	VSL1	NIST	NRC	CENAM	INM	IMGC	PTB	KCRV
	-0.219 (0.295) [0.461]	-0.519 (0.295) [0.761]	-0.249 (0.295) [0.491]	0.141 (0.220) [0.323]		(0.257) [0.473]	(0.440) [0.428]	(0.441) [0.428]	-0.509 (0.276) [0.736]	(0.168) [0.279]	0.141 (0.314) [0.382]	C860
	-0.029 (0.295) [0.293]	-0.569 (0.295) [0.811]	-0.389 (0.295) [0.634]	-0.009 (0.220) [0.216]		(0.247) [0.573]	(0.430) [0.500]	(0.141) [0.310]	-0.079 (0.276) [0.220]	(0.168) [0.220]	-0.019 (0.314) [0.309]	C864
VSL1	C564 -0.065 (0.220) [0.250]	(0.295) [0.293]	0.300 (0.396) [0.626]	0.030 (0.344) [0.643]		(0.369) [0.783]	(0.505) [0.676]	(0.290) [0.260]	-0.480 (0.390) [0.260]	(0.382) [0.604]	-0.340 (0.410) [0.678]	C860
VSL1	C681 0.045 (0.220) [0.233]		0.540 (0.396) [0.866]	-0.020 (0.344) [0.338]		(0.360) [0.686]	(0.505) [0.693]	(0.170) [0.591]	-0.390 (0.505) [0.338]	(0.350) [0.386]	-0.110 (0.410) [0.403]	C864
VSL2	C564 -0.095 (0.220) [0.278]		-0.030 (0.283) [0.282]	-0.270 (0.344) [0.596]		(0.366) [0.943]	(0.344) [0.660]	-0.660 (0.344) [0.943]	-0.780 (0.344) [0.943]	(0.560) [0.975]	-0.010 (0.313) [0.917]	C860
VSL2	C681 0.075 (0.220) [0.259]		0.120 (0.283) [0.354]	0.180 (0.344) [0.507]		(0.366) [0.507]	(0.366) [0.843]	0.560 (0.344) [0.843]	0.930 (0.366) [0.930]	(0.490) [0.975]	0.550 (0.410) [0.978]	C864
VSL3	C564 0.095 (0.220) [0.277]		0.160 (0.283) [0.393]	0.190 (0.283) [0.423]		(0.344) [0.673]	(0.344) [0.706]	-0.390 (0.344) [0.673]	-0.510 (0.344) [0.706]	(0.290) [0.575]	-0.390 (0.410) [0.708]	C860
VSL3	C681 0.035 (0.220) [0.227]		0.040 (0.283) [0.317]	-0.080 (0.283) [0.287]		(0.344) [0.663]	(0.344) [0.663]	-0.380 (0.344) [0.663]	-0.750 (0.344) [0.663]	(0.530) [0.945]	-0.470 (0.410) [0.708]	C864
NPL1	C564 -0.235 (0.295) [0.478]		-0.140 (0.344) [0.454]	-0.330 (0.344) [0.425]		(0.344) [0.613]	(0.344) [0.613]	-0.140 (0.344) [0.613]	-0.120 (0.344) [0.613]	(0.100) [0.593]	0.000 (0.344) [0.593]	C860
NPL1	C681 0.245 (0.295) [0.488]		-0.290 (0.344) [0.573]	-0.170 (0.344) [0.454]		(0.344) [0.731]	(0.344) [0.493]	-0.210 (0.344) [0.493]	-0.170 (0.344) [0.493]	(0.100) [0.624]	0.000 (0.344) [0.624]	C860
CSIRO	C564 -0.165 (0.101) [0.248]		-0.100 (0.204) [0.268]	-0.070 (0.204) [0.240]		(0.204) [0.428]	(0.283) [0.309]	-0.260 (0.204) [0.428]	0.070 (0.204) [0.428]	(0.100) [0.624]	0.000 (0.344) [0.624]	C860
CSIRO	C681 -0.025 (0.101) [0.110]		-0.070 (0.204) [0.240]	-0.050 (0.204) [0.222]		(0.204) [0.200]	(0.283) [0.453]	0.010 (0.204) [0.200]	0.220 (0.283) [0.453]	(0.100) [0.624]	0.000 (0.344) [0.624]	C860
KRISS	C564 -0.205 (0.202) [0.372]		-0.140 (0.289) [0.362]	-0.110 (0.289) [0.333]		(0.289) [0.521]	(0.333) [0.330]	0.030 (0.184) [0.197]	-0.040 (0.184) [0.197]	(0.220) [0.620]	0.120 (0.384) [0.459]	C860
KRISS	C681 0.105 (0.202) [0.272]		0.060 (0.269) [0.289]	0.180 (0.269) [0.402]		(0.269) [0.362]	(0.353) [0.624]	0.140 (0.184) [0.282]	0.350 (0.184) [0.282]	(0.230) [0.620]	0.040 (0.384) [0.606]	C864
NIM	C564 -0.045 (0.239) [0.250]		0.020 (0.297) [0.293]	0.050 (0.297) [0.307]		(0.297) [0.386]	(0.297) [0.304]	-0.140 (0.224) [0.484]	0.190 (0.224) [0.484]	(0.160) [0.304]	-0.100 (0.443) [0.476]	C860
NIM	C681 0.155 (0.239) [0.351]		0.110 (0.204) [0.240]	0.050 (0.204) [0.222]		(0.204) [0.200]	(0.283) [0.453]	0.010 (0.204) [0.200]	0.220 (0.283) [0.453]	(0.100) [0.624]	0.000 (0.344) [0.624]	C864
NMC	C564 -0.125 (0.314) [0.684]		-0.360 (0.361) [0.657]	-0.330 (0.361) [0.627]		(0.297) [0.435]	(0.356) [0.693]	0.140 (0.284) [0.693]	-0.190 (0.284) [0.693]	(0.220) [0.620]	0.140 (0.384) [0.591]	C860
NMC	C681 -0.535 (0.314) [0.794]		-0.580 (0.361) [0.877]	-0.460 (0.361) [0.757]		(0.299) [0.797]	(0.410) [0.628]	-0.500 (0.303) [0.628]	-0.510 (0.303) [0.759]	(0.290) [0.996]	-0.640 (0.372) [0.996]	C864
NRLM	C564 -0.045 (0.257) [0.267]		0.020 (0.312) [0.308]	0.050 (0.312) [0.321]		(0.297) [0.398]	(0.297) [0.321]	-0.140 (0.243) [0.398]	0.190 (0.243) [0.398]	(0.120) [0.321]	0.160 (0.344) [0.696]	C860
NRLM	C681 -0.065 (0.257) [0.282]		0.020 (0.312) [0.308]	0.140 (0.312) [0.398]		0.100 (0.312) [0.361]	0.310 (0.369) [0.613]	0.030 (0.243) [0.292]	-0.040 (0.300) [0.304]	-0.040 (0.326) [0.364]	-0.090 (0.334) [0.916]	C864
VNIM	C564 0.545 (0.333) [0.819]		0.610 (0.377) [0.920]	0.640 (0.377) [0.950]		0.450 (0.377) [0.760]	0.780 (0.322) [0.975]	0.710 (0.322) [0.975]	0.750 (0.439) [1.052]	0.590 (0.388) [0.909]	0.590 (0.400) [0.919]	C864
VNIM	C681 0.565 (0.333) [0.839]		0.520 (0.377) [0.830]	0.640 (0.377) [0.910]		0.600 (0.377) [0.950]	0.810 (0.425) [1.160]	0.530 (0.322) [0.855]	0.460 (0.367) [0.762]	0.410 (0.388) [0.729]	0.500 (0.449) [1.461]	C864
		KCRV	VSL1	VSL3	NPL1	CSIRO	RTRSS	NMC	NMC	NMC	NRLM	

## Lamp Properties

Lamp	Current	KCRV	$\bar{u}(KCRV)$	$\bar{u}(KCRV) \leftarrow 1$
C564	4.480	964.115	0.096	
C681	5.508	963.305	0.037	
C860	5.072	962.219	0.155	
C864	4.933	962.159	0.257	

Table 32 : Differences between participants within each loop at nominal temperature 1000°C.

Given in each cell is the difference (top) the associated uncertainty (k=2) (round brackets) and the QDE [square brackets].

The sign of the difference with KCRV is defined as: 'column participant - KCRV'.

The sign of the difference between participants is defined as : 'row participant - column participant'.

Loop 1 : Lower left corner of the matrix.

Loop 2 : Upper right corner of the matrix.

	KCRV	NPL1	NPL2	NPL3	VSL1	NIST	NRC	CENAM	INM	IMGC	PTB
	(0.291)[0.395]	(0.291)[0.715]	(0.215)[0.515]	(0.215)[0.301]	(0.486)[0.588]	(0.252)[0.422]	(0.447)[0.439]	(0.291)[0.765]	(0.178)[0.281]	(0.329)[0.324]	C860 KCRV
	(0.291)[0.722]	(0.291)[0.611]	(0.215)[0.212]	(0.486)[0.529]	(0.252)[0.495]	(0.447)[0.470]	(0.291)[0.326]	(0.178)[0.235]	(0.329)[0.387]	(0.329)[0.387]	C864 KCRV
VSL1	C564 (-0.052)	(0.291)[0.701]	(0.215)[0.611]	(0.215)[0.212]	(0.486)[0.529]	(0.252)[0.495]	(0.447)[0.470]	(0.291)[0.326]	(0.178)[0.235]	(0.329)[0.387]	C860 NPL1
VSL1	C564 (0.215)[0.233]	(0.396)[0.646]	(0.396)[0.451]	(0.344)[0.563]	(0.536)[0.798]	(0.369)[0.673]	(0.356)[0.605]	(0.356)[0.606]	(0.322)[0.555]	(0.425)[0.513]	C860 NPL1
VSL1	C681 (0.148)	(0.396)[0.716]	(0.396)[0.626]	(0.344)[0.380]	(0.556)[0.653]	(0.369)[0.663]	(0.522)[0.596]	(0.336)[0.389]	(0.322)[0.426]	(0.425)[0.422]	C864 NPL1
VSL2	C564 (-0.082)	(0.291)[0.701]	(0.215)[0.611]	(0.215)[0.212]	(0.486)[0.529]	(0.252)[0.495]	(0.447)[0.470]	(0.291)[0.326]	(0.178)[0.235]	(0.329)[0.387]	C860 NPL2
VSL2	C681 (0.215)[0.260]	(0.283)[0.282]	(0.396)[0.527]	(0.344)[0.883]	(0.536)[1.117]	(0.369)[0.993]	(0.522)[0.919]	(0.336)[0.399]	(0.322)[0.875]	(0.425)[0.830]	C864 NPL2
VSL2	C681 (0.032)	(0.283)[0.880]	(0.396)[0.390]	(0.344)[0.480]	(0.536)[0.580]	(0.369)[0.750]	(0.522)[0.550]	(0.336)[0.380]	(0.322)[0.550]	(0.425)[0.350]	C864 NPL2
VSL3	C564 (0.148)	(0.283)[0.317]	(0.396)[0.426]	(0.344)[0.763]	(0.536)[1.037]	(0.369)[1.053]	(0.522)[0.979]	(0.336)[0.706]	(0.322)[0.815]	(0.425)[0.700]	C860 NPL3
VSL3	C681 (0.132)	(0.283)[0.433]	(0.396)[0.463]	(0.344)[0.683]	(0.536)[0.917]	(0.369)[0.793]	(0.522)[0.729]	(0.336)[0.576]	(0.322)[0.675]	(0.425)[0.630]	C864 NPL3
NPL1	C564 (-0.002)	(0.291)[0.505]	(0.215)[0.294]	(0.215)[0.282]	(0.486)[0.400]	(0.252)[0.390]	(0.447)[0.390]	(0.291)[0.326]	(0.178)[0.235]	(0.329)[0.387]	C860 VSL1
NPL1	C681 (0.215)[0.212]	(0.283)[0.294]	(0.396)[0.527]	(0.344)[0.673]	(0.536)[0.947]	(0.369)[0.963]	(0.522)[0.889]	(0.336)[0.616]	(0.322)[0.725]	(0.425)[0.610]	C860 VSL1
NPL1	C564 (0.292)	(0.291)[0.200]	(0.283)[0.170]	(0.283)[0.140]	(0.486)[0.660]	(0.522)[0.521]	(0.447)[0.521]	(0.486)[0.521]	(0.450)[0.521]	(0.377)[0.455]	C860 VSL1
NPL1	C681 (0.491)	(0.344)[0.484]	(0.396)[0.454]	(0.344)[0.683]	(0.536)[0.521]	(0.369)[0.521]	(0.447)[0.521]	(0.486)[0.521]	(0.450)[0.521]	(0.377)[0.455]	C860 VSL1
CSIRO	C564 (-0.222)	(0.344)[0.270]	(0.396)[0.190]	(0.344)[0.474]	(0.344)[0.503]	(0.520)[0.500]	(0.447)[0.527]	(0.486)[0.527]	(0.450)[0.527]	(0.377)[0.444]	C860 VSL1
CSIRO	C681 (0.132)	(0.344)[0.553]	(0.396)[0.080]	(0.344)[0.531]	(0.344)[0.505]	(0.520)[0.528]	(0.557)[0.528]	(0.651)[0.719]	(0.556)[1.167]	(0.506)[1.054]	C860 NIST
CSIRO	C564 (0.088)[0.204]	(0.204)[0.249]	(0.294)[0.222]	(0.294)[0.448]	(0.294)[0.222]	(0.283)[0.354]	(0.283)[0.240]	(0.294)[0.240]	(0.294)[0.240]	(0.230)[0.230]	C864 NIST
NIM	C681 (0.018)	(0.204)[0.030]	(0.294)[0.208]	(0.294)[0.222]	(0.294)[0.203]	(0.283)[0.473]	(0.537)[0.618]	(0.651)[0.639]	(0.556)[0.662]	(0.506)[0.498]	C860 NIST
KRISS	C564 (-0.152)	(0.204)[0.208]	(0.294)[0.208]	(0.294)[0.222]	(0.294)[0.203]	(0.283)[0.473]	(0.537)[0.618]	(0.651)[0.639]	(0.556)[0.662]	(0.506)[0.498]	C860 NRC
KRISS	C681 (0.196)[0.313]	(0.289)[0.323]	(0.289)[0.297]	(0.289)[0.521]	(0.333)[0.379]	(0.184)[0.184]	(0.220)[0.220]	(0.369)[0.393]	(0.344)[0.393]	(0.256)[0.255]	C864 NRC
NIM	C564 (-0.032)	(0.060)	(0.269)[0.289]	(0.269)[0.362]	(0.269)[0.333]	(0.333)[0.604]	(0.184)[0.242]	(0.220)[0.220]	(0.170)[0.220]	(0.180)[0.220]	C860 NIST
NIM	C681 (0.252)[0.254]	(0.312)[0.308]	(0.312)[0.321]	(0.312)[0.437]	(0.312)[0.321]	(0.369)[0.524]	(0.243)[0.302]	(0.300)[0.339]	(0.243)[0.339]	(0.230)[0.339]	C864 NIST
NIM	C681 (0.208)	(0.160)	(0.240)	(0.240)	(0.240)	(0.430)	(0.190)	(0.120)	(0.170)	(0.120)	C860 NIST
NMC	C564 (0.452)	(0.312)[0.418]	(0.312)[0.467]	(0.312)[0.467]	(0.312)[0.467]	(0.369)[0.733]	(0.184)[0.184]	(0.220)[0.220]	(0.170)[0.220]	(0.180)[0.220]	C860 NRC
NMC	C681 (0.552)	(0.361)[0.697]	(0.361)[0.667]	(0.361)[0.697]	(0.361)[0.697]	(0.410)[0.539]	(0.303)[0.569]	(0.330)[0.588]	(0.334)[0.736]	(0.322)[0.925]	C864 NRC
NRLM	C564 (-0.002)	(0.310)[0.806]	(0.361)[0.897]	(0.361)[0.847]	(0.410)[0.668]	(0.303)[0.819]	(0.350)[0.948]	(0.350)[1.076]	(0.344)[1.076]	(0.425)[0.419]	C860 CENAM
NRLM	C681 (0.252)[0.249]	(0.312)[0.321]	(0.312)[0.343]	(0.312)[0.408]	(0.312)[0.343]	(0.369)[0.554]	(0.243)[0.331]	(0.300)[0.350]	(0.252)[0.462]	(0.354)[0.632]	C864 CENAM
NRLM	C681 (0.108)	(0.060)	(0.140)	(0.140)	(0.140)	(0.370)	(0.200)	(0.320)	(0.290)	(0.360)	C860 INM
VNIM	C564 (0.438)	(0.312)[0.328]	(0.312)[0.398]	(0.312)[0.370]	(0.369)[0.633]	(0.243)[0.292]	(0.339)[0.296]	(0.339)[0.384]	(0.339)[0.384]	(0.358)[0.495]	C864 IMGC
VNIM	C564 (0.329)[0.709]	(0.377)[0.800]	(0.377)[0.830]	(0.377)[0.604]	(0.425)[0.1040]	(0.322)[0.835]	(0.367)[0.892]	(0.400)[0.799]	(0.400)[0.799]	(0.358)[0.495]	C864 IMGC
VNIM	C681 (0.228)	(0.180)	(0.260)	(0.230)	(0.230)	(0.450)	(0.210)	(0.120)	(0.120)	(0.120)	C860 INM
VNIM	C681 (0.329)[0.500]	(0.377)[0.492]	(0.377)[0.571]	(0.377)[0.541]	(0.425)[0.800]	(0.322)[0.426]	(0.367)[0.426]	(0.400)[0.393]	(0.400)[0.393]	(0.400)[0.455]	NRLM
						NPL1	CSIRO	VSL3	RTRSS	NMC	

### Lamp Properties

Lamp	Current	KCRV	$u(KCRV)$	$k=1$
C564	4.721	1002.130	0.117	
C681	5.822	1001.760	0.058	
C860	5.380	1000.280	0.151	
C864	5.236	1000.190	0.191	

Table 33 : Differences between participants within each loop at nominal temperature 1064°C.

Given in each cell is the difference (top) the associated uncertainty (k=2) (round brackets) and the QDE [square brackets].

The sign of the difference with KCRV is defined as: 'column participant - KCRV'.

The sign of the difference between participants is defined as: 'row participant - column participant'.

**Loop 1 :** Lower left corner of the matrix.

**Loop 2 :** Upper right corner of the matrix.

	KCRV	NPL1	NPL2	NPL3	VSL1	NIST	NRC	CENAM	INM	IMGC	PTB	
	-0.236 (0.324)	-0.376 (0.503)	-0.124 (0.324)	-0.126 (0.395)	0.124 (0.252)	0.084 (0.534)	0.134 (0.287)	0.094 (0.515)	-0.526 (0.342)	0.174 (0.201)	0.004 (0.339)	C860
	-0.126 (0.324)	-0.376 (0.395)	-0.236 (0.324)	-0.236 (0.503)	0.024 (0.252)	0.184 (0.534)	0.164 (0.287)	0.114 (0.515)	-0.106 (0.342)	0.084 (0.201)	-0.096 (0.250)	C864
VSL1	-0.085 (0.252)	0.140 (0.424)	-0.110 (0.468)	-0.110 (0.468)	-0.360 (0.628)	-0.320 (0.400)	-0.370 (0.400)	-0.410 (0.551)	-0.240 (0.392)	-0.410 (0.392)	-0.240 (0.400)	C860
VSL1	0.019 (0.252)	0.250 (0.424)	0.110 (0.600)	0.110 (0.468)	0.666 (0.628)	0.815 (0.400)	0.666 (0.628)	0.815 (0.400)	0.240 (0.392)	0.630 (0.392)	0.210 (0.400)	C860
VSL2	-0.105 (0.252)	-0.020 (0.311)	-0.105 (0.306)	-0.105 (0.600)	-0.150 (0.806)	-0.150 (0.954)	-0.150 (0.806)	-0.150 (0.954)	-0.500 (0.553)	-0.720 (0.553)	-0.500 (0.447)	C864
VSL2	0.061 (0.252)	0.080 (0.311)	0.140 (0.342)	0.140 (0.494)	0.400 (0.706)	0.560 (0.867)	0.540 (0.867)	0.490 (0.954)	-0.330 (0.533)	-0.330 (0.631)	-0.330 (0.740)	NPL1
VSL3	0.115 (0.252)	0.220 (0.323)	0.200 (0.456)	0.200 (0.456)	0.746 (0.556)	0.710 (0.587)	0.746 (0.556)	0.710 (0.587)	-0.260 (0.533)	-0.260 (0.761)	-0.300 (0.580)	C860
VSL3	-0.031 (0.252)	-0.050 (0.253)	-0.030 (0.326)	-0.030 (0.326)	-0.350 (0.566)	-0.400 (0.727)	-0.350 (0.566)	-0.400 (0.727)	-0.350 (0.533)	-0.320 (0.497)	-0.340 (0.510)	C864
NPL1	0.564 (0.324)	-0.185 (0.454)	-0.100 (0.413)	-0.100 (0.413)	-0.300 (0.606)	0.040 (0.557)	-0.100 (0.537)	0.030 (0.537)	-0.050 (0.533)	-0.050 (0.631)	-0.050 (0.633)	C864
NPL1	-0.111 (0.324)	-0.130 (0.381)	-0.050 (0.440)	-0.050 (0.440)	-0.250 (0.397)	-0.210 (0.422)	-0.250 (0.422)	-0.210 (0.422)	-0.220 (0.533)	-0.220 (0.761)	-0.300 (0.580)	NPL3
CSIRO	0.125 (0.128)	-0.040 (0.230)	-0.040 (0.233)	-0.040 (0.233)	-0.240 (0.222)	0.060 (0.319)	-0.260 (0.319)	0.060 (0.319)	-0.400 (0.533)	-0.400 (0.761)	-0.320 (0.580)	C864
CSIRO	0.049 (0.128)	0.030 (0.155)	0.030 (0.226)	0.030 (0.226)	0.110 (0.295)	0.080 (0.410)	0.110 (0.410)	0.080 (0.410)	-0.100 (0.581)	-0.100 (0.497)	-0.130 (0.519)	C864
KRISS	-0.145 (0.234)	-0.060 (0.337)	-0.040 (0.314)	-0.040 (0.314)	-0.260 (0.505)	-0.040 (0.203)	-0.260 (0.203)	-0.040 (0.203)	-0.020 (0.563)	-0.020 (0.631)	-0.050 (0.459)	C860
KRISS	0.159 (0.234)	0.140 (0.352)	0.220 (0.386)	0.220 (0.465)	0.190 (0.435)	0.270 (0.567)	0.190 (0.435)	0.110 (0.435)	0.100 (0.563)	0.100 (0.631)	-0.060 (0.459)	NRC
NIM												CENAM
NIM												CENAM
NMC	-0.465 (0.342)	-0.380 (0.746)	-0.360 (0.699)	-0.360 (0.679)	-0.580 (0.899)	-0.280 (0.641)	-0.340 (0.641)	-0.340 (0.641)	-0.320 (0.630)	-0.320 (0.630)	-0.400 (0.530)	C860
NMC	-0.611 (0.342)	-0.630 (0.893)	-0.550 (0.949)	-0.550 (0.869)	-0.580 (0.899)	-0.500 (0.861)	-0.660 (0.861)	-0.500 (0.861)	-0.770 (0.860)	-0.770 (0.860)	-0.600 (0.459)	C864
NRLM	0.015 (0.287)	0.100 (0.282)	0.120 (0.341)	0.120 (0.341)	-0.100 (0.385)	-0.100 (0.385)	-0.100 (0.385)	-0.100 (0.385)	0.140 (0.357)	0.160 (0.357)	0.170 (0.459)	C860
NRLM	0.109 (0.287)	0.090 (0.347)	0.170 (0.377)	0.170 (0.451)	0.422 (0.422)	0.439 (0.547)	0.422 (0.547)	0.439 (0.547)	-0.220 (0.283)	-0.220 (0.336)	-0.400 (0.459)	IMGC
VNIM	0.035 (0.342)	0.120 (0.341)	0.445 (0.463)	0.445 (0.463)	-0.080 (0.411)	0.388 (0.582)	0.220 (0.426)	0.180 (0.426)	0.220 (0.377)	0.180 (0.492)	0.020 (0.405)	C864
VNIM	-0.221 (0.342)	-0.240 (0.503)	-0.160 (0.560)	-0.160 (0.560)	-0.190 (0.511)	-0.110 (0.480)	-0.270 (0.535)	-0.380 (0.535)	-0.110 (0.690)	-0.330 (0.690)	-0.330 (0.690)	NRLM
												NMC

### Lamp Properties

Lamp	Current	KCRV	u(KCRV)	k=1
C564	5.169	1066.290	0.114	
C681	6.399	1066.110	0.038	
C860	5.944	1064.350	0.117	
C864	5.788	1064.240	0.117	

Table 34 : Differences between participants within each loop at nominal temperature 1084°C.

Given in each cell is the difference (top) the associated uncertainty (k=2) (round brackets) and the QDE [square brackets].

The sign of the difference with KCRV is defined as: 'column participant - KCRV'.

The sign of the difference between participants is defined as: 'row participant - column participant'.

Loop 1 : Lower left corner of the matrix.  
 Loop 2 : Upper right corner of the matrix.

	KCRV	NPL1	NPL2	NPL3	VSL1	NIST	NRC	CENAM	INM	IMGC	PTB
	-0.233 (0.321)	-0.393 (0.497)	-0.133 (0.321)	-0.127 (0.398)	0.127 (0.248)	0.107 (0.332)	0.077 (0.340)	-0.523 (0.542)	0.167 (0.213)	0.057 (0.349)	C860 KCRV
	-0.169 (0.321)	-0.377 (0.434)	-0.209 (0.643)	-0.031 (0.473)	0.248 (0.248)	0.141 (0.391)	0.121 (0.552)	-0.089 (0.573)	0.081 (0.213)	-0.059 (0.349)	C864 KCRV
VSL1	C564 (0.248)	-0.068 (0.276)	0.160 (0.512)	-0.100 (0.459)	-0.360 (0.666)	-0.340 (0.678)	-0.340 (0.410)	-0.400 (0.600)	-0.081 (0.305)	-0.059 (0.350)	C860 NPL1
VSL1	C681 (0.248)	0.042 (0.256)	0.210 (0.560)	0.040 (0.422)	-0.200 (0.507)	-0.310 (0.410)	-0.290 (0.600)	-0.250 (0.600)	-0.100 (0.439)	-0.110 (0.453)	C864 NPL1
VSL2	C564 (0.248)	-0.078 (0.285)	-0.010 (0.305)	-0.260 (0.609)	-0.520 (0.826)	-0.500 (0.372)	-0.470 (0.410)	-0.560 (0.600)	-0.450 (0.453)	-0.450 (0.453)	C860 NPL2
VSL2	C681 (0.248)	0.038 (0.254)	0.080 (0.342)	0.170 (0.522)	0.410 (0.716)	0.520 (0.372)	0.520 (0.410)	0.500 (0.600)	0.460 (0.555)	0.320 (0.555)	C864 NPL2
VSL3	C564 (0.248)	0.132 (0.336)	0.210 (0.466)	0.210 (0.311)	-0.260 (0.566)	-0.240 (0.372)	-0.240 (0.410)	-0.240 (0.600)	-0.300 (0.550)	-0.190 (0.453)	C860 NPL3
VSL3	C681 (0.248)	-0.018 (0.244)	-0.060 (0.327)	0.020 (0.306)	-0.240 (0.546)	-0.350 (0.372)	-0.330 (0.410)	-0.300 (0.600)	-0.290 (0.550)	-0.150 (0.453)	C864 NPL3
NPL1	C564 (0.321)	-0.198 (0.462)	-0.130 (0.449)	-0.120 (0.430)	-0.330 (0.636)	-0.400 (0.372)	-0.400 (0.372)	-0.400 (0.565)	-0.400 (0.560)	-0.400 (0.565)	C860 VSL1
NPL1	C681 (0.321)	-0.138 (0.404)	-0.180 (0.487)	-0.100 (0.413)	-0.120 (0.430)	-0.110 (0.372)	-0.110 (0.372)	-0.110 (0.565)	-0.090 (0.560)	-0.090 (0.565)	C864 VSL1
CSIRO	C564 (0.121)	-0.098 (0.197)	-0.030 (0.226)	-0.020 (0.222)	-0.230 (0.224)	-0.100 (0.414)	-0.100 (0.303)	-0.100 (0.565)	-0.120 (0.560)	-0.090 (0.565)	C864 VSL1
CSIRO	C681 (0.121)	0.072 (0.171)	0.030 (0.224)	0.030 (0.226)	0.090 (0.295)	0.210 (0.275)	0.210 (0.303)	0.210 (0.565)	0.284 (0.560)	0.284 (0.565)	C864 VSL1
KRISS	C564 (0.196)	-0.108 (0.270)	-0.040 (0.277)	-0.030 (0.272)	-0.240 (0.464)	-0.090 (0.376)	-0.010 (0.165)	-0.060 (0.162)	-0.050 (0.980)	-0.050 (0.980)	NIST
KRISS	C681 (0.196)	0.162 (0.323)	0.120 (0.345)	0.200 (0.424)	0.180 (0.404)	0.300 (0.340)	0.090 (0.580)	0.090 (0.226)	0.230 (0.580)	0.200 (0.580)	NIST
NIM											NIST
NIM											NIST
NMC	C564 (0.340)	-0.488 (0.677)	-0.420 (0.739)	-0.410 (0.729)	-0.620 (0.939)	-0.290 (0.439)	-0.390 (0.655)	-0.380 (0.358)	-0.630 (0.980)	-0.050 (0.347)	C860 NRC
NMC	C681 (0.340)	-0.638 (0.917)	-0.680 (0.999)	-0.600 (0.919)	-0.920 (0.938)	-0.500 (0.439)	-0.800 (0.861)	-0.800 (0.975)	-0.710 (0.358)	-0.347 (0.347)	C864 NRC
NRLM	C564 (0.284)	0.052 (0.296)	0.120 (0.403)	0.130 (0.341)	-0.080 (0.413)	0.250 (0.341)	0.160 (0.369)	0.160 (0.263)	0.540 (0.367)	-0.090 (0.581)	C860 CENAM
NRLM	C681 (0.284)	0.142 (0.376)	0.100 (0.385)	0.180 (0.441)	0.160 (0.341)	0.280 (0.397)	0.120 (0.577)	0.120 (0.345)	0.879 (0.412)	0.040 (0.621)	C864 CENAM
VNIM	C564 (0.397)	-0.008 (0.390)	0.060 (0.445)	0.070 (0.451)	-0.140 (0.507)	-0.280 (0.484)	-0.280 (0.592)	-0.280 (0.412)	-0.200 (0.780)	-0.060 (0.467)	INM
VNIM	C681 (0.397)	0.198 (0.526)	-0.010 (0.602)	-0.240 (0.439)	-0.160 (0.525)	-0.180 (0.439)	-0.060 (0.544)	-0.060 (0.484)	-0.270 (0.584)	-0.340 (0.412)	INM
											NRLM
											NRLM
											NRLM

### Lamp Properties

Lamp	Current	KCRV	u(KCRV)	k=1
C564	5.322	1086.670	0.111	
C681	6.594	1086.480	0.039	
C860	6.141	1085.440	0.123	
C864	5.980	1085.280	0.104	

Table 35 : Differences between participants within each loop at nominal temperature 1100°C.  
 Given in each cell is the difference (top) the associated uncertainty (k=2) (round brackets) and the QDE [square brackets].  
 The sign of the difference with KCRV is defined as: 'column participant - KCRV'.

The sign of the difference between participants is defined as : 'row participant - column participant'.  
 Loop 1 : Lower left corner of the matrix.  
 Loop 2 : Upper right corner of the matrix.

	KCRV	NPL1	NPL2	NPL3	VSL1	NIST	NRC	CENAM	INM	IMGC	PTB	
	(0.338) [0.626]	(0.338) [0.666]	(0.338) [0.438]	(0.245) [0.305]	(0.330) [0.318]	(0.330) [0.092]	(0.337) [0.548]	(0.531) [0.528]	(0.357) [0.842]	(0.210) [0.324]	(0.376) [0.369]	C860
	(0.338) [0.529]	(0.338) [0.689]	(0.338) [0.530]	(0.245) [0.241]	(0.330) [0.629]	(0.330) [0.088]	(0.531) [0.548]	(0.337) [0.393]	(0.357) [0.393]	(0.210) [0.226]	(0.376) [0.402]	C864
VSL1	C564 -0.069	(0.245) [0.275]	(0.338) [0.449]	(0.453) [0.565]	(0.338) [0.769]	(0.628) [1.176]	(0.425) [0.766]	(0.611) [0.903]	(0.467) [0.586]	(0.367) [0.802]	(0.482) [0.756]	C860
VSL1	C681 0.035	(0.245) [0.249]	(0.338) [0.536]	(0.453) [0.445]	(0.338) [0.550]	(0.628) [0.917]	(0.425) [0.680]	(0.611) [0.833]	(0.467) [0.540]	(0.367) [0.592]	(0.482) [0.562]	C864
VSL2	C564 -0.089	(0.245) [0.293]	(0.331) [0.306]	(0.453) [0.603]	(0.338) [0.809]	(0.628) [1.216]	(0.425) [0.800]	(0.611) [0.942]	(0.467) [0.549]	(0.367) [0.842]	(0.482) [0.796]	C860
VSL2	C681 0.045	(0.245) [0.256]	(0.331) [0.342]	(0.453) [0.527]	(0.338) [0.709]	(0.628) [1.076]	(0.425) [0.840]	(0.611) [0.992]	(0.467) [0.694]	(0.367) [0.732]	(0.482) [0.717]	C864
VSL3	C564 0.111	(0.245) [0.314]	(0.331) [0.436]	(0.311) [0.456]	(0.338) [0.580]	(0.628) [0.987]	(0.425) [0.571]	(0.611) [0.718]	(0.467) [0.774]	(0.367) [0.612]	(0.482) [0.571]	C860
VSL3	C681 -0.035	(0.245) [0.250]	(0.331) [0.334]	(0.311) [0.305]	(0.338) [0.560]	(0.628) [0.927]	(0.425) [0.690]	(0.611) [0.843]	(0.467) [0.549]	(0.367) [0.602]	(0.482) [0.571]	C864
NPL1	C564 -0.259	(0.338) [0.537]	(0.338) [0.511]	(0.338) [0.491]	(0.338) [0.689]	(0.583) [0.695]	(0.336) [0.357]	(0.565) [0.560]	(0.405) [0.983]	(0.405) [0.450]	(0.422) [0.495]	C860
NPL1	C681 -0.215	(0.338) [0.494]	(0.338) [0.570]	(0.338) [0.491]	(0.338) [0.501]	(0.583) [0.659]	(0.336) [0.357]	(0.565) [0.587]	(0.405) [0.427]	(0.405) [0.380]	(0.422) [0.435]	C864
CSIRO	C564 -0.099	(0.116) [0.194]	(0.224) [0.226]	(0.224) [0.220]	(0.224) [0.394]	(0.322) [0.426]	(0.250)	(0.608) [0.754]	(0.750) [0.884]	(0.860)	(0.300)	C860
CSIRO	C681 0.075	(0.116) [0.170]	(0.224) [0.233]	(0.224) [0.304]	(0.224) [0.295]	(0.322) [0.555]	(0.240)	(0.608) [0.610]	(0.750) [0.745]	(0.860)	(0.300)	C860
KRIS	C564 -0.109	(0.227) [0.297]	(0.297) [0.301]	(0.297) [0.293]	(0.297) [0.465]	(0.377) [0.463]	(0.204)	(0.283) [0.581]	(0.440) [0.972]	(0.333) [0.370]	(0.456) [0.456]	C864
KRIS	C681 0.125	(0.227) [0.312]	(0.297) [0.339]	(0.297) [0.415]	(0.297) [0.405]	(0.377) [0.656]	(0.204)	(0.283) [0.582]	(0.440) [0.545]	(0.333) [0.335]	(0.456) [0.549]	C864
NIM	C564 0.001	(0.300) [0.296]	(0.356) [0.375]	(0.356) [0.390]	(0.356) [0.408]	(0.425) [0.610]	(0.230)	(0.283) [0.335]	(0.344) [0.397]	(0.621) [1.111]	(0.550) [0.573]	C860
NIM	C681 0.315	(0.300) [0.296]	(0.356) [0.375]	(0.356) [0.390]	(0.356) [0.408]	(0.425) [0.610]	(0.230)	(0.283) [0.335]	(0.344) [0.397]	(0.621) [1.111]	(0.550) [0.573]	C864
NMC	C564 -0.509	(0.300) [0.562]	(0.336) [0.573]	(0.336) [0.653]	(0.336) [0.643]	(0.425) [0.889]	(0.233)	(0.283) [0.473]	(0.344) [0.474]	(0.621) [0.701]	(0.550) [0.543]	C860
NMC	C681 -0.645	(0.300) [0.562]	(0.338) [0.787]	(0.338) [0.759]	(0.338) [0.739]	(0.453) [0.623]	(0.322)	(0.410)	(0.510)	(0.620)	(0.560)	C860
NRLM	C564 0.051	(0.282) [0.294]	(0.341) [0.403]	(0.341) [0.422]	(0.341) [0.354]	(0.412) [0.649]	(0.263)	(0.323) [0.473]	(0.344) [0.474]	(0.621) [0.701]	(0.550) [0.543]	C860
NRLM	C681 0.155	(0.282) [0.294]	(0.341) [0.403]	(0.341) [0.481]	(0.341) [0.471]	(0.412) [0.709]	(0.263)	(0.323) [0.675]	(0.377) [0.710]	(0.425) [0.860]	(0.585) [0.700]	C864
VNIM	C564 -0.149	(0.282) [0.387]	(0.341) [0.403]	(0.341) [0.480]	(0.341) [0.460]	(0.411) [0.610]	(0.260)	(0.322) [0.623]	(0.377) [0.670]	(0.425) [0.770]	(0.585) [0.700]	C864
VNIM	C681 -0.245	(0.434) [0.510]	(0.474) [0.490]	(0.474) [0.478]	(0.474) [0.651]	(0.528) [0.560]	(0.422)	(0.422) [0.424]	(0.465) [0.461]	(0.505) [0.573]	(0.495) [0.609]	C864
VNIM	C681 -0.349	(0.434) [0.603]	(0.474) [0.671]	(0.474) [0.593]	(0.474) [0.602]	(0.528) [0.519]	(0.422)	(0.422) [0.667]	(0.465) [0.753]	(0.505) [0.975]	(0.528) [0.834]	NRLM
						NPL1	CSTO	VSL3	RUTS	NIM	NMC	

## Lamp Properties

Lamp	Current	KCRV	u(KCRV)	k=1
C564	5.441	1102.110	0.103	
C681	6.745	1101.890	0.041	
C860	6.284	1100.450	0.115	
C864	6.120	1100.350	0.084	

Table 36 : Differences between participants within each loop at nominal temperature 1200°C.  
 Given in each cell is the difference (top) the associated uncertainty (k=2) (round brackets) and the QDE [square brackets].  
 The sign of the difference with KCRV is defined as: 'column participant - KCRV'.  
 The sign of the difference between participants is defined as: 'row participant - column participant'.

Loop 1 : Lower left corner of the matrix.  
 Loop 2 : Upper right corner of the matrix.

	KCRV	NPL1	NPL2	NPL3	VSL1	NIST	NRC	CENAM	INM	IMGC	PTB
VSL1	(0.410) [0.736]	(0.410) [0.786]	(0.410) [0.676]	(0.410) [0.743]	(0.405) [-0.425]	(0.257) [0.264]	(0.627) [0.780]	(0.333) [0.405]	(0.627) [0.615]	(0.331) [0.960]	(0.031) [0.264]
C564	(0.410) [0.693]	(0.410) [0.763]	(0.410) [0.561]	(0.410) [0.565]	(0.355) [-0.75]	(0.247) [0.290]	(0.627) [0.647]	(0.333) [0.383]	(0.627) [0.616]	(0.331) [0.537]	(0.015) [0.217]
C681	(0.257) [0.318]	(0.257) [0.252]	(0.257) [0.125]	(0.339) [0.334]	(0.355) [-0.205]	(0.356) [0.561]	(0.466) [0.824]	(0.758) [1.267]	(0.512) [0.693]	(0.758) [0.979]	(0.447) [0.848]
VSL2	(0.257) [0.337]	(0.257) [0.185]	(0.339) [0.080]	(0.339) [0.334]	(0.366) [0.595]	(0.466) [0.874]	(0.758) [1.068]	(0.512) [0.664]	(0.758) [1.068]	(0.512) [0.699]	(0.447) [0.738]
VSL2	(0.257) [0.299]	(0.257) [0.266]	(0.150) [0.045]	(0.339) [0.367]	(0.566) [0.561]	(0.466) [0.75]	(0.758) [1.068]	(0.512) [0.640]	(0.758) [1.020]	(0.512) [0.680]	(0.447) [0.844]
VSL3	(0.257) [0.195]	(0.257) [0.308]	(0.339) [0.431]	(0.339) [0.450]	(0.339) [0.090]	(0.466) [0.764]	(0.758) [1.207]	(0.512) [0.634]	(0.758) [0.921]	(0.512) [0.755]	(0.447) [0.758]
VSL3	(0.257) [0.195]	(0.257) [0.308]	(0.339) [0.376]	(0.339) [0.333]	(0.339) [0.260]	(0.466) [0.714]	(0.758) [1.117]	(0.512) [0.722]	(0.758) [1.048]	(0.512) [0.649]	(0.447) [0.758]
NPL1	(0.410) [0.722]	(0.410) [0.664]	(0.410) [0.645]	(0.410) [0.814]	(0.410) [0.220]	(0.605) [0.744]	(0.627) [0.742]	(0.530) [0.530]	(0.620) [0.740]	(0.530) [0.668]	(0.460) [0.460]
NPL1	(0.410) [0.315]	(0.410) [0.653]	(0.410) [0.694]	(0.410) [0.615]	(0.310) [-0.230]	(0.466) [0.605]	(0.600) [-0.600]	(0.210) [0.210]	(0.420) [-0.210]	(0.300) [0.300]	(0.552) [0.914]
CSIRO	(0.100) [0.095]	(0.100) [0.177]	(0.010) [0.100]	(0.243) [0.239]	(0.243) [0.245]	(0.030) [-0.140]	(0.290) [0.243]	(0.402) [0.621]	(0.330) [-0.510]	(0.210) [0.200]	(0.420) [-0.420]
CSIRO	(0.100) [0.045]	(0.100) [0.127]	(0.243) [0.258]	(0.243) [0.331]	(0.130) [0.130]	(0.140) [0.341]	(0.360) [0.402]	(0.220) [0.691]	(0.220) [-0.220]	(0.170) [0.170]	(0.040) [-0.040]
KRISS	(0.257) [0.318]	(0.339) [0.335]	(0.339) [0.334]	(0.339) [0.431]	(0.310) [-0.150]	(0.466) [0.644]	(0.466) [0.664]	(0.280) [-0.010]	(0.600) [0.734]	(0.400) [0.501]	(0.680) [0.680]
KRISS	(0.257) [0.318]	(0.339) [0.393]	(0.339) [0.470]	(0.339) [0.480]	(0.110) [0.190]	(0.220) [0.200]	(0.420) [0.420]	(0.510) [-0.180]	(0.395) [0.739]	(0.400) [0.395]	(0.310) [-0.310]
NIM	(0.333) [0.374]	(0.333) [0.265]	(0.400) [0.393]	(0.400) [0.395]	(0.010) [0.030]	(0.140) [0.130]	(0.290) [0.243]	(0.400) [0.621]	(0.030) [0.318]	(0.668) [0.965]	(0.490) [0.490]
NIM	(0.333) [0.539]	(0.400) [0.599]	(0.400) [0.679]	(0.339) [0.431]	(0.020) [0.020]	(0.050) [0.050]	(0.239) [0.239]	(0.466) [0.664]	(0.030) [0.318]	(0.665) [0.685]	(0.449) [0.449]
NMC	(0.371) [0.910]	(0.433) [0.856]	(0.433) [0.836]	(0.433) [0.1006]	(-0.500) [-0.480]	(-0.050) [-0.050]	(0.420) [0.420]	(0.510) [-0.180]	(0.395) [0.736]	(0.390) [0.900]	(0.312) [0.352]
NMC	(0.371) [1.110]	(0.433) [1.156]	(0.433) [1.076]	(0.433) [1.066]	(-0.720) [-0.710]	(-0.140) [-0.140]	(0.290) [0.290]	(0.433) [0.266]	(0.000) [0.000]	(0.877) [1.021]	(0.180) [0.180]
NRLM	(0.314) [0.349]	(0.384) [0.507]	(0.384) [0.527]	(0.384) [0.383]	(0.270) [0.350]	(0.190) [0.210]	(0.470) [0.512]	(0.580) [0.712]	(0.320) [0.318]	(0.638) [0.794]	(0.070) [0.070]
NRLM	(0.314) [0.205]	(0.384) [0.527]	(0.384) [0.606]	(0.384) [0.616]	(0.210) [0.300]	(0.050) [0.050]	(0.280) [0.280]	(0.510) [-0.010]	(0.400) [0.492]	(0.638) [0.710]	(0.497) [0.521]
VNIM	(0.636) [0.990]	(0.721) [0.916]	(0.721) [0.897]	(0.721) [1.064]	(-0.320) [-0.300]	(-0.470) [-0.460]	(0.339) [0.804]	(0.466) [0.804]	(-0.490) [0.532]	(0.658) [0.933]	(0.449) [0.490]
VNIM	(0.636) [1.030]	(0.721) [1.054]	(0.721) [0.975]	(0.721) [0.965]	(-0.460) [-0.370]	(-0.510) [-0.490]	(0.400) [0.473]	(0.440) [0.393]	(-0.490) [0.393]	(0.631) [0.951]	(0.330) [0.330]
RKRV							VSL1	NPL1	NPL1	NPL1	NPL1
							VSL1	VSL1	VSL1	VSL1	VSL1
							CSIRO	CSIRO	CSIRO	CSIRO	CSIRO

### Lamp Properties

Lamp	Current	KCRV	$u(KCRV)$	$u(KCRV)$ k=1
C564	6.2272	1202.020	0.087	
C681	7.795	1202.050	0.046	
C860	7.298	1200.590	0.052	
C864	7.107	1200.460	0.034	

































Figure 12 : Loop 1, difference from KCRV for participant VSL1 , star/dashed : lamp C564, plus/solid : C681

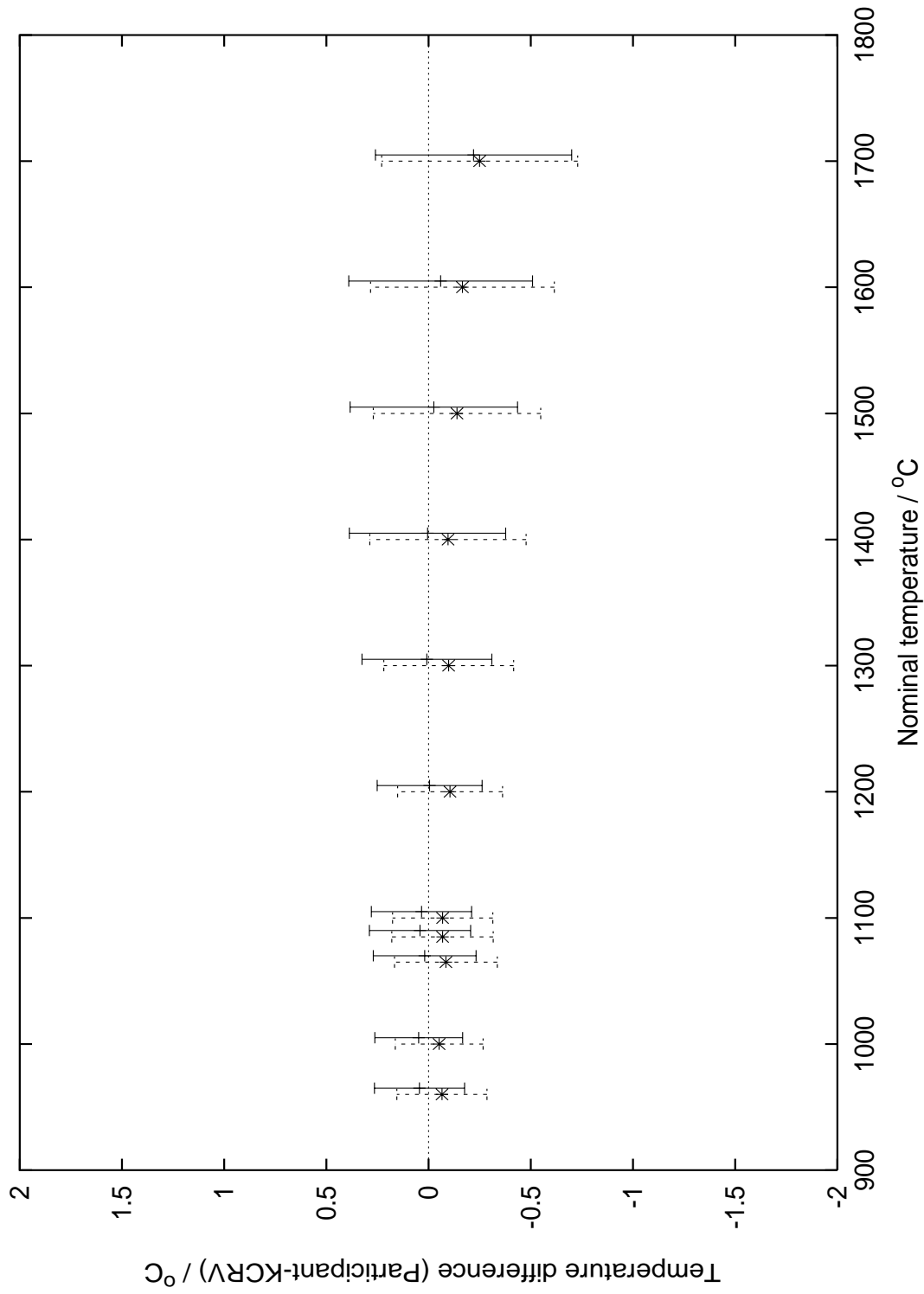


Figure 13 : Loop 1, difference from KCRV for participant VSL2 , star/dashed : lamp C564, plus/solid : C681

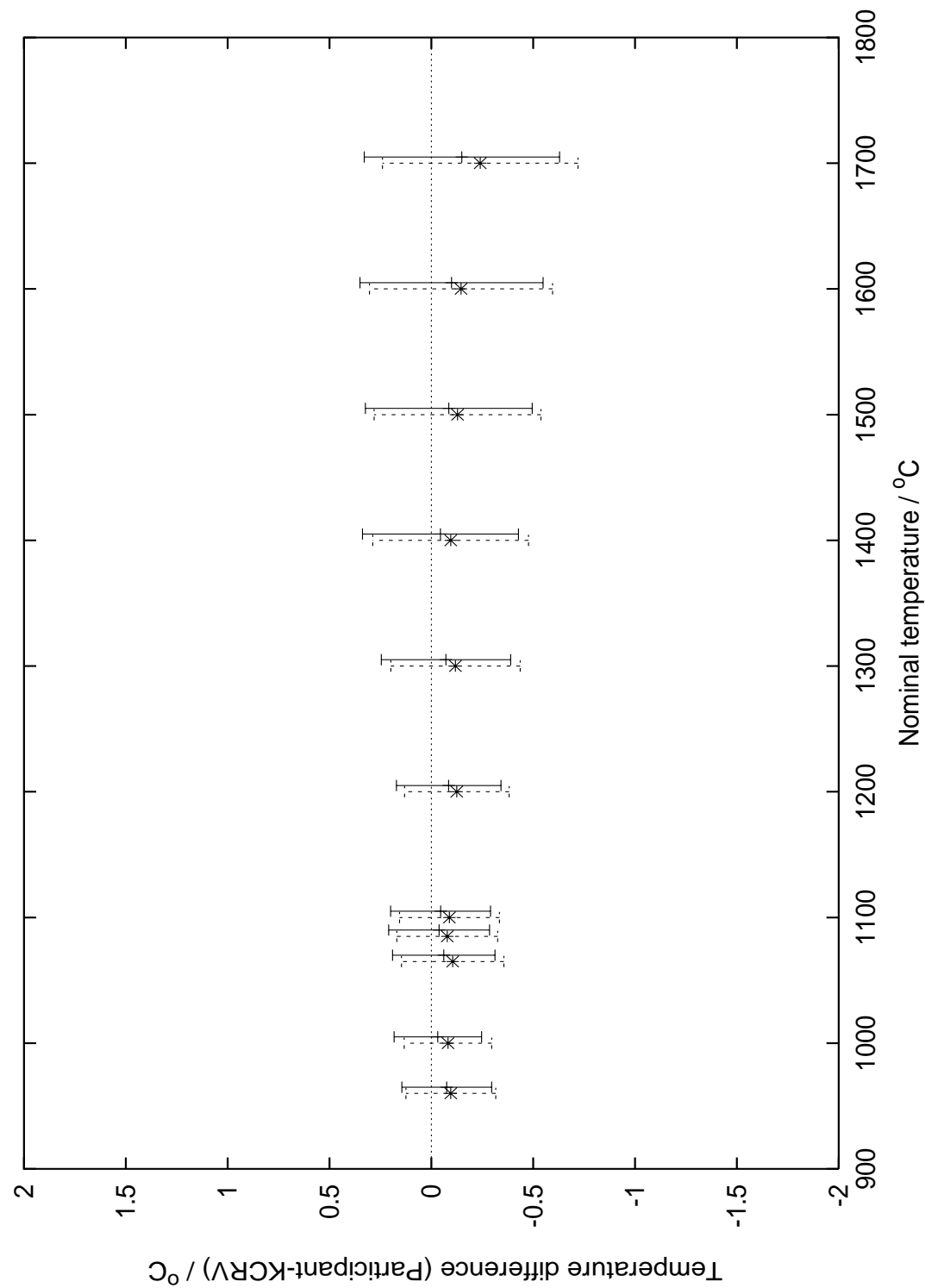


Figure 14 : Loop 1, difference from KCRV for participant VSL3 , star/dashed : lamp C564, plus/solid : C681

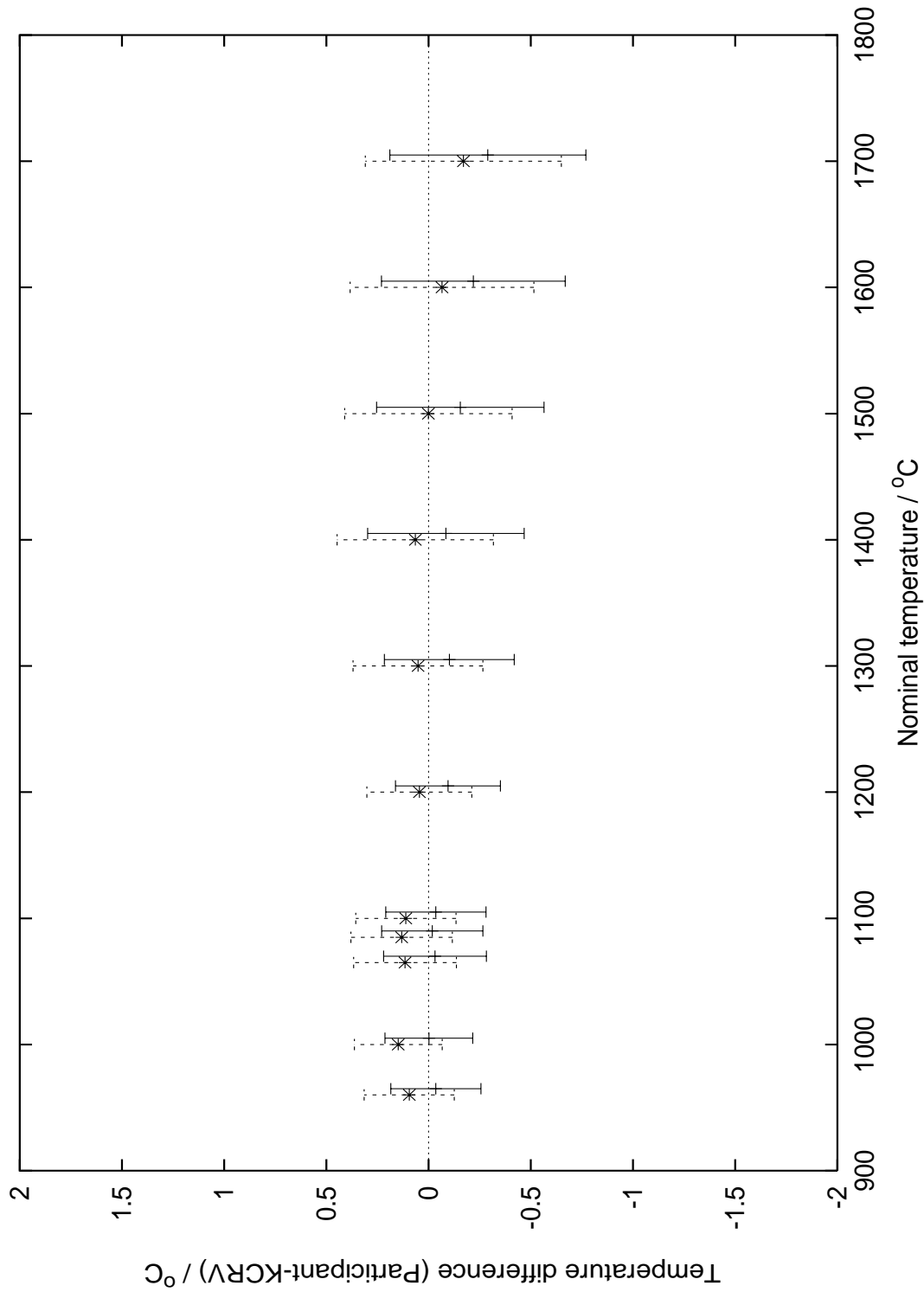


Figure 15 : Loop 1, difference from KCRV for participant NPL1 , star/dashed : lamp C564, plus/solid : C681

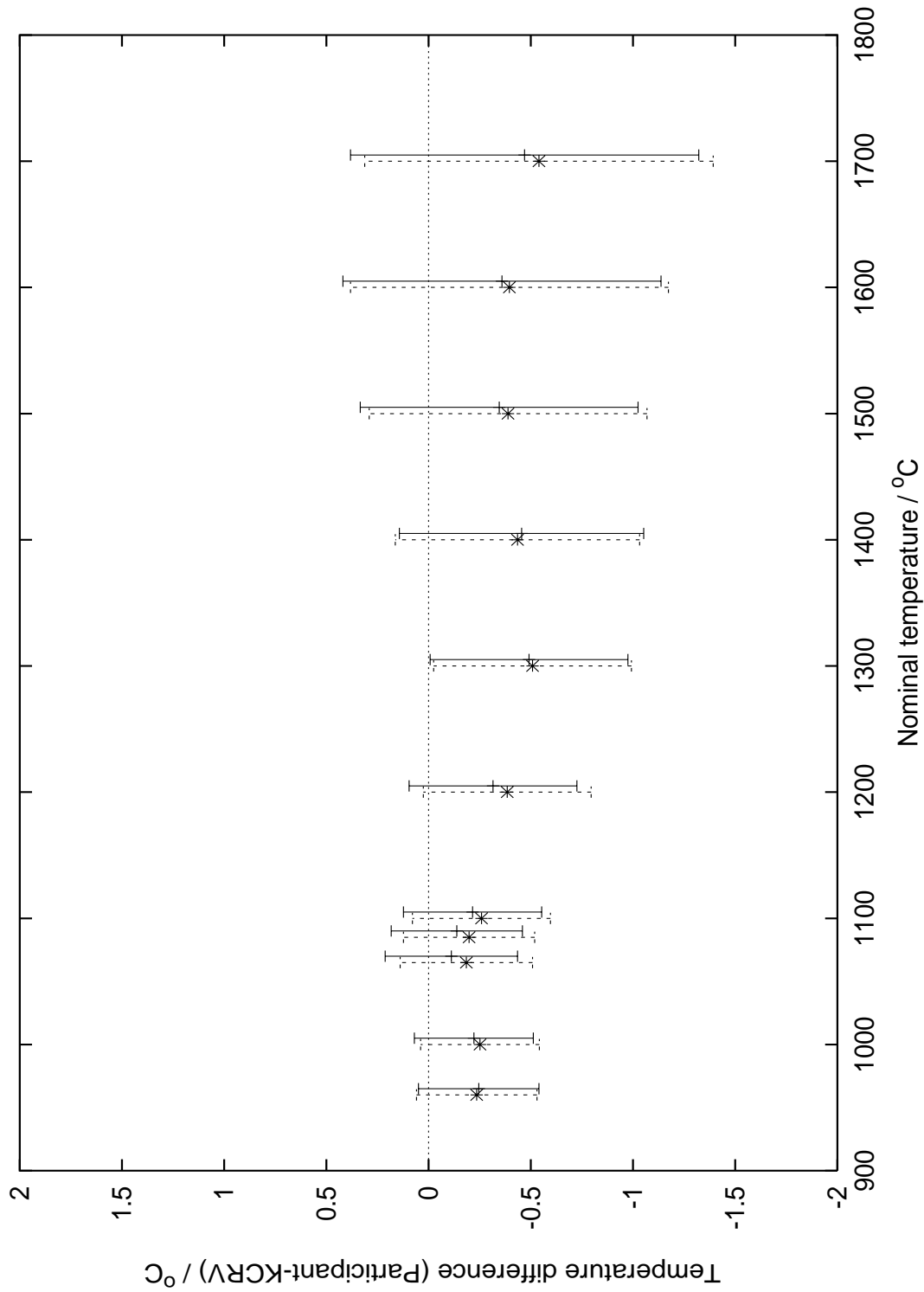


Figure 16 : Loop 1, difference from KCRV for participant CSIRO , star/dashed : lamp C564, plus/solid : C681

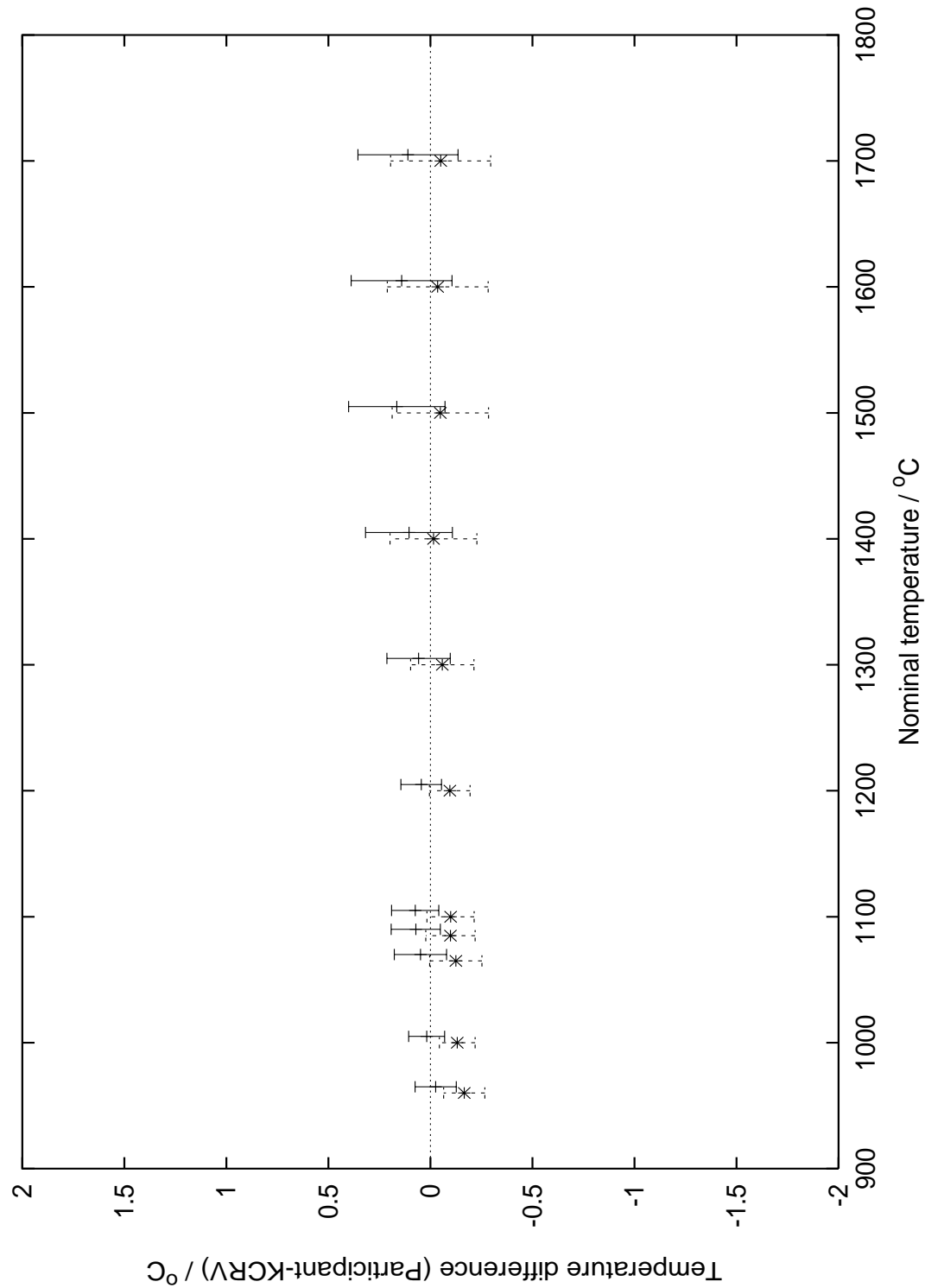


Figure 17 : Loop 1, difference from KCRV for participant KRISS , star/dashed : lamp C564, plus/solid : C681

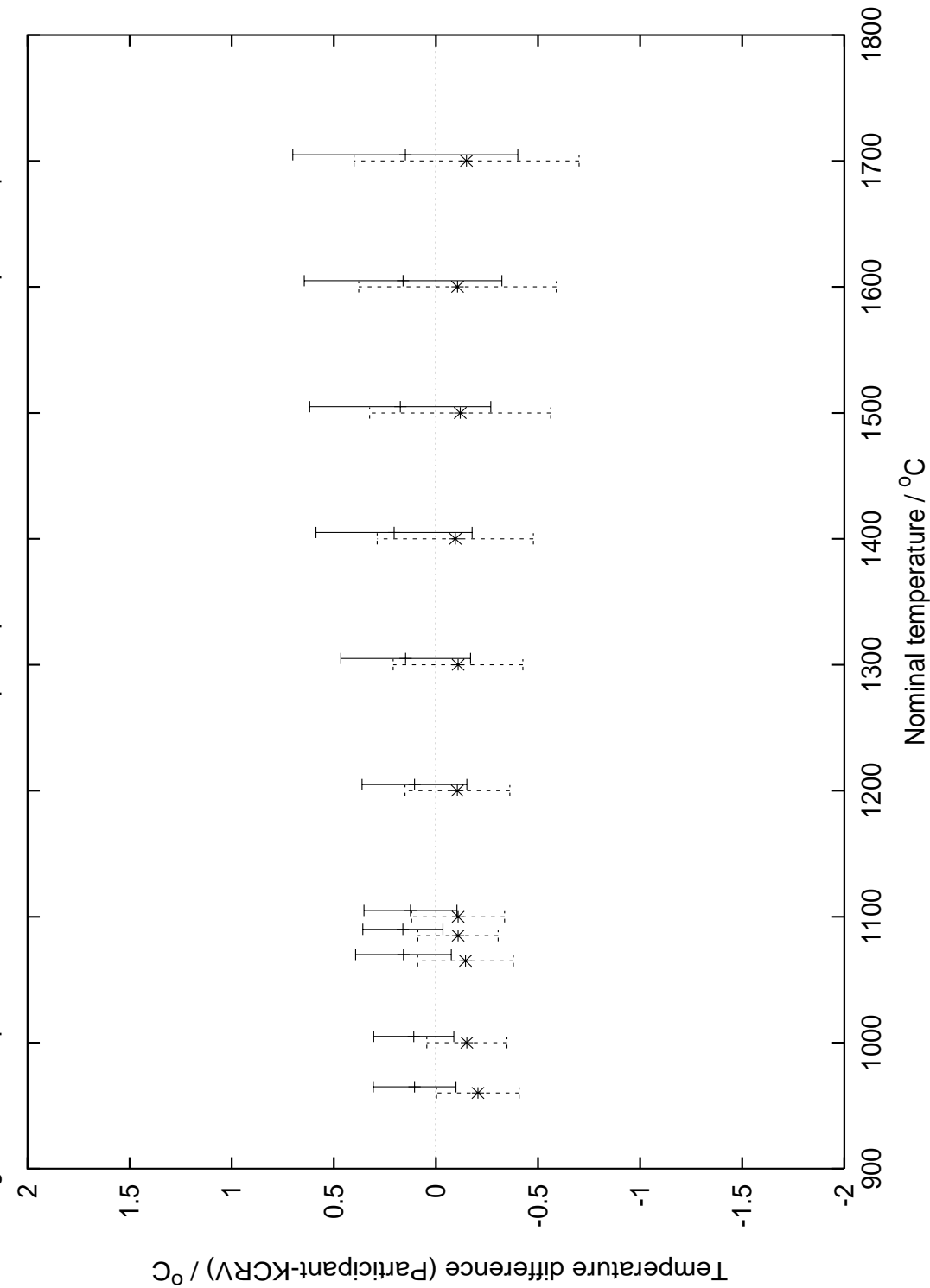


Figure 18 : Loop 1, difference from KCRV for participant NIM , star/dashed : lamp C564, plus/solid : C681

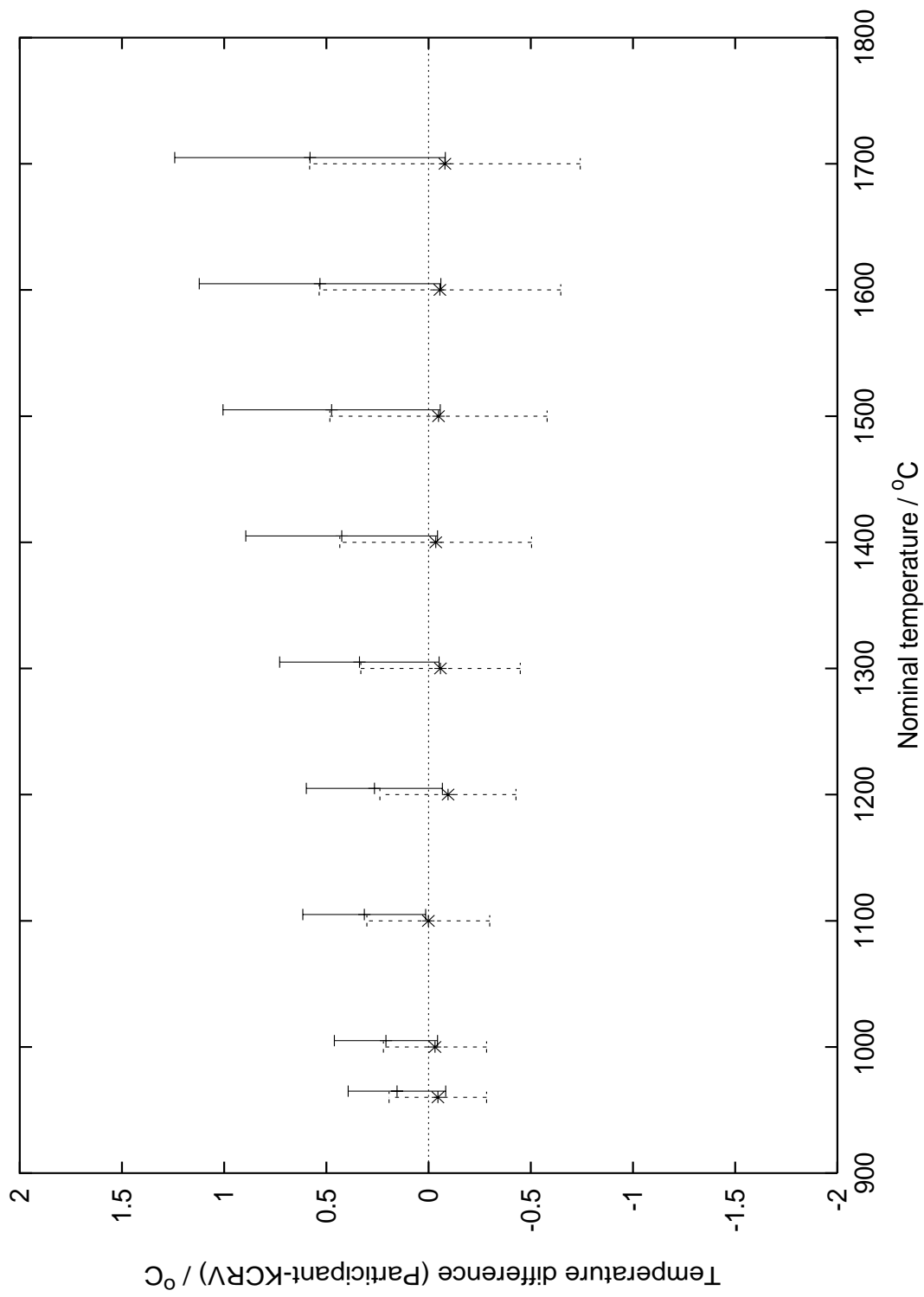


Figure 19 : Loop 1, difference from KCRV for participant NMC , star/dashed : lamp C564, plus/solid : C681

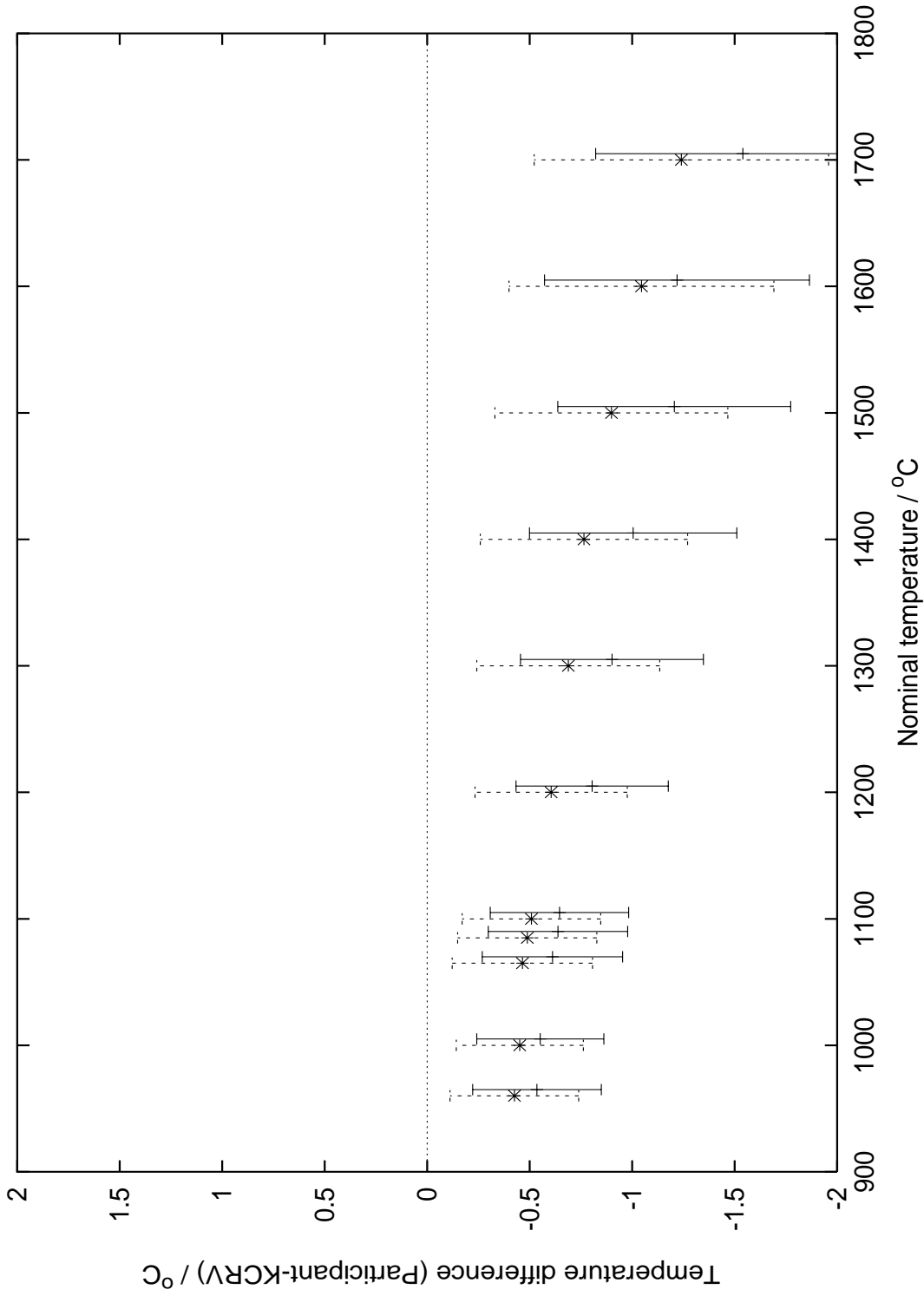


Figure 20 : Loop 1, difference from KCRV for participant NRLM , plus/dashed : lamp C564, star/dashed : lamp C681

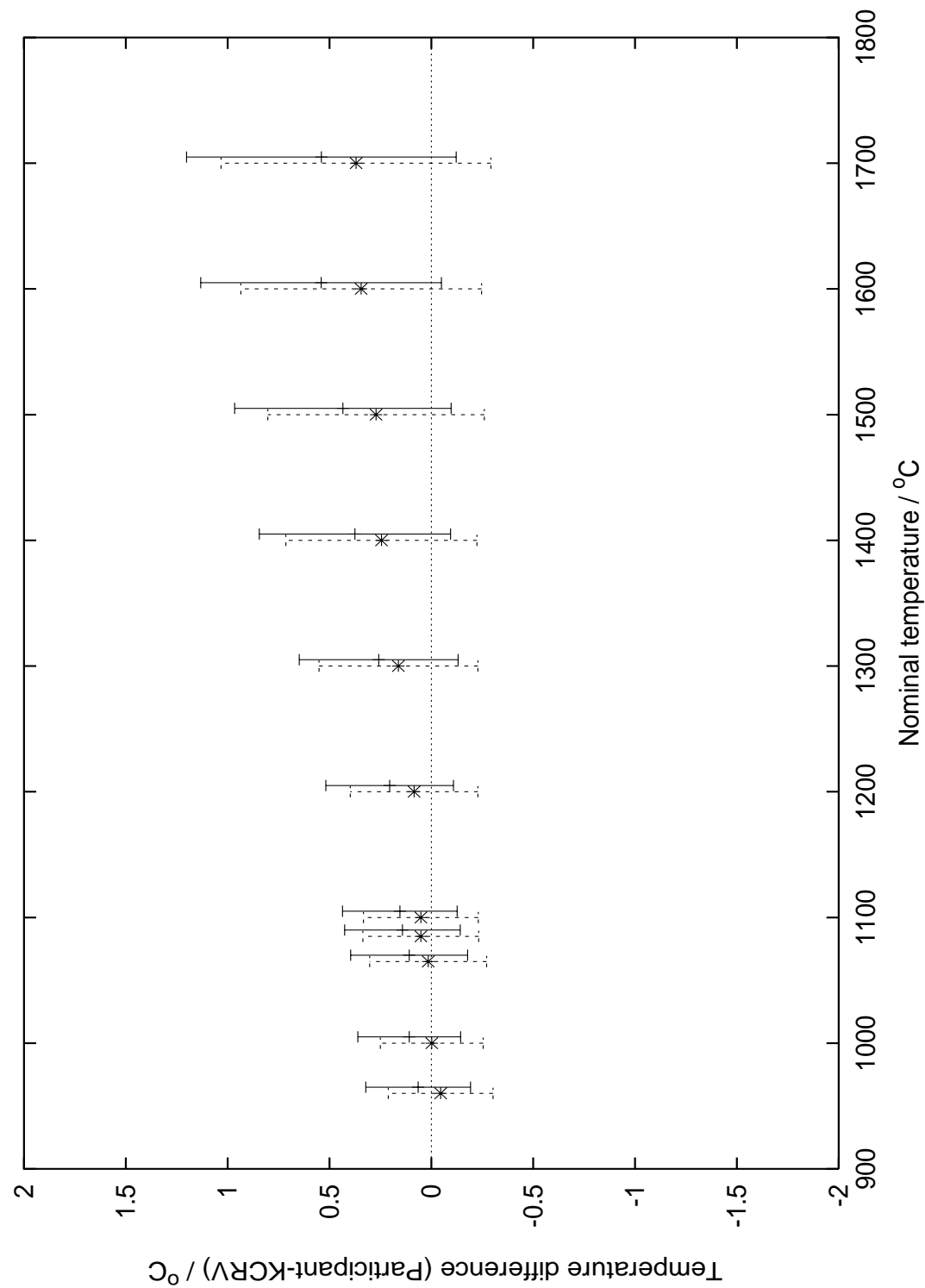


Figure 21 : Loop 1, difference from KCRV for participant VNIIM , star/dashed : lamp C564, plus/solid : C681

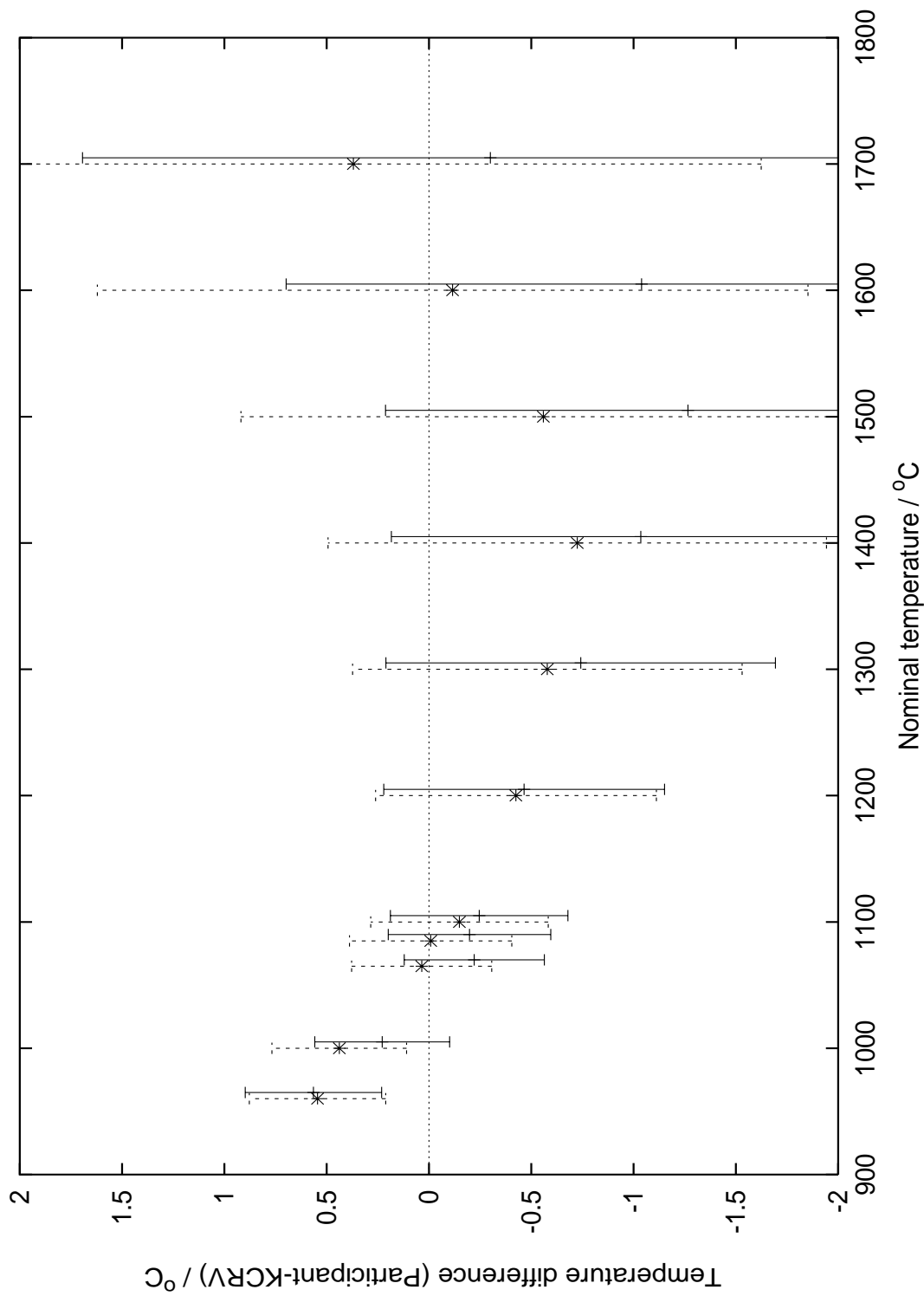


Figure 22 : Second loop, difference from KCRV for participant NPL1 , star/dashed : lamp C860, plus/solid : C864

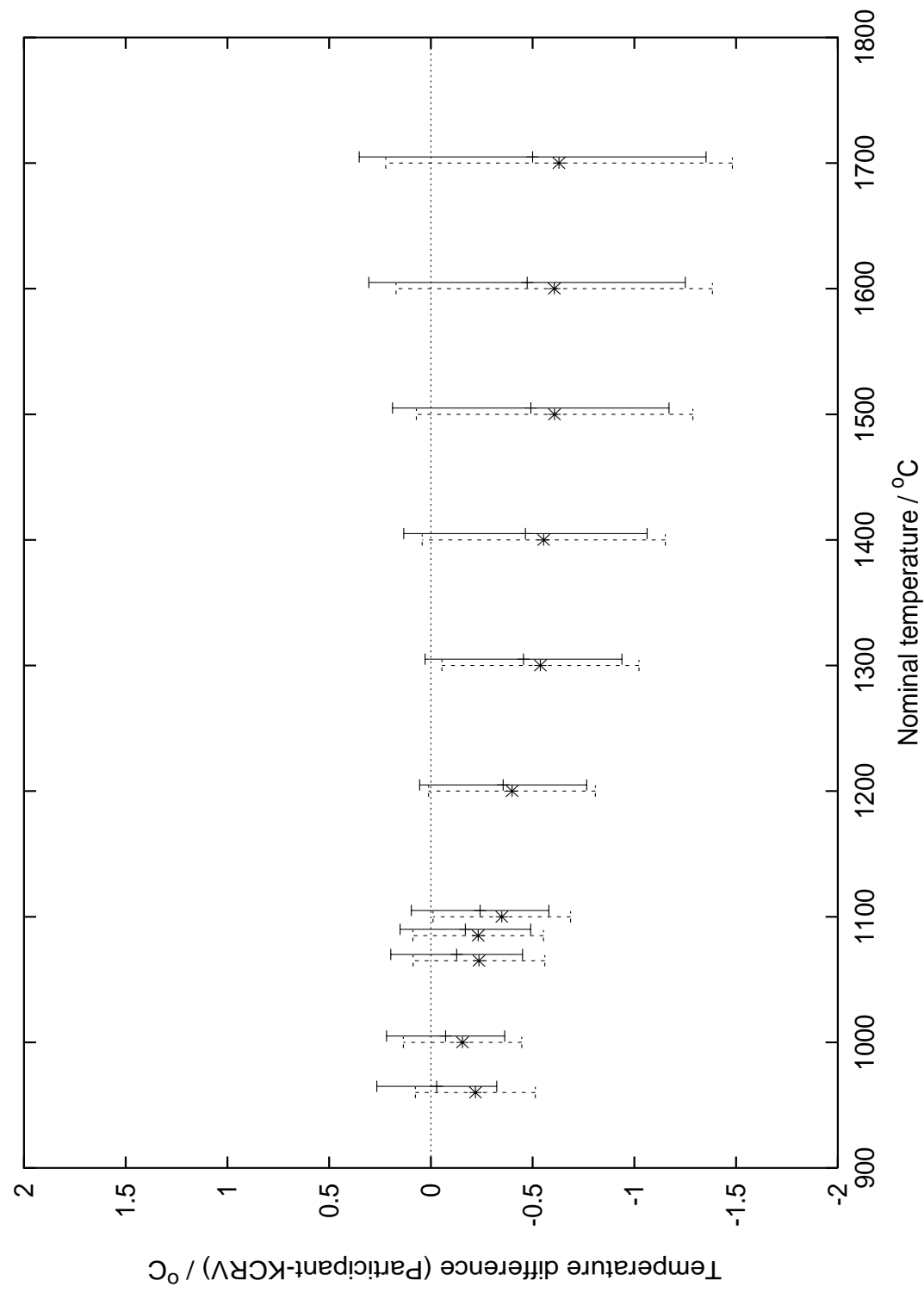


Figure 23 : Second loop, difference from KCRV for participant NPL2 , star/dashed : lamp C860, plus/solid : C864

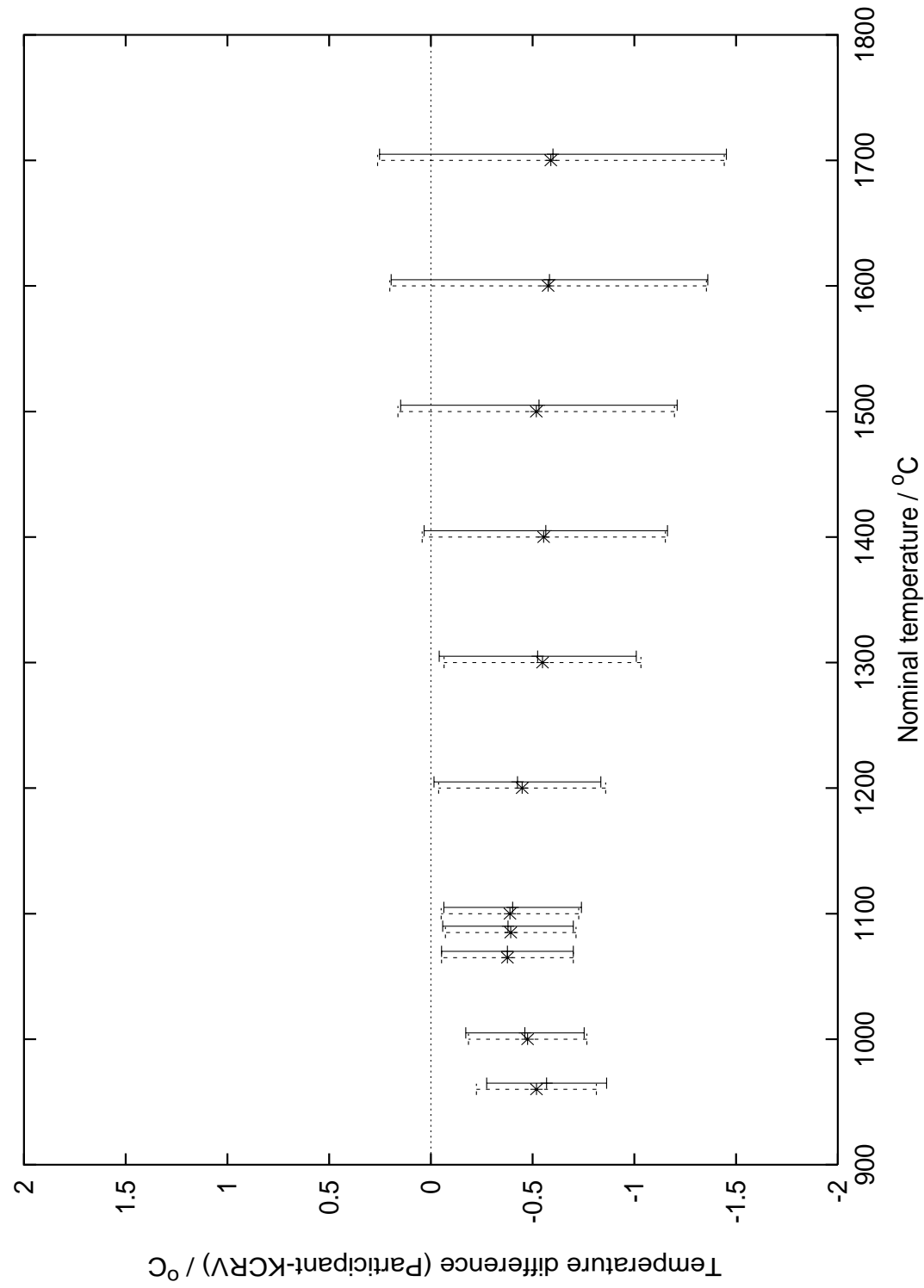


Figure 24 : Second loop, difference from KCRV for participant NPL3 , star/dashed : lamp C860, plus/solid : C864

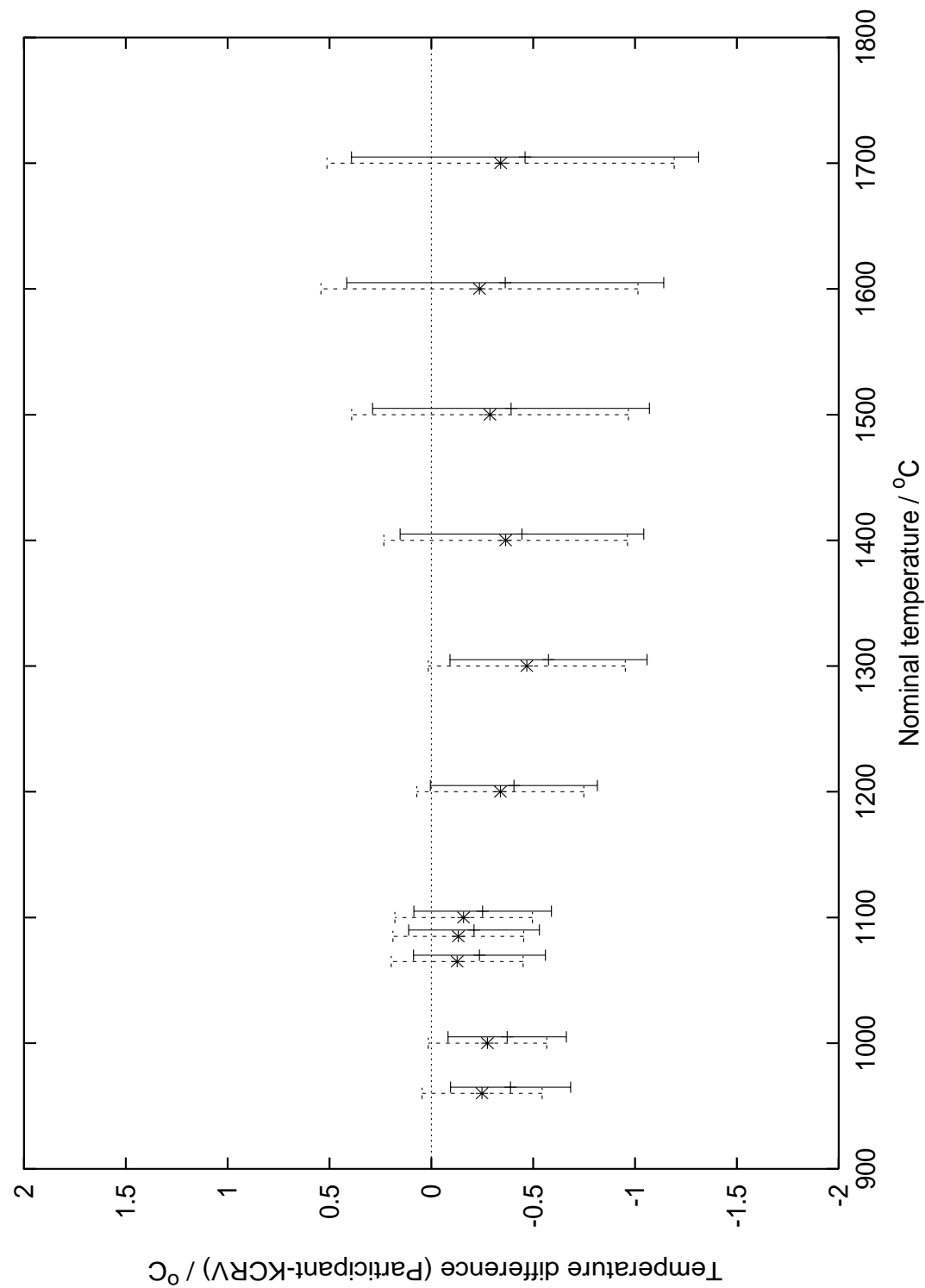


Figure 25 : Second loop, difference from KCRV for participant VSL1 , star/dashed : lamp C860, plus/solid : C864

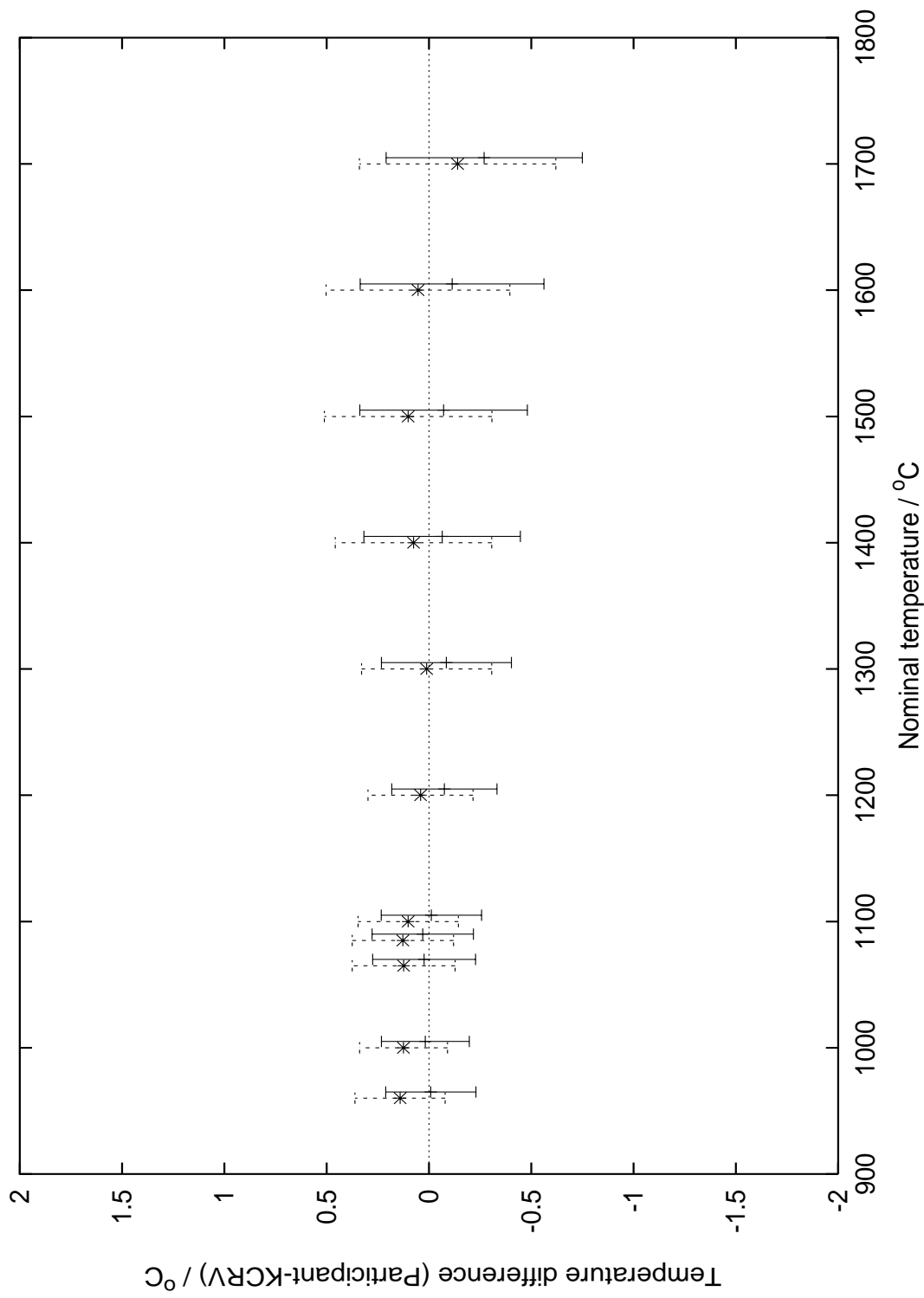


Figure 26 : Second loop, difference from KCRV for participant NIST , star/dashed : lamp C860, plus/solid : C864

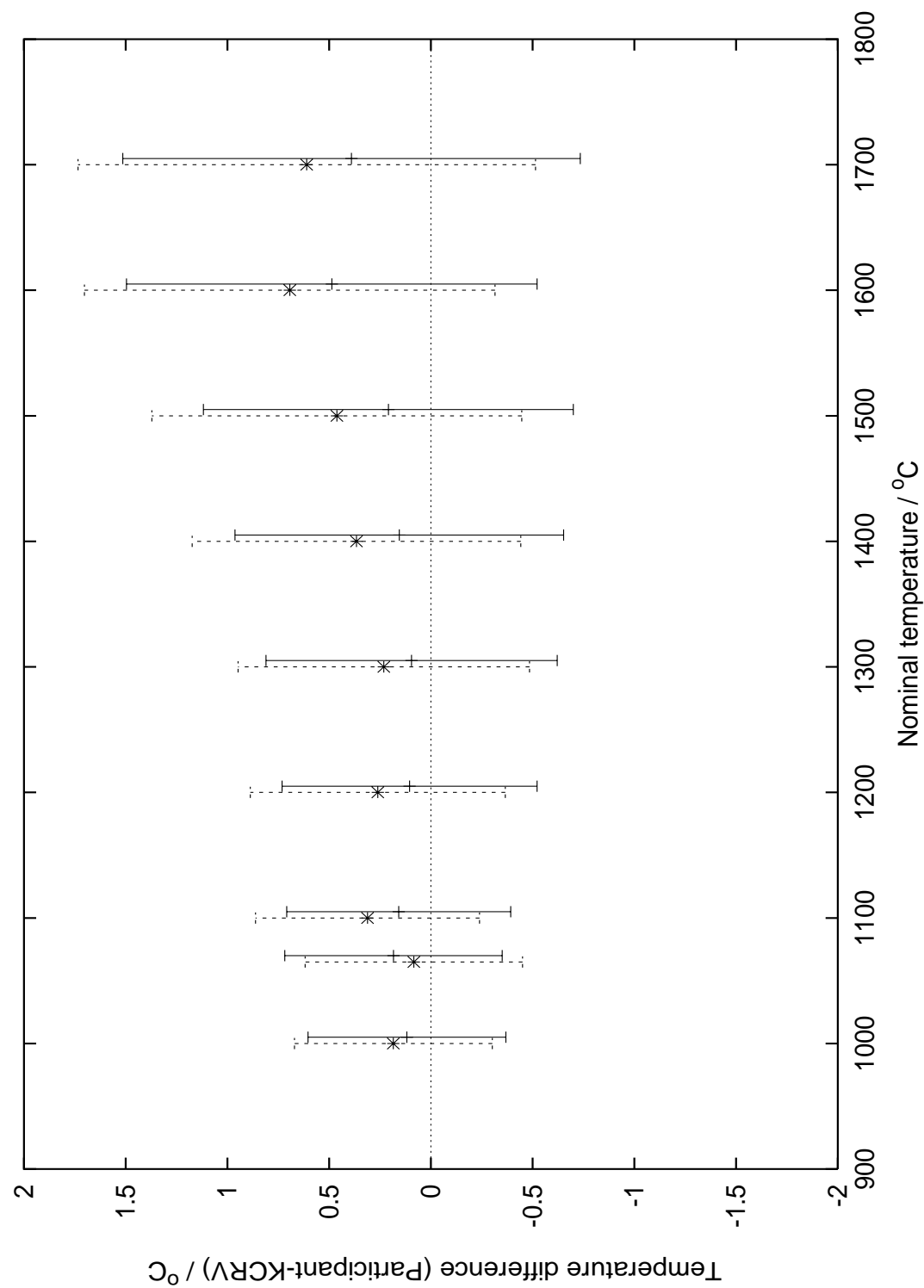


Figure 27 : Second loop, difference from KCRV for participant NRC , star/dashed : lamp C860, plus/solid : C864

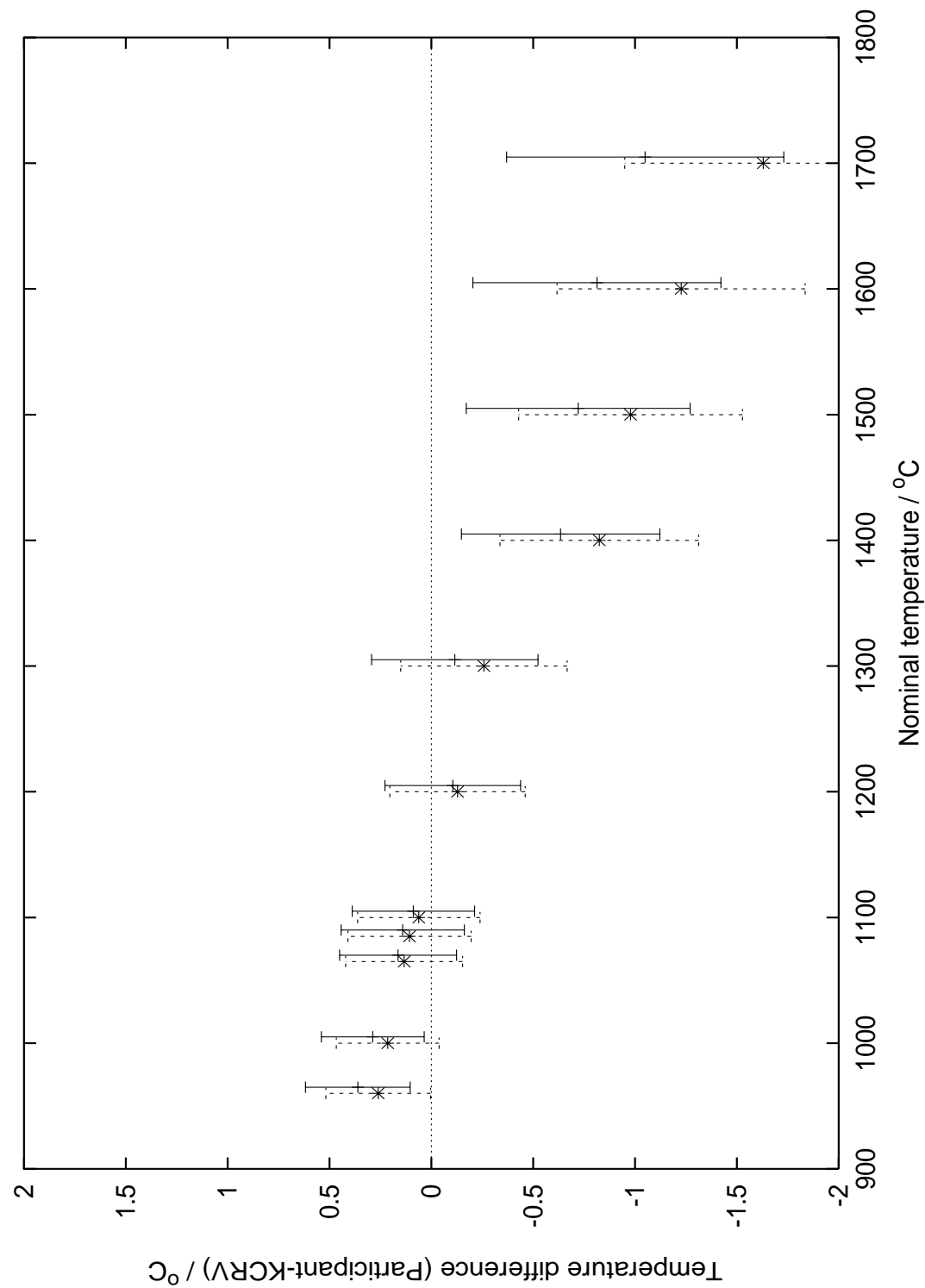


Figure 28 : Second loop, difference from KCRV for participant CENAM , star/dashed : lamp C860, plus/solid : C864

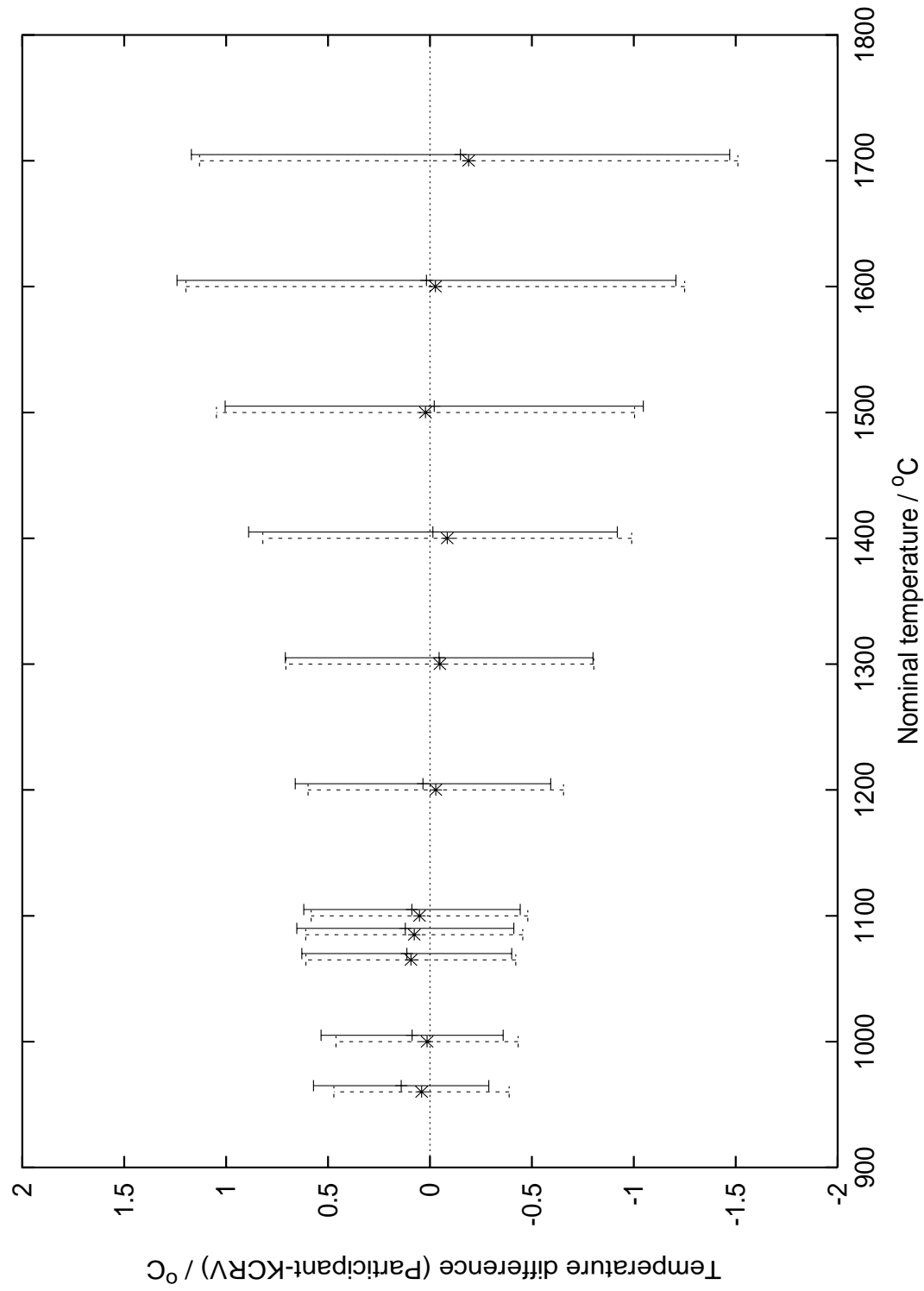


Figure 29 : Second loop, difference from KCRV for participant INM , star/dashed : lamp C860, plus/solid : C864

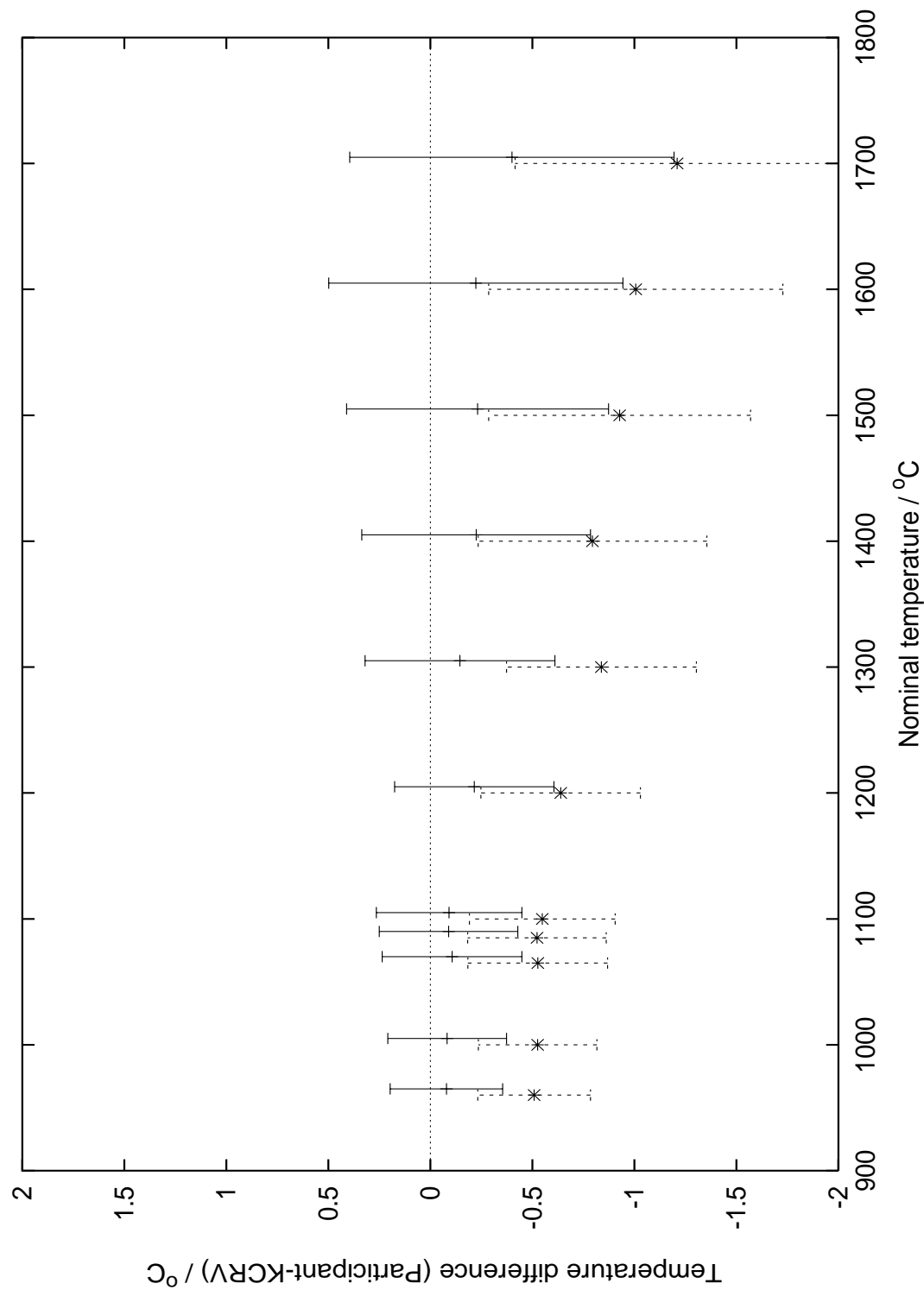


Figure 30 : Second loop, difference from KCRV for participant IMGC , star/dashed : lamp C860, plus/solid : C864

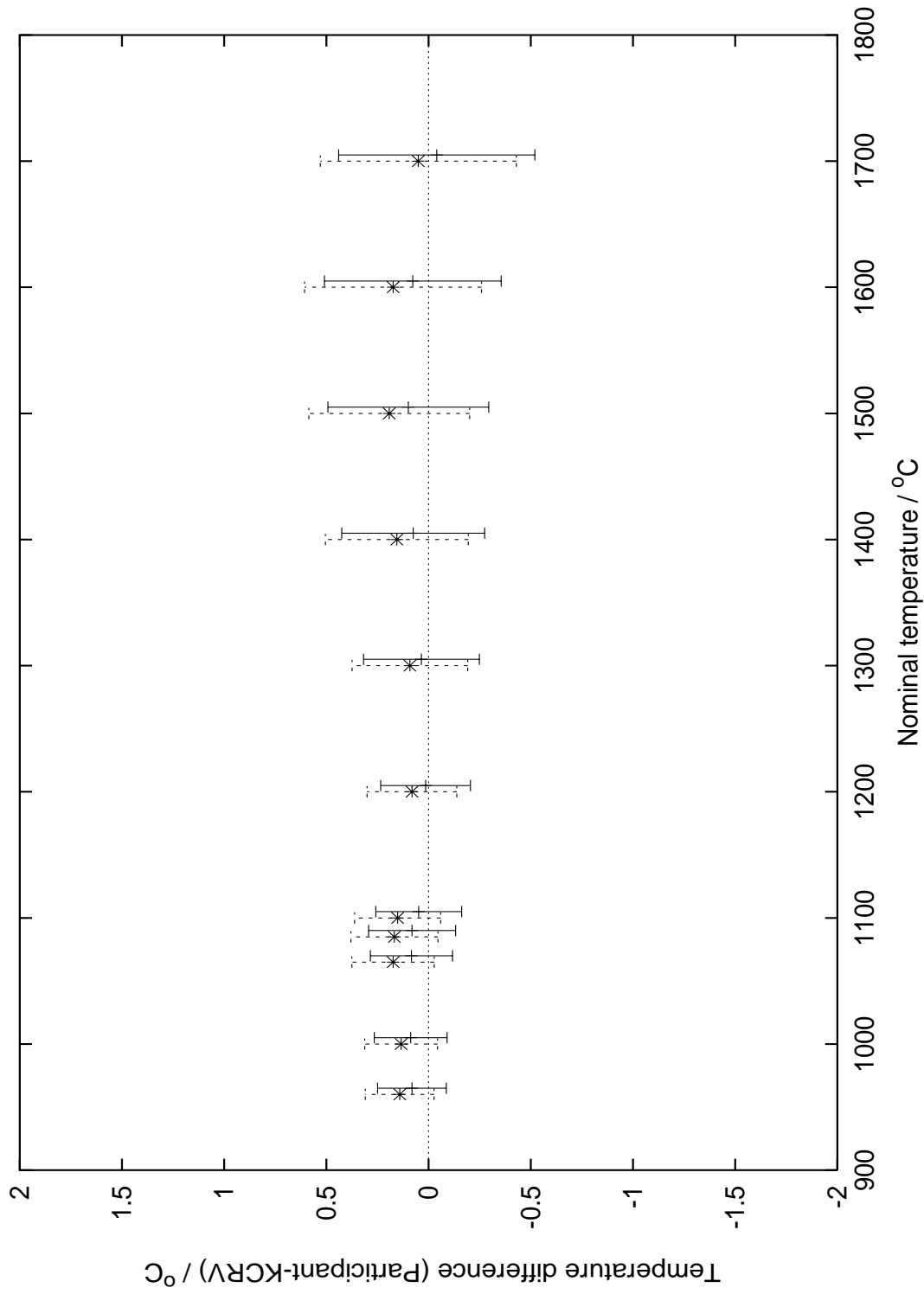
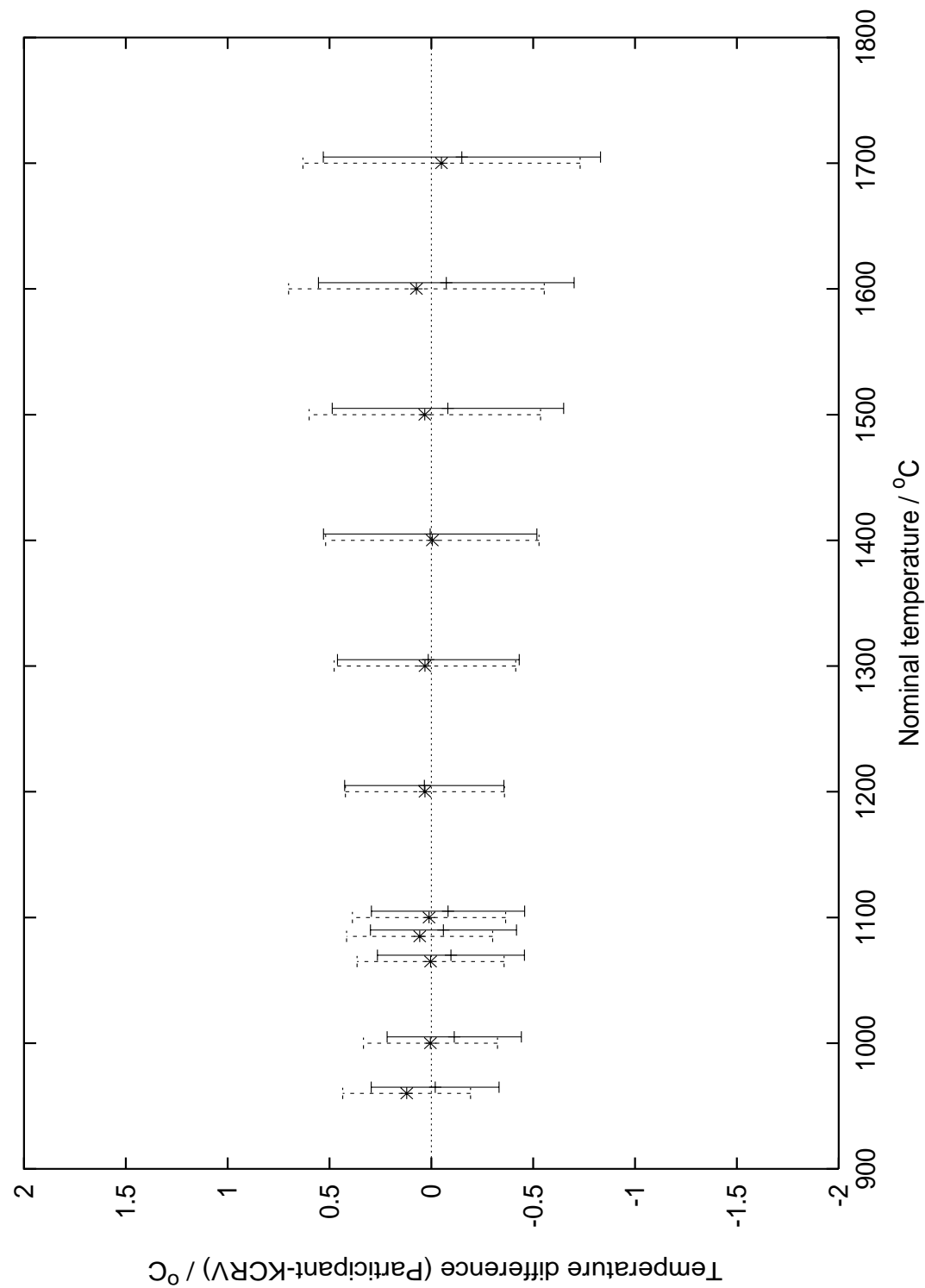


Figure 31 : Second loop, difference from KCRV for participant PTB , star/dashed : lamp C860, plus/solid : C864



## **Appendices**

### ***Appendix I. Protocol used in the comparison***

This appendix contains the protocol as used in the comparison. Although the layout seems to be changed, the contents remain the same as the original. The protocol was drafted by NMi-VSL, Dr P. Bloembergen, in June 1997.

# **PROTOCOL TO THE COMPARISON OF LOCAL REALIZATIONS OF THE ITS-90 BETWEEN THE SILVER POINT AND 1700°C USING VACUUM TUNGSTEN-STRIP LAMPS AS TRANSFER STANDARDS**

## **1. Introduction**

## **2. Organization**

- 2.1. Coordinating institutes
- 2.2. Transfer standards
- 2.3. Circulation patterns
- 2.4. Transport of the transfer lamps
- 2.5. Coordination

## **3. Technical aspects**

- 3.1. Initialization of the comparison
- 3.2. Instructions / guidelines for lamp calibrations

## **4. Reporting**

- 4.1. Experimental and theoretical procedures
- 4.2. Presentation of the results
- 4.3. Uncertainties
- 4.4. Time schedule
- 4.5. Editing and publication

## **Appendices**

- Appendix A: Circulation schemes
- Appendix B: The dependence of spectral radiance temperature on wavelength
- Appendix C: Form to confirm the receipt of the transfer standards
- Appendix D:
  - Lamp data
    - Instructions as to the handling of the lamps
    - Currents to be set during calibration of the lamps
    - Temperature coefficient  $dT_\lambda/dT_b (T_\lambda)$

## **1. Introduction**

The CCT decided during its 19th session in September 1996 to undertake an international comparison of local realizations of the ITS-90 above the silver point, using high-stability vacuum tungsten strip lamps as transfer standards. This comparison has been qualified as a key comparison with the potential effect of entailing documented bilateral agreements as to the equivalence of local realizations of the ITS-90 in the temperature range, envisaged. To this end results of the intercomparison will be evaluated in the first trimester of 1999, to prepare their discussion during the next CCT meeting in June 1999. The definitive results to be communicated in September 1999 will be eventually published in *Metrologia*.

## **2. Organization**

### **2.1. Coordinating institutes**

The intercomparison will be coordinated by:

Nederlands Meetinstituut - Van Swinden Laboratorium (NMi-VSL).  
P.O. Box 654  
2600 AR Delft  
The Netherlands

**Contact Persons:**

Dr. P. Bloembergen. Phone: + 31 15 2691 660  
Ing. R. Bosma. Fax: + 31 15 261 2971  
E-mail: PBloembergen@NMi.nl  
RBosma@NMi.nl

**Supporting institute:**

NPL: supplying one of the sets of transfer lamps  
and coordinating their transport.

**Contact Persons:**

Dr. R. L. Rusby Phone: - 44 181 943 6742  
Dr. G. Machin Fax: - 44 181 943 6755  
E-mail: graham.machin@newton.npl.co.uk  
rlr@newton.npl.co.uk

## **2.2. Transfer standards**

### **2.2.1. General specification**

- Two sets of GEC high-stability vacuum tungsten-strip lamps, identified by number, strip width, supplied with a water-cooled base, the polarity of the current connectors being indicated. Both lamps of a set are mounted in a metal case, to be hand carried when transferring the set of lamps between the participating institutes.

- Two double-wire cables are going with the lamps, essentially serving as current leads and voltage leads such that the room- temperature resistance  $R_{amb}$  of the lamp elements, comprising tungsten strip and its internal support, can be measured (along with the temperature  $T_{amb}$ , measured with a calibrated PRT inserted in the lamp base) just before calibrating them. After the calibration has been completed  $R_{amb}$  and  $T_{amb}$  should be measured again just before transferring the lamps to their next destination. All of this is to additionally monitor changes in the physical constitution of the lamp element, possibly induced during transport of the lamps (cf. 3.2.1). The procedure has been proposed by C.K. Ma of NRC.

### **2.2.2. Attached documentation**

- Appendix D:
  - Instructions as to the handling of the lamps, including an indication of the maximum lamp current and lamp temperature, not to be surpassed.
  - Currents to be set during calibration of the lamps.
  - Temperature coefficients  $dT_\lambda/dT_b$ , where  $T_\lambda$  and  $T_b$  represent the spectral radiance temperature and the lamp-base temperature, respectively.
- A pro-forma quotation as required by EC customs regulations.
- An ATA carnet when circulating the case outside the EC.

The mentioned documents are to be reattached to the case when transferred between the participating institutes.

### **2.3. Circulation patterns**

#### 2.3.1. Time schedule

- Two sets of transfer tungsten-strip lamps, as specified in 2.2, will be circulated following the two circulation schemes, indicated in Appendix A.
- The set designated as I, to be supplied by NMi-VSL, will be given a follow-up such as to eventually comply with the envisaged Euromet comparison, running in conjunction with the international key comparison.
- The set designated as II will be supplied by NPL, piloting the corresponding circulation.
- By circulating two sets of lamps in parallel, each of the institutes involved in the international key comparison, carried out under the auspices of the CCT, has completed its measurements by May 1999. By 1 June 1999 an interim synthesis report, to be drafted by NMi-VSL, based upon the results of these measurements, will be distributed among the members of the CCT.
- By 1 September 1999 the final synthesis report, to be drafted by NMi-VSL, will be distributed among the members of the CCT.
- By the end of June 2000 the final report on the Euromet comparison will be completed.

#### 2.3.2. Operations

- Apart from the periods interfering with the holiday seasons each institute is allocated nominally two months to complete its operations in each of the circulation schemes I and II. In the last week of this period at the latest the set of lamps in question has to be transferred to the next institute, indicated in the time schedule 2.3.1 (Appendix A).
- In the first week after receipt of the set I or II, the 'receipt confirmation form', added to this protocol (Appendix C), has to be filled in and sent to VSL or NPL, respectively. Before dispatching the confirmation form  $R_{amb}$  (2.2.1) should have been measured and the lamps should have been restabilized and checked for their repeatability (cf. 3.2.1).
- One month before transferring the set of lamps to its next destination a concise interim status report has to be sent to VSL and NPL in circulation schemes I and II, respectively; a copy of the report in scheme II should be sent in parallel to VSL as well.
- Within two months after completion of the measurements for the set (I or II) in question, the final report drafted along the lines, set out below, should be sent to VSL.

### **2.4. Transport of the transfer lamps**

#### 2.4.1. Means of transport between institutes: cabin baggage.

#### 2.4.2. Customs provisions:

- EC countries: a pro forma invoice, to be shown on request of the customs officials.

- Countries outside the EC: an ATA carnet consisting of several forms applying to the exportation and importation of the transfer lamps. Customs procedures must be strictly obeyed; when leaving or entering a country the forms should be filled in carefully; this is to the responsibility of the institute, which is to take the lamps to their next destination, indicated in the table. The institute to receive the lamps should carefully recheck the ATA forms, attached.
- VNIIM and NIM: Since neither China nor Russia yet has joined the ATA organization, importation and exportation rights, to be associated with the pro-forma invoice, have to be accounted for. Customs procedures should have been settled between the institutes involved before transport to and from NIM in scheme I and to and from VNIIM in scheme II. The importation and exportation should proceed via official agents in China and Russia, respectively.
- An ATA carnet is valid for one year; in arranging the circulation schemes special care has been taken to cope with this boundary condition.

#### **2.4.3. Insurance**

- The two sets of transfer lamps will be insured by the institutes, supplying the lamps, i.e. VSL and NPL ; the insurance includes transport and stay covering the whole period of the comparison; it does not include however the operations during the actual calibration of the lamps.
- Two fully characterized spare lamp will be kept stand-by, one of them being stationed at VSL, the other one at NPL. In case of damage action may be taken to replace a lamp out of a set of transfer lamps, the precise nature of the action, to be discussed between VSL and NPL, depending on the circumstances at the time of the accident.

#### **2.5. Coordination**

- The coordination will be based upon the time schedule, given in 2.3.1, and the feedback mechanisms specified in 2.3.2.

### **3. Technical aspects**

Below we give just an inventory, in short form, of those aspects, which should be taken into consideration when initializing or executing the comparison.

#### **3.1. Initialization of the comparison by VSL and NPL**

##### **3.1.1. Lamp functions**

- Description and identification of lamps; strip dimensions; specifying maximum radiance temperature  $T_{\lambda}(I_{max})$  and maximum lamp current ( $I_{max}$ ) not to be surpassed when calibrating the lamp (Appendix D).

##### **Ageing and initial stabilization**

Ageing: to be performed at a temperature 100 K higher than the stabilization temperature; duration: 100 hrs.

Stabilization: The highest temperature of calibration (maximum radiance temperature) is to be identified as the stabilization temperature. The initial stabilization should lead to a final drift rate not higher than 0,3 K / 100 hrs. It seems that this can be obtained for a lamp of 1,5 mm nominal width of the strip at a stabilization temperature of 1700°C, the associated ageing temperature being 1800°C. If the drift rate of no more than 0,3 K / 100 hrs cannot be obtained, then the stabilization should be repeated at  $T_{\lambda}(I_{max}) = 1650^{\circ}\text{C}$ .

Specifying the drift rate of the stabilized lamp: during the stabilization at  $I = I_{\max}$  the radiance temperature  $T_\lambda(I_{\max})$  is continuously monitored; from this the drift rate in K / 100 hrs can be easily determined and specified. A constant drift rate is expected after about 60 hrs.

#### - Determination of positioning effects

Effects induced by the rotation of the strip around the vertical axis: for the measurement of these effects the target field and the edges of the tungsten strip must be vertical. The angular distribution of the radiance may have a maximum of some tenths of a percent and about 4 degrees width due to inter-reflection inside the lamp. The pilot institute will define an angle in the most uniform region of the horizontal angular radiance distribution as reference angle for the subsequent measurements.

The influence of tilting of the strip (through rotation around the horizontal axis perpendicular to the optical axis of the radiation thermometer viewing the strip) should be verified being sufficiently low at the reference angle, as defined in the horizontal plane.

#### - Specifying the variation of spectral radiance temperature with wavelength

The function  $dT_\lambda/d\lambda$  versus spectral radiance temperature  $T_\lambda$  has been given in Appendix B in graphical and tabular display for the reference wavelengths 650 nm and 950 nm. The functions have been calculated by PTB, taking a window transmission of 0.92, from values of the spectral emissivity of tungsten reported by L.N. Latyev, V. Ya. Chekovsky and E.N. Shestakov: High Temp.-High Press.2 (1970) 175-181. Estimated standard deviation ( $s$ ) in  $dT_\lambda/d\lambda$ : 10 % of its absolute value. The polynomial representations, with  $T_\lambda$  and  $dT_\lambda/d\lambda$  given in °C and K/nm, respectively, are:

$$dT_\lambda/d\lambda = \sum_i a[i] \cdot [T_\lambda]^i, \text{ with } i = 0 \text{ to } 2, \text{ and:}$$

$$\begin{aligned} \text{For } \lambda_r = 650 \text{ nm:} \quad a[0] &= -0.35422504 \cdot 10^{-1} \\ a[1] &= 2.70716088 \cdot 10^{-5} \\ a[2] &= -0.10980270 \cdot 10^{-6} \end{aligned}$$

$$\text{Associated standard deviation (in } dT_\lambda/d\lambda\text{): } s = 2.607 \cdot 10^{-4} \text{ K / nm}$$

$$\begin{aligned} \text{For } \lambda_r = 950 \text{ nm:} \quad a[0] &= 4.65847984 \cdot 10^{-3} \\ a[1] &= -0.81968285 \cdot 10^{-4} \\ a[2] &= -0.94845913 \cdot 10^{-7} \end{aligned}$$

$$\text{Associated standard deviation (in } dT_\lambda/d\lambda\text{): } s = 2.243 \cdot 10^{-4} \text{ K / nm}$$

- Providing the temperature coefficient  $dT_\lambda/dT_b[T_\lambda]$ , where  $T_b$  represents the base temperature. The corresponding data are given in Appendix D, going with the documents added to the lamps.

#### - Proposal as to the shape of the polynomial representation of the $T_\lambda$ vs. $I$ characteristic.

A polynomial of the sixth order would be sufficient describing  $T_\lambda = T_\lambda(I)$ . Since it is proposed to perform the calibration at fixed prescribed lamp currents  $I$  no inverse function is needed (cf. 3.2.2).

### 3.1.2. Specification of measurement and reference conditions

#### Measurement conditions

- a. Orientation of the strip: in conjunction with the procedure to orient the lamp, to be specified in 3.2.
- b. Target field diameter  $\approx 0.75$  mm.
- c. Viewing distance  $< 1500$  mm.
- d. Lamp-current settings  $I(j)$  as defined in Appendix D.

#### Reference conditions

Reference conditions in principle apply to the influence parameters listed below. To obtain comparable results in principle corrections should be applied whenever the actual value of a given parameter would differ from the reference value. In practice corrections will have to be applied only for the parameters listed under a, d, e, f (f only for RH when  $\lambda_r = 950$  nm).

- a.  $\lambda_r = 650$  nm;  $\lambda_r = 950$  nm.
- b. Aperture ratio: f/8
- c. Target center position with respect to the notch: (0.5.d'; 0), d' referring to the minimum effective width of the strip at the notch position.
- d. The effective source diameter  $\square_d$  of the tungsten strip (with a nominal length of 1 mm) is roughly:  $2 \times d$  mm, d referring to the strip width; it can be measured differentially by focusing onto an illuminated slit (centrally obscured) of width d and length l, or onto an image of the strip itself. It is the effective diameter  $\Phi_d$  (to be specified in conjunction with the SSE as measured for circular sources as a function of the source diameter), which has to be referred to, when correcting for the size-of-source effect in transferring radiances from a fixed-point blackbody radiator to the strip. Note: the effective aperture of the cavity radiator may be different from its geometric aperture due to the (inhomogeneous) radiance field surrounding the cavity. For details we refer to the preprint of the paper on 'The characterization of radiation thermometers subject to the size-of-source effect', presented at Tempmeko 96.
- e. Base temperature  $T_b = 20$  °C
- f.  $T_{amb} = 23$  °C; RH = 0 %

## **3.2. Instructions / guidelines for lamp calibrations**

### 3.2.1. Preparations

#### 3.2.1.1. Initialization

##### -Measurement of the room-temperature resistance $R_{amb}$ of the lamp element

The lamps are transported in a metal case being embedded in flexible plastic foam. Two electrically screened double-wire cables are going with the lamps, one comprising the current leads (to be connected to the current terminals of the lamp) and the other the voltage leads (to be connected to the outer in / outlet brass tubes in circulation scheme I, or to tags attached to the lamp-base in scheme II), such that the room-temperature resistance  $R_{amb}$  of the lamp element, comprising tungsten strip and its internal support, can be measured (along with the temperature  $T_{amb}$ , measured with a calibrated PRT, inserted in the lamp base). The measurement of  $R_{amb}/T_{amb}$  should be done just before starting the calibration of the lamps.

After the calibration has been completed  $R_{\text{amb}}$  and  $T_{\text{amb}}$  should be measured again just before transfer of the lamps to their next destination. All of this is to additionally monitor changes in the physical constitution of the lamp element, possibly induced during transport of the lamps.

It is suggested performing the measurement of the resistance (about 50 m $\Omega$ ) using an ASL F18 bridge at currents of 50 and  $50\sqrt{2}$  mA, 30 Hz, in conjunction with a reference resistor smaller than 1 Ohm, preferably 0.1 or even 0.05 Ohm, such as to arrive at an accuracy of the zero-current resistance better than 2 in  $10^5$ . During the measurements the lamp should be placed in the case in its normal position, the case closed, as far as possible, and grounded. Further instructions are going with the lamps.

#### Mounting the lamps for calibration.

Current-lead connections to the lamps. Stabilizing the base temperature and monitoring its temperature  $T_b$ .

Current switching and setting (maximum 1 A / min).

#### 3.2.1.2. Positioning and checking

##### - Procedure to orient the lamp.

- The lamp is rotated around the axis of the radiation thermometer until the edges of the strip appear vertical when observed from the position of the radiation thermometer.
- The horizontal reference angle and the correct tilting angle (preferably zero degrees) are set by adjustment of the notch and of a mark on the rear window of the lamp such as to be in line with the optical axis of the radiation thermometer (e.g. by means of a pilot laser).
- The lamp is shifted sideward to center it into the reference target position.

During the manipulations described below the radiance temperature should be set to a value smaller than 1500 °C.

##### - Focusing

All calibrations as well as the investigation of positioning effects require accurate focusing. The focal distances of lens thermometers (when not adequately corrected for chromatic effects) may be very different from wavelength to wavelength. Focusing in the visible may lead to enormous errors at 950 nm; at this wavelength careful photoelectric focusing is mandatory. A procedure, suggested by the PTB, is to define the target distance to the thermometer as the distance where the apparent width of the strip image is a minimum. For this purpose the lamp is moved in a direction perpendicular to the optical axis by a micrometer drive. There are two positions where the thermometer signal amounts to only 5 % of its value in the centered position. The difference of the respective micrometer readings is a measure for the apparent width, the minimum width defining the target distance to be set.

##### - Decentering of the target field

It is recommended that all participants measure the horizontal spatial radiance distribution (for  $\lambda_r = 650$  nm) at the height of the notch. If a sufficiently flat portion is not observed, the target size (defined by the thermometer) is too large.

##### - Effects due to the rotation of the strip around the vertical axis

The participants should measure the angular distribution of the radiance in the horizontal plane to provide information on whether its shape is the same for different thermometers or not.

The use of a neutral density filter helps to find the origin of an inter-reflection peak, if any. A neutral density filter of transmissivity 0.1 causes a peak in the angular distribution to effectively disappear if it is due to an inter-reflection between lamp and thermometer.

If an inter-reflection peak is observed around the angular coordinates, set by following the orientation procedure recommended above, measures should be taken in consultation with the pilot institute.

### 3.2.1.3. Restabilization of the lamp after transportation

- The day before the actual measurements (at the latest) the lamp should be restabilized.
- Measurement of the radiance temperature at a lamp current  $I = I(5)$ , defined in Appendix D, and corresponding with a radiance temperature of about 1100 °C (for  $\lambda_r = 650$  nm).
- Restabilization of the lamp at  $T_{\lambda}(I_{max}) \approx 1700$  °C for one hour.
- Measurement of the radiance temperature at  $I = I(5)$ . The difference with the former temperature, to be registered, is expected not to be larger than 0,05 K (650 nm) or 0,1 K (950 nm). However, no further attempt should be made to achieve improved stability because it might give rise to an unacceptable total burning time when aimed at by several institutes.
- Switching off the lamp current. The lamp should be left at 'zero current' to settle down overnight.

### 3.2.2. Measurements.

- Cleaning the window: every day before starting the measurements cleaning with a few drops of pure alcohol and immediately drying subsequently using lens cleaning paper.
- Centering of the target field (at each current to be set) at the level of the notch. Viewing the notch at the object distance, corresponding with  $\lambda_r = 950$  nm, can be accomplished by temporarily reducing the aperture ratio, using an external diaphragm, thereby increasing the depth of focus.
- Measurements should be performed at the currents  $I(j)$  given in Appendix D which is included in the documents attached to the lamps. The currents should be set to approach  $I(j)$  within a few mA; later on the radiance temperatures, as measured, should be converted to correspond with the nominal values  $I(j)$ .

By measuring in the direction of increasing current only, after having restabilized the lamp, as indicated above (3.2.1), hysteresis effects can be avoided. Minimum equilibration times: 30 minutes, and 15 minutes for radiance temperatures (650 nm) in the ranges 900 °C - 1100 °C ( $I \leq I(5)$ ) and  $> 1100$  °C ( $I > I(5)$ ), respectively;  $I(5)$  is given in Appendix D. At each current the result should be obtained as the average of at least ten measurements.

The currents to be set correspond (for  $\lambda_r$  650 nm) roughly with the following nominal radiance temperatures (in °C) in the order as indicated: T(Ag), 1000, T(Au), T(Cu), 1100, 1200, 1300, 1400, 1500, 1600, 1700 °C. Whenever a fixed-point radiance temperature is transferred to the lamp the corresponding (average) current(s) should be registered and eventually reported.

The measurements should be performed at a reference wavelength  $\lambda_r$  around 650 nm, and may be performed additionally around  $\lambda_r = 950$  nm, if at least the time schedule is maintained.

- After completion of the measurements at  $T_{\lambda}(I_{max})$ , the current should be switched off - in a controlled fashion - and the lamp left to settle down overnight.
- A second series of measurements - in the direction of increasing current only - should be performed along the lines indicated above.

- Recommended maximum burning time of the lamps: 30 hours.
- After the calibration has been completed  $R_{\text{amb}}$  and  $T_{\text{amb}}$  should be measured again just after having packed the lamps in the case, to be transferred to its next destination. During the measurements the case should be closed, as far as possible, and grounded (cf. 3.2.1)

## **4. Reporting**

An inventory of aspects, inherent in the reporting of each contribuant to the intercomparison is given in this section. Experimental and theoretical procedures, presentation of results and uncertainties are reviewed in concise form only.

### **4.1. Experimental and theoretical procedures**

#### 4.1.1. Realization of the ITS-90

- Description of equipment, including reference thermometer and reference fixed - point blackbody radiator.
- Description of experimental procedures.
- Formal definition/derivation of the spectral radiance temperature with explicit reference to corrections applied.

#### 4.1.2. Transfer of radiance temperatures to strip lamps.

- Description of equipment and procedures, including corrections.

### **4.2. Presentation of results**

#### 4.2.1. Local conditions to be specified

##### 4.2.1.1. Reference thermometer

- Effective wavelength ( $\lambda_e$ ) / local reference wavelength ( $\lambda_{rl}$ ).
- Half-width of spectral response function.
- Aperture ratio; f-number.
- Target distance.
- Target field dimensions.
- Size-of-source effect (SSE) covering a range in source radii ( $r_0, r_{\text{max}}$ ), with  $r_{\text{max}} > R_b$ ,  $r_0 < d/2$ ,  $R_b$  and  $d$  referring to the effective aperture radius of the reference fixed-point blackbody radiator (to be specified) and the width of the tungsten strip, respectively (cf 3.1.2). The SSE should be measured at wavelengths near to each of the reference wavelengths, included in the scale definition.
- Effective source diameter  $\Phi_d$  of the strip, specified in conjunction with the SSE, as measured for the circular sources (cf. 3.1.2).

#### 4.2.1.2. Transfer lamps

- Orientation of the lamp, if and only if it differs from the reference orientation.
- Nominal base temperature and its stability.
- Total burning time.

#### 4.2.1.3. Ambient conditions

- $T_{amb}$ , RH; mean, maximum and minimum values.

#### 4.2.2. Measurement results

- If using the intermediate of the (mean) effective wavelength  $\lambda_e$ , the following entries to a table surveying direct and corrected measurement results could be envisaged. Alternatively  $\lambda_e$  could be replaced by the (fixed) local reference wavelength  $\lambda_{rl}$ .

Table A:

No: number of measurement;  $I(j)$ : lamp current as defined in Appendix D;  $I(l)$ : lamp current, as set;  $I(j) - I(l)$ ; R: ratio of photo-currents  $i(T_\lambda)/i\{T(FP)\}$ , the temperature  $T(FP)$  referring to the fixed-point temperature as defined in the ITS-90;  $T_\lambda = T_\lambda(\lambda_e; T_b)$ ;  $T_\lambda(\lambda_e; T_b) := T_\lambda$  (corrected for the SSE);  $T_\lambda(\lambda_e; T_b) := T_\lambda$  (corrected for SSE and non-linearity); [ $\lambda_r = 950$  nm;  $T_\lambda$ ; RH = 0 %].

Table B:

No: number of measurement;  $\lambda_e$ ;  $T_\lambda(\lambda_e; T_b)$ ;  $\partial T_\lambda / \partial \lambda$ ;  $\partial T_\lambda / \partial \lambda \cdot (\lambda_r - \lambda_e)$ ;  $T_\lambda(\lambda_r; T_b)$ ;  $T_b$  ( $^{\circ}$ C);  $\partial T_\lambda / \partial T_b$ ;  $\partial T_\lambda / \partial T_b \cdot (20 - T_b)$ ;  $T_\lambda := T_\lambda\{\lambda_r; I(l)\} := T_\lambda\{\lambda_r; 20; I(l)\}$ ;  $\partial T_\lambda / \partial \lambda_i$ ;  $\partial T_\lambda / \partial \lambda_i \cdot \{I(j) - I(l)\}$ ;  $T_\lambda(j) := T_\lambda\{\lambda_r; I(j)\}$ .

- In the last column of table B the final results  $T_\lambda(j) = T_\lambda\{\lambda_r; I(j)\}$ , at the currents  $I(j)$ , as specified in Appendix D, are to be tabulated. The parameter  $\partial T_\lambda / \partial \lambda_i$ , denoted in Table B, can be derived from a polynomial expansion  $T_\lambda = T_\lambda\{\lambda_r; I(l)\}$

- In addition:  $T(FP)$  vs.  $I\{T(FP)\}$ , where the temperature  $T(FP)$  refers to the ITS-90 fixed-point temperature, as transferred to the strip, should be separately reported. Two values of  $I\{T(FP)\}$  should be given, i.e. the directly measured value and the value, obtained after correction for the SSE.

Finally: specify the values  $R_{amb}$  and  $T_{amb}$ , as measured upon receipt of the lamps, and just before transferring them to their next destination (cf. 3.2.1 and 3.2.2).

### **4.3. Uncertainties**

#### 4.3.1. Identification of uncertainty components

Here we confine ourselves to identifying uncertainty components through the physical parameters involved and the associated corrections.

##### I. Reference blackbody radiator.

- Realization of the reference temperature. Subcomponents: impurities, emissivity, temperature difference  $\Delta T$  across the bottom section of the cavity in view

##### II. Reference thermometer

###### II.1. Ratio of photo-currents

- Photo current - measurement.
- Photo current - resolution.
- Linearity

## II.2. Size of source effect (SSE)

### II.3. Spectral parameters

- Spectral response function, including (especially) the spectral transmission of the interference filter and the spectral responsivity of the detector. Stability of the interference filter.
- Blocking.

- Mean effective wavelength ( $\lambda_e$ ), a variable, linking up additionally with the spectral characteristics of the transfer lamps around the fixed reference wavelengths  $\lambda_{rl}$  (local value) and  $\lambda_r$  (reference value).

### II.4. Possible additional parameters

- Transmission of neutral density filter(s).
- Absorption by water vapour ( $\lambda_r = 950$  nm).

## III. Transfer lamps.

### III.1. Lamp current

- Lamp currents  $I(l)$ , as set.
- Lamp-currents  $I(j)$ , as prescribed.

### III.2. Radiance temperature

- Short-term stability.
- Drift.

- Dependence on wavelength:  $T_\lambda = T_\lambda(\lambda); dT_\lambda/d\lambda(\lambda)$ .
- Dependence on base temperature  $T_\lambda = T_\lambda(\lambda; T_b)$ .

### Residual parameters:

- Alignment (spatial and angular distribution of radiance).
- Target field
- Cleaning of the window

## IV. Lamp-thermometer composite parameters

- Radiance temperature  $T_\lambda = T_\lambda(\lambda_e; T_b)$ .
- $T_\lambda := T_\lambda(\lambda_e; T_b)$ , corrected for the SSE.
- $T_\lambda := T_\lambda(\lambda_e; T_b)$ , corrected for SSE and non-linearity.

### Conversion to reference conditions:

- $T_\lambda = T_\lambda\{\lambda_e; T_b; I(l)\}$ , corrected to RH = 0 % (only if  $\lambda_r = 950$  nm).
- Reference wavelength  $\lambda_r$ :  $T_\lambda := T_\lambda\{\lambda_r; T_b; I(l)\}$ .
- Base temperature 20°C:  $T_\lambda := T_\lambda\{\lambda_r; 20; I(l)\}$ .
- Lamp currents  $I(j)$ :  $T_\lambda := T_\lambda\{\lambda_r; 20; I(j)\}$ .

### 4.3.2. Specifying uncertainties

#### 4.3.2.1. Representation

Uncertainties have to be specified in accordance with the 'Guide to the expression of uncertainty in measurement', co-edited by BIPM (1993), in terms of the (effective) standard deviations  $sA(i)$ ,  $sB(i)$ ,  $s(i)$ , for the components  $i$  to be taken into consideration. The terms to be included in the propagation of uncertainties should be fully described.

#### 4.3.2.2. Final specifications

- Uncertainty components arranged within the framework given in 4.3.1.
- The uncertainties  $s\{T_\lambda(\lambda_r; I(j))\}$  vs.  $I(j)$  in the specified reference conditions (3.1.2),  $I(j)$  referring to the currents defined in Appendix D.
- The uncertainties  $s\{T_\lambda(\lambda_r; I(j))\}$  vs.  $T_\lambda(\lambda_r; I(j))$  in the specified reference conditions (3.1.2),  $I(j)$  referring to the currents defined in Appendix D.

#### **4.4. Time schedule.**

- The time schedule is given in 2.3.1; in 2.3.2 the reporting has been scheduled: your final report should be sent to VSL within two months after completion of the measurements.

#### **4.5. Editing and publication**

- Format: measurement data: ASCII; text: WP 6.1 or MS Word 5.5.
- Medium:      - Disk  
                      - E-mail

P. Bloembergen.

NMi-VSL, Delft, 1 June 1997.

Enquiry form Appendix to the protocol

1. Confirmation of participation.

Do you wish to participate in the intercomparison as defined above? Yes/No  
If yes, please:

a. Give your complete address together with the names of (at least) two contact persons; furthermore:

- Telephone number(s).
- Fax number(s).
- E-mail address(es).

b. Respond to the following questions / requests (2 - 4) for information.

2. Circulation schemes.

Do you agree with the circulation schemes, as proposed, and the associated operations conditions? Yes/No. If not, please give your comment.

3. Specification of local technical conditions.

3.1. Fixed points

- Fixed-point reference blackbody radiators (Ag, Au, Cu) available in your institute.

3.2. Reference thermometer

- Reference wavelengths (around 650 and 950 nm) available for the realization of the ITS-90.
- Half-width of corresponding spectral response functions.
- Aperture ratio; f-number.
- Target distance.
- Target field dimensions.

3.3. Lamp provisions

- Maximum current of your current supply; stability at maximum current.
- Is a circulating water thermostat to control the lamp base temperature implemented in your system?
- Lamp base temperature, normally set when operating the lamp.

3.4. Ambient conditions

- $T_{amb}$ , Relative Humidity (RH); mean, maximum and minimum values.

4. Technical aspects, reporting

You are invited to give your comments especially to Sections 3 and 4 of the Protocol, such as to contribute to drafting its final version, which should have the function of a guideline to the ensuing intercomparison.

You are requested to send us the filled-in enquiry form within one month after the date, attached to the present draft Protocol.

## Appendix II. Uncertainty budgets

The uncertainty budgets of each participant are presented in this appendix. Reference is made to the CCT-WG5 document, dated November 20<sup>th</sup> 2002 "Uncertainty budgets for realization of scales by radiation thermometry" [1]. The paper is a joint effort of the working group on radiation thermometry of the Consultative Committee for Thermometry (CCT) summarizing the knowledge and experience of all experts in this field.

Realization of the ITS-90 by radiation thermometry is a complex exercise involving a large number of operations and with many influencing parameters. The following paragraphs present the model that can be used for the calculation of the uncertainties as presented in the last chapter of ref [1]. The participant uncertainty budgets are presented along this model.

### Equation models for the calculation of the uncertainty

According to the Guide to the Expression of Uncertainty in Measurement [3] the combined standard uncertainty  $u_c(y)$  is derived as the positive square root of the combined variance  $u_c^2(y)$  obtained from

$$u_c^2(y) = \sum_{i=1}^N \left( \frac{\partial f}{\partial x_i} \right)^2 u^2(x_i) \quad (19)$$

where  $u(x_i)$  is a standard uncertainty component and the quantities  $\partial f/\partial x_i$  are the partial derivatives of  $y$ , often referred to as sensitivity coefficients.

Equation models for both the uncertainty calculation for scale realizations and comparisons are proposed in the following paragraphs.

### Equation model for the scale realizations

By referring to the different uncertainty components reported in the tables, the general equation (20) may be adopted where  $N$  denotes the number of doubling steps in the non-linearity measurement and  $c_{19}$  converts the current uncertainty into temperature. Specific equations for the different calibration schemes are obtained by including the appropriate uncertainty components  $u(x_i)$ , as reported in the working document.

$$\begin{aligned} u_c^2(\lambda, T)_{\text{scale}} = & \left[ u(x_1)^2 + u(x_3)^2 + u(x_4)^2 + u(x_5)^2 + u(x_{20})^2 \left( \frac{T}{T_{\text{ref}}} \right)^4 + \left[ u(x_6)^2 + u(x_7)^2 + u(x_8)^2 + u(x_9)^2 + u(x_{10})^2 + u(x_{11})^2 + u(x_{12})^2 \right] \left( \frac{T}{\lambda} \right)^2 \left( \frac{T}{T_{\text{ref}}} - 1 \right)^2 \right. \\ & \left. + \left[ u(x_2)^2 + u(x_3)^2 + N^2 u(x_1)^2 + u(x_5)^2 + u(x_6)^2 + u(x_7)^2 + u(x_8)^2 + u(x_{22})^2 \right] \left( \frac{\lambda T^2}{c_2} \right)^2 + c_{19}^2 u(x_9)^2 + u(x_2)^2 + u(x_3)^2 \right] \end{aligned} \quad (20)$$

Table 3 of the report summarizes the uncertainty components in the realization of the ITS-90. Two categories of uncertainty are introduced, i.e., a) normal and b) best, referring to uncertainties that a) can be easily obtained at present in national metrology institutes, b) can be obtained with considerable effort by the small number of leading workers in the field. It is worth noting that not all of the components in this table apply for all three realization schemes. As presented in Table 4, the participants realize their scale according to

Participant	NMi-VSL	NPL	CSIRO	KRISS	NIM	NMC	NRLM	VNIIM	NIST	NRC	CENAM	INM	IMGC	PTB
Scheme	3	1	3	3	3	3	3	1	2	3	3	3	3	1

In the following sections the uncertainty budgets are presented as described in each participant comparison report. Additional information from the participants is needed for further harmonization according to the scheme outlined above.

## NMi-VSL

The uncertainty budget(s) as presented in the participant report is quoted below:

Source of uncertainty	Type	Uncertainty ( $2\sigma$ ) /°C				
		$t_{Ag}$	$t_{Au}$	1300 °C	1500 °C	1700 °C
<b>Fixed point</b>						
Realization of fixed point	B	0.017	0.020	0.027	0.035	0.043
Emissivity of fixed point	B	0.001	0.001	0.001	0.001	0.002
<b>Pyrometer</b>						
Response	A+B	0.016	0.013	0.017	0.022	0.027
Linearity	B	0.002	0.002	0.003	0.004	0.005
SSE	B	0.003	0.003	0.005	0.006	0.007
Wavelength	B	0.000	0.008	0.033	0.059	0.089
Drift	B	0.100	0.117	0.163	0.207	0.257
<b>Lamp</b>						
Positioning	B	0.105	0.123	0.171	0.217	0.268
Current	A+B	0.109	0.106	0.117	0.135	0.154
Emissivity	B	0.006	0.007	0.010	0.012	0.015
Transmission of window	B	0.001	0.001	0.002	0.002	0.003
Quality of polynomial fit	A	0.052				
Total ( $2\sigma$ )		0.19	0.21	0.27	0.34	0.42
Total ( $1\sigma$ )		0.10	0.10	0.14	0.17	0.21

## NPL

The uncertainty budget(s) as presented in the participant report is quoted below:

		Uncertainty (°C)	
Source of uncertainty	Type	Ag point	Au point
Statistical	A	0.009	0.008
Reproducibility of melts and freezes	B	0.020	0.013
Realisation (impurities, emissivity)	B	0.010	0.010
DVM resolution	B	0.001	0.001
Total for fixed point (u)		0.024	0.018
Total for fixed point (U)		0.048	0.036

Source of uncertainty	Type	Uncertainty (°C)				
		962 °C	1064 °C	1300 °C	1500 °C	1700 °C
Realisation of fixed point	B	0.024	0.018	-	-	-
Uncertainty from previous measurements (propagated)		-	-	0.14	0.22	0.30
Lamp radiance temperature: statistical reproducibility resolution of DVM drift in reference lamp during comparison	A A B B	0.010 0.020 0.001 0.050	0.010 0.010 0.001 0.050	0.010 0.050 0.001 0.050	0.010 0.020 0.001 0.050	0.010 0.030 0.001 0.050
Current measurements: reproducibility current stability calibration of DVM resolution of DVM calibration of standard resistor current correction	A A B B B B	N/A 0.030 0.060 0.010 0.005 0.001	N/A 0.030 0.060 0.010 0.005 0.001	N/A 0.020 0.050 0.010 0.005 0.001	N/A 0.030 0.040 0.010 0.005 0.001	N/A 0.030 0.040 0.010 0.005 0.001
Base temperature: stability calibration of DVM resolution of DVM calibration of thermocouple measurement of BTC (10%)	B B B B B	0.005 0.007 0.001 0.007 0.001	0.005 0.003 0.001 0.003 0.000	- - - - -	- - - - -	- - - - -

Interference filter/wavelength: calibration of filter temperature coefficient of filter	B B	- -	- -	0.007 0.010	0.010 0.010	0.012 0.010
Alignment of sources	B	0.020	0.020	0.020	0.020	0.020
Size-of-source effect Detector linearity	B B	0.030 -	0.030 -	0.040 -	0.050 -	0.070
Quality of polynomial fit	A	0.020	0.020	0.020	0.020	0.020
<b>Total standard uncertainty u (excluding wavelength conversion)</b>		<b>0.10</b>	<b>0.10</b>	<b>0.17</b>	<b>0.24</b>	<b>0.32</b>
Conversion to 650 nm due to equation	B	0.09	0.11	0.15	0.21	0.26
<b>Total combined standard uncertainty u</b>		<b>0.13</b>	<b>0.15</b>	<b>0.23</b>	<b>0.32</b>	<b>0.41</b>
<b>Expanded uncertainty U (k=2)</b>		<b>0.27</b>	<b>0.29</b>	<b>0.46</b>	<b>0.64</b>	<b>0.82</b>

# CSIRO

The uncertainty budget(s) as presented in the participant report is quoted below:

The discussion of uncertainties is broken into two sections: Firstly a description of the physical parameters that have an effect on the calibration. Secondly, a table of the numerical values (Table 4) of these uncertainties, combined in accordance with the ISO guide to the expression of uncertainty in measurement [i].

Note: Details of the assumptions and mathematical expressions used to convert these parameters into equivalent uncertainties in temperature are given in [ii].

## **Reference black-body radiator**

1. Emissivity: Uncertainty due to physical dimensions of the blackbody, the emissivity of the surface material, and axial gradients in the crucible.
2. Purity: Estimated from the melt and freeze data using the well-known technique of plotting the temperature vs.  $1/F$  where  $F$  is the fraction of metal melted.
3. Gradients: Conduction losses through the wall of the blackbody due to radiative heat losses.
4. Reproducibility/other: Estimate of other systematic errors, determined by a variety of changes to the system, such as purge gas rate, freeze/melt duration, furnace balance etc.

## **Detector**

1. Short term drift: The measured stability of the sensitivity of the pyrometer over a 12-hour period.

## **Linearity**

1. Random: the uncertainty in the measured linearity, resulting from the detector noise
2. Systematic: The estimate of the inherent uncertainty of a doubling step of the doubler apparatus used to measure the linearity of the detector + amplifier + DVM.

## **Size of source effect**

1. BB SOSE: The uncertainty in the SOSE of the fixed-point black-body
2. Systematics: The estimated systematic errors inherent in the SOSE measurement apparatus.
3. Integration: Uncertainty in the integrated SOSE for the strip, resulting from the numerical integration technique used.
4. Strip width: Uncertainty in the SOSE due to uncertainty in the measurement of the width of the lamp filament
5. Curve fit: Uncertainty in the SOSE resulting from the deviation of the fitted curve to the measured SOSE points.

## **Spectral parameters**

1. Calibration: The uncertainty in the wavelength calibration of the monochromator.
2. Leakage: The estimated out-of-band sensitivity of the pyrometer
3. Temperature coefficient: Uncertainty due to known temperature coefficient of the interference filter and the long term (over months) pyrometer temperature stability
4. Reproducibility: The type-A uncertainty derived from repeated measurements of the effective wavelength of the pyrometer.
5. Stability: The measured long term stability of the interference filter

## **Lamp**

1. Base temp: Uncertainty of the measurement of the lamp base temperature.
2. Horiz. posn. : Uncertainty arising from the ability to set the lamp to the specified transverse position.
3. Rotation: Uncertainty arising from the ability to set the lamp to the specified angular position.

4. Supply stability: Short term current stability of the lamp supply.
5. Thermal EMFs: A  $0.01\ \Omega$  resistor was used as a current shunt, thus contribution from stray thermo-voltages may affect the current measurement.
6. DVM calibration: The DVM is calibrated yearly, and this component takes account of drifts over this period.
7. Shunt calibration: The calibration uncertainty of the shunt resistor used to measure the lamp current.
8. Window transmittance: Changes in transmission due to non-reproducibility of the cleaning of the lamp window. No account is made for changes in the window transmittance during the calibration due to effects such as deposition of tungsten etc.)
9. Prism reflectance: Change in pyrometer sensitivity between the prism position for viewing the fixed point and that for viewing the lamp.
10.  $dT/d\lambda$ : Reference wavelength: An estimate of 3% in  $dT_R/d\lambda$ , and a maximum shift of 0.5nm is allowed for in the error budget in converting to the reference wavelength

### **Other parameters**

Several other parameters, for which the uncertainty contribution was considered negligible were:

1. DVM resolution for lamp current measurement.
2. DVM resolution for photocurrent measurement.
3. Detector noise: Signals were averaged over a 5-minute period, resulting in negligible contribution to the uncertainty from the noise in the detector system.
4. Neutral Density filters: Not applicable, since we use the pyrometer to step from the gold point in a single step.
5. Correction of RH: As absorption due to water vapour is negligible at 650nm, no explicit correction is included.

Table 37: Summary of the numerical values of the uncertainty sub-components in the calibration of strip lamps at CSIRO, and their combination into an overall uncertainty estimate.

$\lambda(\text{nm}) = 649.85$

Tref (K) = 1337.33

	T(K)	1235	1337	1573	1773	1973
I(A)	4.48	5.17	7.19	9.24	11.5	
K/nm	0.111	0.131	0.186	0.242	0.307	
K/A	156	141	104	93	87	

Compt.	Sub-component	semi-range or 95% C.L.	$\mu_{\text{I}}$	units	Type	$v_{\text{I}}$	Temp. (deg. C)					
							962	1064	1300	1500	1700	
component uncertainty ( $1\sigma$ ) (mK)												
$\lambda$	calibration	0.02	0.012	nm	B	8	2	0	5	10	17	
	leakage	0.3	1.7E-01	ppm	B	2	4	0	4	6	6	
	temp. coeff.	0.3	0.2	K	B	8	0	0	1	2	2	
	reproducibility		0.010	nm	A	8	1	0	4	9	14	
	stability	0.01	0.006	nm	B	2	1	0	2	5	8	
Ref. BB	emissivity	5.10E-05	2.9E-05	ratio	B	8	2	2	3	4	5	
	purity	10	5.8	mK	B	2	5	6	7	8	9	
	wall gradients	1	0.6	mK	B	2	1	1	1	1	1	
	reprod/other	4	2.3	mK	B	2	2	2	3	3	3	
Detect.	short term drift	1.00E-04	5.8E-05	ratio	A	2	4	5	6	8	10	
SOSE	BB SOSE		2.0E-05	ratio	B	2	1	2	2	3	4	
	systematics		1.0E-05	ratio	B	2	1	1	1	1	2	
	integration		1.0E-05	ratio	B	2	1	1	1	1	2	
	strip width		1.0E-05	ratio	A	2	1	1	1	1	2	
	curve fit		1.0E-05	ratio	A	8	1	1	1	1	2	
Linearity	random		3.0	ppm	A	8	0	0	1	1	1	
	systematic		6.0	ppm/step	B	2	1	0	2	5	8	
Lamp	base temp.	40	23.1	mK	A	40	2	2	1	0	0	
	horiz. posn.	8.0E-05	4.6E-05	ratio	A	2	3	4	5	7	8	
	rotation	2.0E-05	1.2E-05	ratio	A	2	1	1	1	2	2	
	supply stab.	3.0	1.7	ppm	B	40	1	1	1	1	2	
	thermal EMFs	0.5	0.3	uV	B	8	5	4	3	3	3	
	DVM calib.	15	8.7	ppm	B	40	6	6	6	7	9	
	shunt calib.	2	1.2	ppm	B	40	1	1	1	1	1	
	window trans.	1.00E-04	5.8E-05	ratio	A	2	4	5	6	8	10	
	prism refl.	3.00E-05	1.7E-05	ratio	B	2	1	1	2	2	3	
	dT/d $\lambda$	3.00E-02	1.7E-02	rel. err.	B	8	0	0	1	1	1	
TOTAL	$\mu_c$			mK			12.98	13.13	17.78	24.99	34.33	
	$v_{\text{eff}}$						210	24	28	38	41	
	k						1.97	2.06	2.05	2.03	2.02	
	$\mu_{95\%}$			mK			26	27	36	51	69	

Temp. (C)	$\mu_{95\%}$ (mK)
962	26
1000	26
1064	27
1100	29
1200	32
1300	36
1400	44
1500	51
1600	60
1700	69

## KRISS

The uncertainty budget(s) as presented in the participant report is quoted below:

Table 10. Effective standard deviations of calibrations of the lamps at the specified reference conditions.

Effective standard deviation (°C)	Current of C564 Lamp (A)	Current of C681 Lamp (A)	Temp (°C)
0.085	4.480	5.508	964
0.090	4.721	5.822	1002
0.095	5.169	6.399	1066
0.075	5.322	6.594	1086
0.100	5.441	6.745	1102
0.115	6.272	7.795	1201
0.135	7.194	8.948	1301
0.160	8.189	10.183	1402
0.185	9.242	11.487	1502
0.210	10.347	12.851	1602
0.245	11.502	14.273	1703

Table 9: The budgets of uncertainties for the calibration of the lamps

Type	Temperature	964 °C	1066 °C	1086 °C	1703°C
Source of uncertainty		Standard deviation			
Reference blackbody radiator					
B	Impurity	0.008	0.010	0.010	0.021
B	Temp gradient along cavity wall	0.017	0.019	0.020	0.042
B	Emissivity	0.003	0.004	0.004	0.009
B	Temp difference across cavity wall	0.001	0.001	0.001	0.002
Reference thermometer					
B	Ratio of photo current -measurement	0.007	0.008	0.008	0.018
B	Ratio of photo current -resolution	0.009	0.003	0.004	0.003
A	Non-linearity	0.034	0.040	0.000	0.088
A	SSE	0.034	0.040	0.042	0.088
B	Spectral response function	0.017	0.003	0.000	0.138
B	Blocking at the side band	0.000	0.000	0.000	0.003
B	Mean effective wavelength	0.000	0.000	0.000	0.003
Transfer Lamps					
A	Lamp current, as set	0.002	0.002	0.001	0.000
B	Lamp current, as prescribed	0.002	0.002	0.001	0.000
Radiance temperature					
B	Short term stability	0.002	0.001	0.001	0.000
B	Drift	0.017	0.019	0.020	0.042
B	Dependence on wavelength	0.001	0.001	0.001	0.002
B	Dependence on base temp.	0.006	0.002	0.002	0.000
A	Alignment	0.017	0.019	0.020	0.042
B	Target field	0.017	0.019	0.020	0.042
B	Cleaning of the window	0.004	0.005	0.005	0.011

Lamp-thermometer composite					
A	Repeatability of radiance temperature	0.019	0.006	0.009	0.007
B	Correction for SSE	0.034	0.040	0.042	0.088
B	Correction for SSE & non-linearity	0.034	0.040	0.000	0.088
B	Conversion to reference wavelength	0.001	0.001	0.001	0.002
B	Conversion to reference base temperature	0.000	0.000	0.000	0.000
B	Conversion to prescribed lamp current	0.013	0.012	0.012	0.010
Effective standard deviation of type A		0.050	0.061	0.047	0.132
Effective standard deviation of type B		0.060	0.069	0.058	0.202
Overall effective standard deviation		0.085	0.095	0.070	0.245

5/9

SSE corrections  $I_1(t_{Ag}, \lambda)$ , current with furnace SSE correction  $I_2(t_{Ag}, \lambda)$ , current with furnace and lamp SSE correction  $I_3(t_{Ag}, \lambda)$  are as following separately:  
C564: 4.46580A, 4.46558A, 4.46604A  
C681: 5.49624A, 5.49244A, 5.49316A

### 2.3 Lamp resistance and ambient temperature $R_{amb}$ , $T_{amb}$

Before sent the lamps to go to PSB of Singapore,  $R_{amb}$  and  $T_{amb}$  be measured. The bridge 6010B and a 0.1 Ohm standard resistor is used. The measurement currents are 1mA and 1.41mA.  
Lamp1(C564):  $R_{amb}(1)=0.039849$  Ohm,  $T_{amb}(1)=20.80$ C  
Lamp2(C681):  $R_{amb}(2)=0.033987$  Ohm,  $T_{amb}(2)=20.53$ C

## 3. Uncertainty

### 3.1 Effective wavelength

The uncertainty of determination of the effective wavelength is shown as Table 6.  
 $u_i$  is the standard uncertainty of uncertainty component

$$u_c = \sqrt{\sum_1^5 u_i^2} = 0.036\text{nm}, \text{ equivalent freedom } v_{eff} = u_c^4 / \sum_1^5 \frac{u_i^4}{v_i} = 17.$$

**Table 6. Uncertainty of effective wavelength**

i	component of uncertainty	type	estimated		K	$u_i$	$v_i$
				nm			
1	wavelength repeatability of monochromometer	A		0.02	2.50	0.008	8
2	measurement of filter transmittance	A		0.01	2.00	0.005	2
3	wavelength calibration of monochrometer	B		0.02	1.73	0.012	8
4	measurement of detector response	B	3%	0.05	1.73	0.029	8
5	difference of room temperature	B	1C	0.025	1.73	0.014	8
	combined standard uncertainty ( $u_c$ )					0.036	17

### 3.2 Realization of silver freezing point

The uncertainty of realization of the silver freezing point is shown as Table 7.  
 $u_i$  is the standard uncertainty of uncertainty component

$$u_c = \sqrt{\sum_1^8 u_i^2} = 0.0203\text{C}, \text{ equivalent freedom } v = u_c^4 / \sum_1^8 \frac{u_i^4}{v_i} = 26.$$

**Table 7. Uncertainty of realization of silver freezing point**

i	component of uncertainty	type	estimated		K	$u_i$	$v_i$
				C			
1	repeatability of realization	A		0.0136	1.00	0.0136	10
2	emissivity of cavity	B	0.00008	0.0056	1.73	0.0032	8
3	impurity of sample	B		0.0100	1.73	0.0058	8
4	gradient across cavity bottle	B		0.0004	1.73	0.0002	8
5	stability of Ag point lamp	B		0.0100	1.73	0.0058	8
6	effective wavelength	B	0.036nm	0.0040	1.00	0.0040	17
7	electric measurement equipment	B		0.0040	1.73	0.0023	8
8	SSE	B	0.000163	0.0114	1.00	0.0114	6
	combined standard uncertainty ( $u_c$ )					0.0203	26

### 3.3 Extension of temperature scale

The uncertainty of the radiance temperature of C564 and C681 is shown as Table 8 and Table 9.

**Table 8. Uncertainty of temperature of C564**

t	NL	$t_i(\text{AB})$	$\lambda_{\text{v1}}$	$\lambda_e$	SSE	lamp	elec.	$\Delta T$	$t_b$			$\lambda_{\text{v1}}$	
C	C	C	C	C	C	C	C	C	C	$U(k=2.68)$ p=0.99)	$u_{11}$	$u_{e11}$	
961.78	0.0062	0.0000	0.0203	0.0000	0.0000	0.0073	0.0173	0.0171	0.0038	0.0052	0.034	0.090	0.106
1000	0.0055	0.0007	0.0216	0.0002	0.0022	0.0077	0.0173	0.0163	0.0044	0.0040	0.034	0.091	0.113
1100	0.0046	0.0012	0.0251	0.0004	0.0084	0.0090	0.0173	0.0153	0.0007	0.0017	0.037	0.098	0.133
1200	0.0058	0.0020	0.0289	0.0011	0.0155	0.0103	0.0173	0.0152	0.0033	0.0007	0.042	0.113	0.154
1300	0.0071	0.0042	0.0329	0.0032	0.0235	0.0118	0.0173	0.0157	0.0000	0.0000	0.049	0.131	0.177
1400	0.0118	0.0056	0.0373	0.0044	0.0324	0.0133	0.0173	0.0166	0.0028	0.0000	0.058	0.156	0.203
1500	0.0094	0.0057	0.0419	0.0059	0.0422	0.0150	0.0173	0.0176	0.0011	0.0000	0.067	0.180	0.231
1600	0.0079	0.0085	0.0467	0.0072	0.0528	0.0167	0.0173	0.0187	0.0020	0.0000	0.078	0.209	0.260
1700	0.0033	0.0083	0.0518	0.0096	0.0644	0.0185	0.0173	0.0196	0.0019	0.0000	0.090	0.240	0.293
		$v_1$	$v_2$	$v_3$	$v_4$	$v_5$	$v_6$	$v_7$	$v_8$	$v_9$	$v_{10}$	$v_{\text{eff}}$	$v_{11}$
961.78	2	1	26	1	17	8	8	16	8	8	53		
1000	2	11	26	16	17	8	8	15	8	8	53		
1100	2	25	26	16	17	8	8	13	8	8	56		
1200	2	51	26	16	17	8	8	12	8	8	65		
1300	2	25	26	16	17	8	8	11	8	8	69		
1400	2	26	26	16	17	8	8	11	8	8	67		
1500	2	30	26	16	17	8	8	11	8	8	61		
1600	2	33	26	16	17	8	8	10	8	8	55		
1700	2	51	26	16	17	8	8	10	8	8	49		

7/9

**Table 9. Uncertainty of temperature of C681**

$t$	NL	$t_c(A_E)$	$\lambda_{v1}$	$\lambda_e$	SSE	lamp	elec.	$\Delta t$	$t_b$	$\lambda_{v1}$		
C	$u_1$	$u_2$	$u_3$	$u_4$	$u_5$	$u_6$	$u_7$	$u_8$	$u_9$	$U(k=2.68)$	$u_{11}$	$u_{e,11}$
C	C	C	C	C	C	C	C	C	C	$p=0.999$	C	C
961.78	0.0137	0.0000	0.0203	0.0000	0.0000	0.0079	0.0173	0.0151	0.0036	0.0037	0.035	0.093
1000	0.0078	0.0007	0.0216	0.0002	0.0022	0.0084	0.0173	0.0148	0.0041	0.0025	0.034	0.091
1100	0.0050	0.0012	0.0251	0.0004	0.0084	0.0097	0.0173	0.0144	0.0006	0.0008	0.036	0.098
1200	0.0035	0.0020	0.0289	0.0011	0.0155	0.0112	0.0173	0.0147	0.0010	0.0000	0.042	0.112
1300	0.0059	0.0042	0.0329	0.0032	0.0235	0.0128	0.0173	0.0154	0.0019	0.0000	0.049	0.131
1400	0.0006	0.0056	0.0373	0.0044	0.0324	0.0144	0.0173	0.0164	0.0009	0.0000	0.057	0.153
1500	0.0049	0.0057	0.0419	0.0059	0.0422	0.0162	0.0173	0.0175	0.0022	0.0000	0.067	0.180
1600	0.0103	0.0085	0.0467	0.0072	0.0528	0.0181	0.0173	0.0187	0.0025	0.0000	0.079	0.211
1700	0.0070	0.0083	0.0518	0.0096	0.0644	0.0201	0.0173	0.0198	0.0012	0.0000	0.090	0.242
												0.293
												0.306
961.78	2	1	26	1	17	8	8	13	8	8	37	
1000	2	11	26	16	17	8	8	13	8	8	51	
1100	2	25	26	16	17	8	8	12	8	8	55	
1200	2	51	26	16	17	8 *	8	11	8	8	63	
1300	2	25	26	16	17	8	8	11	8	8	69	
1400	2	26	26	16	17	8	8	10	8	8	66	
1500	2	30	26	16	17	8	8	10	8	8	61	
1600	2	33	26	16	17	8	8	10	8	8	56	
1700	2	51	26	16	17	8	8	10	8	8	50	

The uncertainty of the result of extension of temperature scale of C564 and C681 includes 10 or 11 uncertainty components.

#### A type evaluation of uncertainty

- (1)  $u_1$ , the standard uncertainty of the repeatability of extension experiments .

The standard deviation of the average of three times extension experiments. This depends on the repeatability of aiming lamp, reproducibility of lamp itself and the clean of the window of lamp.

- (2)  $u_2$ , non-linearity correction. That is the combined standard uncertainty of linearity measurement of photoelectric comparator system.

#### B type evaluation of uncertainty

- (3)  $u_3$ , realization of silver freezing point.  $u_3=0.0203\text{C}$ ,  $v_3=26$ .

- (4)  $u_4$ , correcting the radiance temperature to the local wavelength  $\lambda_{rl}$ .

- (5)  $u_5$ , determination of effective wavelength.

$$\text{the combined standard uncertainty of effective wavelength, } u_c(\lambda_e)=0.036\text{nm. } u_5=\frac{T^2}{\lambda e} \left( \frac{1}{T_{Ag}} - \frac{1}{T} \right) u_c(\lambda_e)$$

- (6)  $u_6$ , SSE correction of transfer lamp.

$$\text{The accuracy of SSE coefficient } q \text{ is } 15\%. \text{ Equality distribution. At temperature } t, u_6=0.15 q \frac{\lambda e T^2}{c_2} / \sqrt{3}$$

- (7)  $u_7$ , stability of transfer lamp.

Suppose that the instability is  $0.03\text{C}$  and equality distribution.  $u_7=0.03/\sqrt{3}=0.013\text{C}$  .

- (8)  $u_8$ , electric measurement equipment.

including the accuracy of digital voltmeter hp3458A and standard resistor they are used for measuring the current of transfer lamp, ripple and noise of power supply of constant current.

- (9)  $u_9$ , the correction of the deviation of lamp current.

The experiment software corrects the difference between measured lamp current and the set current automatically. Suppose the absolute value of the difference is  $\Delta I$ , and the error of correction is 1%, then

$$\Delta t = 1\% \cdot \Delta I / \frac{dI}{dt}, \text{ equality distribution, } u_9 = \Delta t / \sqrt{3}.$$

- (10)  $u_{10}$ , measurement and instability of base temperature ,  $0.1\text{C}$ .

$$u_{10}=0.1 \times \frac{dt}{dt_b} / \sqrt{3}, \quad v_{10}=8$$

Combining 10 items of standard uncertainties mentioned above, the combined standard uncertainty  $u_c = \sqrt{\sum_{i=1}^{10} u_i^2}$ , and the equivalent freedom  $v_{eff} = u_c^4 / \sum_{i=1}^{10} u_i^4$ . Uncertainty  $u_c$  of temperature  $t_s$  of C564 and C681 is in the condition,  $\lambda_{rl}=659.54\text{nm}$ , lamp current specifies by CCT inter-comparison document, base temperature  $t_b=20.0\text{C}$ , ambient temperature  $t_{room}=20\text{C}$ .

From 962 up to 1700C,  $u_c=0.034 \sim 0.090\text{C}$ ,  $U=0.090 \sim 0.24\text{C}$  ( $K=2.68$ ,  $p=0.99$ ,  $v=37-66$ ).

- (11)  $u_{11}$ , correcting the radiance temperature to the reference wavelength  $\lambda_r$ ,  $650\text{nm}$

The correction value is  $\frac{dT}{d\lambda} (\lambda_r - \lambda_{rl})$ , the standard deviation of  $\frac{dT}{d\lambda}$  is 10% of its absolute value.

$$u_{11}=0.10 \times \frac{dT}{d\lambda} (\lambda_r - \lambda_{rl})$$

$$u_{11}=0.106 \sim 0.293\text{C}$$

Combining  $u_{11}$  and  $u_c$ , represented as  $u_{c11}$ .

$$u_{c11} = \sqrt{u_{11}^2 + u_c^2} = \sqrt{\sum_{i=1}^{11} u_i^2}.$$

$u_{c11}=0.111 \sim 0.306\text{C}$ , from  $t_{Ag}$  up to 1700C.

Because the freedom of  $u_{11}$  is not given, so that the effective freedom of  $u_{c11}$  can not be calculated exactly and the extended uncertainty  $U_{c11}$  can not be provided with the level of confidence.

## 4. Final results

## NMC

The uncertainty budget(s) as presented in the participant report is quoted below:

Table D1. Uncertainty budget of lamp 1 (C564) (all the uncertainties are in °C)

I(j) (A)	T <sub>λ</sub> final (°C)	Prop. of s(Tag)	Prop. of s(λe)	s(λr)	s(I)	s(Tb)	s(rnd)	s(pos)	s(drift signal)	s(drift lamp)	s(amb)	s(NL)	u	U (k=2 95%)
4.480	963.689	0.057	0.000	0.014	0.031	0.005	0.050	0.045	0.019	0.090	0.069	0.005	0.149	0.30
4.721	1001.677	0.061	0.006	0.015	0.029	0.003	0.046	0.048	0.020	0.090	0.073	0.005	0.152	0.30
5.169	1065.834	0.067	0.017	0.017	0.026	0.002	0.046	0.053	0.022	0.090	0.081	0.006	0.161	0.32
5.322	1086.178	0.069	0.021	0.018	0.025	0.002	0.045	0.055	0.023	0.090	0.083	0.006	0.164	0.33
5.441	1101.600	0.071	0.024	0.018	0.024	0.001	0.045	0.056	0.023	0.090	0.085	0.006	0.166	0.33
6.272	1201.414	0.081	0.044	0.021	0.022	0.001	0.045	0.064	0.027	0.090	0.098	0.007	0.185	0.37
7.194	1301.399	0.093	0.067	0.025	0.020		0.045	0.073	0.031	0.090	0.112	0.008	0.208	0.42
8.189	1401.654	0.105	0.092	0.028	0.019		0.045	0.083	0.035	0.090	0.127	0.009	0.234	0.47
9.242	1501.818	0.118	0.120	0.032	0.018		0.045	0.093	0.039	0.090	0.142	0.010	0.265	0.53
10.347	1601.973	0.131	0.150	0.037	0.017		0.045	0.104	0.043	0.090	0.159	0.011	0.299	0.60
11.502	1702.323	0.146	0.183	0.041	0.016		0.045	0.116	0.048	0.090	0.176	0.012	0.337	0.67

Table D2. Uncertainty budget of lamp 2 (C681) (all the uncertainties are in °C)

I(j) (A)	T <sub>λ</sub> final (°C)	Prop. of s(Tag)	Prop. of s(λe)	s(λr)	s(I)	s(Tb)	s(ran d.)	s(pos. )	s(drift signal)	s(drift lamp)	s(Tamb)	s(NL)	u	U (k=2 95%)
5.508	962.967	0.057	0.000	0.014	0.024	0.003	0.048	0.046	0.019	0.019	0.069	0.005	0.118	0.24
5.822	1001.208	0.061	0.006	0.015	0.022	0.002	0.044	0.048	0.020	0.019	0.073	0.005	0.122	0.24
6.399	1065.499	0.067	0.017	0.017	0.020	0.001	0.042	0.053	0.022	0.019	0.081	0.005	0.132	0.26
6.594	1085.836	0.069	0.021	0.018	0.020	0.001	0.042	0.055	0.023	0.019	0.083	0.006	0.136	0.27
6.745	1101.240	0.071	0.024	0.018	0.019	0.001	0.042	0.056	0.023	0.019	0.085	0.006	0.139	0.28
7.795	1201.236	0.081	0.044	0.021	0.017		0.042	0.065	0.027	0.019	0.098	0.007	0.161	0.32
8.948	1301.468	0.093	0.067	0.025	0.016		0.042	0.074	0.031	0.019	0.112	0.008	0.187	0.37
10.183	1401.710	0.105	0.092	0.028	0.015		0.042	0.084	0.035	0.019	0.127	0.009	0.217	0.43
11.487	1501.828	0.118	0.120	0.032	0.014		0.042	0.094	0.039	0.019	0.142	0.010	0.249	0.50
12.851	1601.891	0.131	0.150	0.037	0.014		0.042	0.105	0.043	0.019	0.159	0.011	0.285	0.57
14.273	1701.690	0.146	0.182	0.041	0.013		0.042	0.116	0.048	0.019	0.176	0.012	0.325	0.65

# NRLM

- 3.2. Specifying uncertainties.
- 3.2.1. Representation.
  - I . Reference blackbody radiator.
    - $U_{T90}$ : Realization of the reference temperature
    - $U_{imp}$ : Impurities;
    - $U_{emj}$ : Emissivity;
    - $U_{tdif}$ : Temperature difference across the bottom section of the cavity in view;.
  - II .Reference Thermometer
    - II .1. Ratio of photo-currents
      - $U_{phot}$ : Photo current measurement;
      - $U_{per}$ : Photo current resolution;
      - $U_{lin}$ : Linearity;
    - II .2. Size of source effect.
      - $U_{sse}$ : Size of source effect
  - II .3. Spectral parameters.
    - $U_{srf}$ : Spectral response function;
    - $U_{stf}$ : Stability of the interference filter;
    - $U_{bloc}$ : Blocking of the filter wing;
- III . Transfer lamps.
  - III .1. Lamp current.
    - $U_{les}$ : Lamp currents  $I(l)$  as set.
    - $U_{lep}$ : Lamp currents  $I(l)$  as prescribed.
  - III .2. Radiance temperature.
    - $U_{sts}$ : Short term stability.
    - $U_{ridr}$ : Drift.
    - $U_{rdw}$ : Dependence on wavelength.
    - $U_{ridt}$ : Dependence on temperature.
- Residual parameters
  - $U_{ralign}$ : Alignment (spatial and angular distribution of radiance)
  - $U_{tf}$ : Target field

$U_{\text{rew}}$ : Cleaning of the window

IV. Lamp-thermometer composite parameters.

$U_{\text{rt}}$ : Radiance temperature

$U_{\text{rts}}$ : Radiance temperature, corrected for the SSE

$U_{\text{rtsl}}$ : Radiance temperature, corrected for the SSE and non-linearity

$U_{\text{refc}}$ : Conversion to reference conditions:

$U_{\text{rw}}$ : Reference wavelength

$U_{\text{bt}}$ : Base temperature 20C

$U_{\text{lc}}$ : Lamp currents  $I(j)$

3.2.2. Final specifications.

$I(j)$  and  $T$  in the specified reference conditions vs. the uncertainties  $s$  are shown in Table C.

Table D shows values of uncertainty components arranged within the framework given in 3.1.

TABLE D C 564

TypeA	TypeB	Calculated from 564.1 data	962	1000	1064	1085	1100	1200	1300	1400	1500	1600	1700			
U <sub>90</sub>	○	standard uncertainty	0.1	K	0.083	0.088	0.097	0.100	0.102	0.118	0.134	0.152	0.171	0.190	0.211	
U <sub>1apn</sub>	○		0.99999													
U <sub>em</sub>	○		± 0.0005		0.034	0.037	0.040	0.042	0.043	0.049	0.056	0.063	0.071	0.079	0.088	
U <sub>diff</sub>	○		± 0.01	K	± 2mm											
U <sub>fm</sub>	○		0.03 %		0.021	0.022	0.024	0.025	0.026	0.029	0.034	0.038	0.043	0.048	0.053	
U <sub>per</sub>	○		0.05 pA		0.039	0.024	0.012	0.009	0.008	0.003	0.001	0.001	0.000	0.000		
U <sub>lin</sub>	○		0.05 %/deg		-0.008	-0.006	-0.001	0.000	0.001	0.009	0.018	0.028	0.039	0.051	0.065	
U <sub>ssu</sub>	○		0.03 %		0.021	0.022	0.024	0.025	0.026	0.029	0.034	0.038	0.043	0.048	0.053	
U <sub>inf</sub>	○		0.1 nm		-0.017	-0.012	-0.003	0.000	0.002	0.019	0.038	0.060	0.083	0.109	0.138	
U <sub>eff</sub>	○		0.05 nm													
U <sub>tot</sub>	○		1.00E-06													
U <sub>BS</sub>	○		0.0045 %													
U <sub>ep</sub>	○		---													
U <sub>res</sub>	○		o of 16 data		K	0.010	0.012	0.004	0.003	0.003	0.002	0.002	0.003	0.002	0.002	
U <sub>drh</sub>	○		Difference of No. 2 No. 1		K	-0.019	-0.025	-0.003	-0.012	-0.013	-0.011	-0.030	-0.029	-0.031	-0.022	
U <sub>rw</sub>	○		10% of dV/Tm		K	0.008	0.009	0.010	0.010	0.010	0.011	0.013	0.014	0.016	0.018	
U <sub>rdt</sub>	○		5% of dV/K(Tb)		K	-0.004	-0.004	-0.002	-0.002	-0.002	-0.001					
U <sub>ralign</sub>	○		RLLD 0.05mm ANG 0.1°		K	0.020	0.022	0.024	0.025	0.025	0.029	0.033	0.037	0.042	0.047	
U <sub>rf</sub>	○		---													
U <sub>rew</sub>	○		0.03 %		0.021	0.022	0.024	0.025	0.026	0.029	0.034	0.038	0.043	0.048	0.053	
U <sub>rt</sub>	○		U <sub>Trin</sub> +U <sub>tem1</sub> +U <sub>per</sub> +U <sub>err</sub>		K	0.101	0.101	0.108	0.112	0.114	0.132	0.154	0.179	0.207	0.238	0.272
U <sub>rs</sub>	○		U <sub>rt</sub> +SSE		K	0.104	0.104	0.111	0.114	0.117	0.136	0.158	0.183	0.211	0.243	0.277
U <sub>rls</sub>	○		U <sub>rt</sub> +SSE+non-L linear		K	0.104	0.104	0.111	0.114	0.117	0.136	0.159	0.185	0.215	0.248	0.285
U <sub>rw</sub>	○		dλ/e-a+(λ-r-λ)da		K	0.014	0.015	0.016	0.017	0.017	0.020	0.023	0.026	0.029	0.033	0.036
U <sub>rt</sub>	○		dTB <sub>b</sub> +(20-Tb)db		K	0.013	0.012	0.008	0.005	0.004	0.002	0.000	0.000	0.000	0.000	
U <sub>c</sub>	○		dI(I)-c+(I(j)-I(l))dc		K	0.033	0.032	0.031	0.031	0.032	0.034	0.036	0.039	0.041	0.044	
			combined stand. uncertainty		K	0.116	0.118	0.122	0.126	0.128	0.147	0.173	0.200	0.230	0.263	0.301
			expanded uncertainty		K	0.233	0.236	0.244	0.251	0.256	0.295	0.346	0.400	0.461	0.527	0.601

TABLE D C 68/

TypeA	TypeB	Calculated from 681-1 data	952	1000	1064	1085	1100	1200	1300	1400	1500	1600	1700			
U <sub>Tca</sub>	○	standard uncertainty	0.1	0.1 K	0.083	0.088	0.097	0.100	0.102	0.118	0.134	0.152	0.171	0.190	0.211	
U <sub>tapp</sub>	○		0.99999													
U <sub>tem</sub>	○		$\pm 0.0005$		0.034	0.037	0.040	0.042	0.043	0.049	0.056	0.063	0.071	0.079	0.088	
U <sub>tdif</sub>	○		$\pm 0.01$ K	$\pm 2$ mm												
U <sub>tm</sub>	○		0.03 %		0.021	0.022	0.024	0.025	0.026	0.029	0.034	0.038	0.043	0.048	0.053	
U <sub>per</sub>	○		0.05 pA		0.039	0.024	0.012	0.009	0.008	0.003	0.001	0.001	0.000	0.000		
U <sub>lin</sub>	○		0.005 %/deg		-0.008	-0.006	-0.001	0.000	0.001	0.009	0.018	0.028	0.039	0.051	0.065	
U <sub>sse</sub>	○		0.03 %		0.021	0.022	0.024	0.025	0.026	0.029	0.034	0.038	0.043	0.048	0.053	
U <sub>rf</sub>	○		0.1 nm		-0.017	-0.012	-0.003	0.000	0.002	0.019	0.038	0.060	0.083	0.109	0.138	
U <sub>sf</sub>	○		0.05 nm													
U <sub>loc</sub>	○		1.00E-06													
U <sub>es</sub>	○		0.0045 %													
U <sub>ep</sub>	○		$\sigma$ of 16 data	K	0.009	0.007	0.006	0.003	0.003	0.003	0.001	0.001	0.005	0.001	0.002	
U <sub>sts</sub>	○		Difference of No. 2-No. 1 K		0.035	0.017	0.016	-0.003	-0.014	0.029	0.033	0.034	0.036	0.035	-0.017	
U <sub>trit</sub>	○		10% of dt/1nm	K	0.008	0.009	0.010	0.010	0.010	0.010	0.011	0.013	0.014	0.016	0.018	0.020
U <sub>trw</sub>	○		5% of dt/1K(Tb)	K	-0.002	-0.002	-0.001	-0.001	-0.001	-0.001	-0.001	-0.001	-0.001	-0.001	-0.001	
U <sub>train</sub>	○		RJID 0.05mm AMG 0.1°	K	0.027	0.028	0.031	0.032	0.033	0.038	0.043	0.049	0.055	0.061	0.068	
U <sub>trf</sub>	○															
U <sub>trw</sub>	○		0.03 %		0.021	0.022	0.024	0.025	0.026	0.029	0.034	0.038	0.043	0.048	0.053	
U <sub>trt</sub>	○		UTC(t <sub>tem</sub> +t <sub>pcm</sub> +t <sub>per</sub> +t <sub>sr</sub> )K		0.101	0.101	0.108	0.112	0.114	0.132	0.154	0.179	0.207	0.238	0.272	
U <sub>trs</sub>	○		U <sub>rt-SSE</sub>	K	0.104	0.104	0.111	0.114	0.117	0.136	0.158	0.183	0.211	0.243	0.277	
U <sub>rst</sub>	○		U <sub>rt+SSE+non-Lin</sub> a	K	0.104	0.104	0.111	0.114	0.117	0.136	0.159	0.185	0.215	0.248	0.285	
U <sub>rw</sub>	○		$d\lambda_e \cdot a + (\lambda_e - \lambda_{e0}) da$	K	0.014	0.015	0.016	0.017	0.017	0.020	0.023	0.026	0.029	0.033	0.036	
U <sub>ra</sub>	○		$d(\lambda_b \cdot b) / (20 - 1b) db$	K	0.004	0.002	0.001	0.001	0.002	0.000	0.000	0.000	0.000	0.000		
U <sub>re</sub>	○		$d(l(1) \cdot c + l(1(j)) - l(1)) dc$	K	0.031	0.031	0.031	0.031	0.032	0.034	0.036	0.039	0.042	0.044		
		combined stand. uncert.	K	0.120	0.117	0.124	0.126	0.130	0.152	0.176	0.203	0.234	0.268	0.303		
		expanded uncertainty	K	0.240	0.233	0.248	0.253	0.260	0.304	0.352	0.406	0.468	0.535	0.607		

## VNIIM

The uncertainty budget(s) as presented in the participant report is quoted below:

No	Uncertainty components	Uncertainty values [°C] for T [°C]:			
		961.78	1064.18	1084.62	1700
1.	<u>Reference blackbody radiator</u>				
1.1.	Impurities	0.01	0.01	0.02	
1.2.	Emissivity	0.02	0.02	0.02	
1.3.	Temperature difference across the bottom of cavity	0.01	0.01	0.01	
2.	<u>Reference thermometer</u>				
2.1.	<i>Ratio of photo-currents</i>				
2.1.1.	Photocurrent - measurement	0.01	0.005	0.005	0.03
2.1.2.	Photocurrent - resolution	0.02	0.007	0.007	0.1
2.1.3.	Linearity				0.3
2.2.	Size of source effect	0.08	0.12	0.12	0.2
2.3.	<i>Spectral parameters</i>				
2.3.1.	Spectral response function	0.06	0.05	0.05	0.2
3.	<u>Transfer lamps</u>				
3.1.	Lamp current	0.04	0.03	0.03	0.1
3.2.	Radiance temperature	0.06	0.05	0.05	0.5
3.3.	Residual parameters	0.06	0.04	0.04	0.3
4.	<u>Lamp-thermometer composite parameters</u>				
4.1.	Radiance temperature	0.05	0.04	0.04	0.6
4.2.	Conversion to reference conditions:	0.05	0.03	0.03	0.3
Combined uncertainty u		0.16	0.16	0.16	0.99
Expanded uncertainty U (k=2; 95%)		0.32	0.32	0.32	1.98

## NIST

The uncertainty budget(s) as presented in the participant report is quoted below:

20. The Uncertainty analysis is summarized in Tables C, D, & E below:

Table C: Working Standard lamp Expanded Uncertainties

Source of Uncertainty	Type	Expanded Uncertainties (°C)
Refractive index	B	0.03
Wavelength	B	0.37
Freezing temperature of gold	B	0.30
Second radiation constant	B	0.03
Emissivity of Au	B	0.02
First radiation constant	B	0.00
Ratio of WS signal to Au signal	A	0.03
WS amplifier calibration correction	A	0.01
WS linearity correction	A	0.11
WS size of source correction	A	0.06
WS amplifier gain	B	0.00
Au amplifier calibration correction	A	0.01
Au linearity correction	A	0.11
Au size of source correction	A	0.02
Au amplifier gain	B	0.00
Digital voltmeter	B	0.00
WS current	B	0.11
WS stability	B	0.11
Expanded uncertainty $U = ku_c(T)$ , where $k = 2$		0.53

Table D: Test lamp vs. Au Expanded Uncertainties

Source of Uncertainty	Type	Expanded Uncertainties (°C)
Refractive index	B	0.03
Wavelength	B	0.37
Freezing temperature of gold	B	0.30
Second radiation constant	B	0.03
Emissivity of Au	B	0.02
First radiation constant	B	0.00
Ratio of TL signal to Au signal	A	0.09
TL amplifier calibration correction	A	0.01
TL linearity correction	A	0.11
TL size of source correction	A	0.06
TL amplifier gain	B	0.00
Au amplifier calibration correction	A	0.01
Au linearity correction	A	0.11
Au size of source correction	A	0.02
Au amplifier gain	B	0.00
Digital voltmeter	B	0.00
TL current	B	0.13
TL stability	B	0.11
Expanded uncertainty $U = ku_c(T)$ , where $k = 2$		0.54

Table E: Test lamp Expanded Uncertainties

Source of Uncertainty	Type	Expanded Uncertainties [ °C]							
		Temperature [ °C]							
1. Calibration of the reference radiance temperature lamp relative to the 1990 NIST Radiance Temperature Scale	A	0.37	0.43	0.49	0.56	0.64	0.71	0.80	0.88
2. Test lamp temperature determination	A	0.07	0.09	0.10	0.11	0.13	0.14	0.16	0.18
3. Current measurement	B	0.14	0.13	0.12	0.11	0.11	0.11	0.11	0.10
4. Mean effective wavelength measurement for the NIST Photoelectric Pyrometer	B	0.06	0.04	0.02	0.01	0.05	0.09	0.13	0.18
5. Test lamp alignment	B	0.12	0.14	0.16	0.19	0.21	0.24	0.27	0.30
6. 1990 NIST Radiance Temperature Scale relative to the Thermodynamic Temperature Scale	B	0.21	0.24	0.28	0.32	0.36	0.40	0.45	0.50
Expanded uncertainty $U = ku_c(T)$ , where $k = 2$		0.47	0.54	0.61	0.69	0.78	0.88	0.98	1.09

## **NRC**

The uncertainty budget(s) and calculations as presented in the participant report were not available in Word. Please refer to full report as sent in by NRC (report pages 29 through 42).

## CENAM

The uncertainty budget(s) as presented in the participant report is quoted below:

### 4.3 Uncertainties

#### 4.3.1 Uncertainty components

We detected the uncertainty components listed below. The "S" number in the description is related with the headings in TABLE C and the capital letter inside brackets indicates the type of uncertainty respectively with the described component. The combination of them was carried out as indicated in the "Guide for the expression of uncertainties" of the BIPM [3]. The expanded uncertainty was obtained for  $k = 2$ .

- **S1 (B)**  
Uncertainty on the reference temperature determination (from the silver point blackbody).
- **S2 (B)**  
Uncertainty on the effective wavelength calculation of the utilised pyrometer.
- **S3 (B)**  
Uncertainty due to the resolution in the measurement of the pyrometer's photocurrent.
- **S4 (B)**  
Uncertainty on the determination of the linearity of the photodetector.
- **S5 (B)**  
Uncertainty on the determination of the SSE error.
- **S6 (B)**  
Uncertainty on the measurement of the pyrometer's photocurrent when using different ranges, due to different amplifier's gain.
- **S7 (B)**  
Uncertainty due to the effects of the room lights and the offset of the electronic circuit of the measurement unit of the pyrometer.
- **S8 (B)**  
Uncertainty of the measurements of the digital multimeter connected to the analog output of the measurement unit of the pyrometer.
- **S9 (B)**  
Uncertainty of the digital multimeter utilised to measure the voltage of the shunt resistor to determine the current supplied to the strip filament of the lamps.
- **S10 (B)**  
Uncertainty on the reported value of the shunt resistor (from the manufacturer's report).
- **S11 (A)**  
Uncertainty due to the stability of the radiance temperature of the lamp under study, during its calibration.
- **S12 (B)**  
Uncertainty on the applied wavelength corrections for the determination of the radiance temperature of the lamps.
- **S13 (B)**  
Uncertainty on the applied corrections to the actual values of the supplied currents to get the reference currents specified in the protocol.
- **S14 (B)**  
Uncertainty due to the focusing and the alignment between the pyrometer and the lamp under study.

On the next page

Table C. Estimated uncertainties of the measured radiance temperatures on the calibration of lamps C860 and C864

<b>Lamp C860</b>											
<i>t</i> / °C	961,85	999,85	1063,85	1084,85	1099,85	1199,85	1299,85	1399,85	1499,85	1599,85	1699,85
<i>S1</i> / °C	0,029	0,031	0,034	0,035	0,036	0,041	0,047	0,053	0,060	0,066	0,074
<i>S2</i> / °C	0,000	0,014	0,039	0,048	0,054	0,101	0,153	0,210	0,274	0,343	0,418
<i>S3</i> / °C	0,003	0,002	0,001	0,001	0,001	0,000	0,000	0,000	0,000	0,000	0,000
<i>S4</i> / °C	0,008	0,008	0,009	0,010	0,010	0,011	0,013	0,015	0,016	0,018	0,020
<i>S5</i> / °C	0,040	0,042	0,047	0,048	0,049	0,057	0,065	0,073	0,082	0,092	0,102
<i>S6</i> / °C	0,000	0,000	0,009	0,010	0,010	0,011	0,013	0,015	0,016	0,018	0,020
<i>S7</i> / °C	0,003	0,002	0,001	0,001	0,001	0,000	0,000	0,000	0,000	0,000	0,000
<i>S8</i> / °C	0,001	0,001	0,001	0,001	0,001	0,001	0,001	0,001	0,001	0,001	0,001
<i>S9</i> / °C	0,007	0,007	0,007	0,007	0,007	0,007	0,008	0,008	0,008	0,009	0,010
<i>S10</i> / °C	0,030	0,031	0,032	0,033	0,033	0,035	0,037	0,039	0,042	0,046	0,052
<i>S11</i> / °C	0,003	0,003	0,003	0,003	0,003	0,003	0,003	0,003	0,003	0,003	0,003
<i>S12</i> / °C	0,000	0,000	0,000	0,000	0,000	0,000	0,000	0,000	0,000	0,000	0,000
<i>S13</i> / °C	0,003	0,007	0,004	0,002	0,002	0,005	0,006	0,008	0,001	0,001	0,007
<i>S14</i> / °C	0,199	0,212	0,234	0,241	0,247	0,284	0,324	0,366	0,411	0,459	0,509
<i>S=[Σ(S<sub>j</sub>)]<sup>1/2</sup></i>	0,208	0,221	0,247	0,256	0,262	0,312	0,369	0,434	0,507	0,586	0,673
<i>u (k=2)</i> / °C	0,42	0,44	0,49	0,51	0,52	0,62	0,74	0,87	1,0	1,2	1,3
<b>Lamp C864</b>											
<i>t</i> / °C	961,85	999,85	1063,85	1084,85	1099,85	1199,85	1299,85	1399,85	1499,85	1599,85	1699,85
<i>S1</i> / °C	0,029	0,031	0,034	0,035	0,036	0,041	0,047	0,053	0,060	0,066	0,074
<i>S2</i> / °C	0,000	0,014	0,039	0,048	0,054	0,101	0,153	0,210	0,274	0,343	0,418
<i>S3</i> / °C	0,003	0,002	0,001	0,001	0,001	0,000	0,000	0,000	0,000	0,000	0,000
<i>S4</i> / °C	0,008	0,008	0,009	0,010	0,010	0,011	0,013	0,015	0,016	0,018	0,020
<i>S5</i> / °C	0,040	0,042	0,047	0,048	0,049	0,057	0,065	0,073	0,082	0,092	0,102
<i>S6</i> / °C	0,000	0,000	0,009	0,010	0,010	0,011	0,013	0,015	0,016	0,018	0,020
<i>S7</i> / °C	0,003	0,002	0,001	0,001	0,001	0,000	0,000	0,000	0,000	0,000	0,000
<i>S8</i> / °C	0,001	0,001	0,001	0,001	0,001	0,001	0,001	0,001	0,001	0,001	0,001
<i>S9</i> / °C	0,007	0,007	0,007	0,007	0,007	0,007	0,008	0,008	0,008	0,009	0,010
<i>S10</i> / °C	0,030	0,031	0,032	0,033	0,033	0,035	0,037	0,039	0,042	0,046	0,052
<i>S11</i> / °C	0,003	0,003	0,003	0,003	0,003	0,003	0,003	0,003	0,003	0,003	0,003
<i>S12</i> / °C	0,000	0,000	0,000	0,000	0,000	0,000	0,000	0,000	0,000	0,000	0,000
<i>S13</i> / °C	0,007	0,006	0,008	0,007	0,003	0,000	0,002	0,005	0,006	0,009	0,001
<i>S14</i> / °C	0,199	0,212	0,234	0,241	0,247	0,284	0,324	0,366	0,411	0,459	0,509
<i>S=[Σ(S<sub>j</sub>)]<sup>1/2</sup></i>	0,208	0,221	0,247	0,256	0,262	0,312	0,369	0,434	0,507	0,586	0,673
<i>u (k=2)</i> / °C	0,42	0,44	0,49	0,51	0,52	0,62	0,74	0,87	1,01	1,17	1,35

## INM

The uncertainty budget(s) as presented in the participant report is quoted below:

### 2.6 Table of uncertainties

We give the values of uncertainties for the lowest medium and highest temperature.

	Uncertainty on parameter		960°C		1300°C		1700°C	
Wavelength	650	950	650	950	650	950	650	950
Reference black body radiator	0.03K	0.035 K	0.023	0.026	0.038	0.043	0.061	0.068
Photo current measurement	0.015%	0.015%	0.010	0.014	0.016	0.022	0.026	0.035
Photo current linearity	0.01%	0.01%	0.007	0.009	0.011	0.015	0.017	0.024
Size of source effect	0.06%	0.07%	0.040	0.064	0.065	0.105	0.102	0.165
Blocking	-	-	0.026	-	0.102	-	0.22	-
Wavelength knowledge	0.02 nm	-	0.003	0.003	0.008	0.006	0.028	0.020
Lamp current: resistor and Voltmeter calibration	0.005%	-	0.030	0.030	0.036	0.036	0.049	0.049
Lamp short term stability Drift	-	-	-	-	-	-	-	-
Dependence on base temperature dT with dB	0.2°C	-	0.01	0.01	-	-	-	-
Alignment	0.1 mm	L860	0.008	0.011	0.013	0.018	0.020	0.028
	0.1 mm	L864	0.053	0.074	0.086	0.120	0.136	0.188
Orientation	0,2°	L864	0.095	0.131	0.154	0.214	0.243	0.336
Final uncertainty		L860	0.064	0.079	0.134	0.123	0.259	0.193
Final uncertainty		L864	0.126	0.170	0.222	0.274	0.380	0.430

## IMGC

The uncertainty budget(s) as presented in the participant report is quoted below:

### Uncertainties

The uncertainties in the final radiance temperature  $T_\lambda$  originate from the combination of the uncertainties in the measured  $T_\lambda(\lambda_e; T_b)$  and the uncertainties in the corrections. A map of the various uncertainty sources is shown in Table 8.

The standard uncertainty estimates at the various calibration points are reported in Tables 9 and Table 10. Because the uncertainties were the same for the two lamps, only those referring to lamp 1 have been reported. The labels in the tables should be read as follows:

- $s(T_{Ag})$ : uncertainty in the fixed-point calibration
- $s(\lambda_e)$ : uncertainty in the effective wavelength
- $s(R)$ : uncertainty in the signal ratio
- $s(x;y;\theta;\varphi)$ : uncertainty in positioning
- $s(SSE)$ : uncertainty in the size-of-source effect correction
- $s[T_\lambda(\lambda)]$ : uncertainty in the wavelength correction
- $s[T_\lambda(T_b)]$ : uncertainty in the base temperature correction
- $s[T_\lambda(I)]$ : uncertainty in the current correction

Table 8: Layout of uncertainties in lamp calibration

Uncertainty in final $T_\lambda$							
$T_\lambda(\lambda_e; T_b)$				Corrections			
FP calibration	$\lambda_e$	R	Position	SSE	$\Delta T_\lambda(\lambda)$	$\Delta T_\lambda(T_b)$	$\Delta T_\lambda(I)$
<ul style="list-style-type: none"> <li>• Impurities</li> <li>• Emissivity</li> <li>• Temperature drop</li> <li>• Random (resolution)</li> </ul>		<ul style="list-style-type: none"> <li>• Non-linearity</li> <li>• Random</li> </ul>			<ul style="list-style-type: none"> <li>• <math>\lambda_e</math></li> <li>• <math>\partial T_\lambda / \partial \lambda</math></li> </ul>	<ul style="list-style-type: none"> <li>• <math>T_b</math></li> <li>• <math>\partial T_\lambda / \partial T_b</math></li> </ul>	<ul style="list-style-type: none"> <li>• <math>I(j)-I(l)</math></li> </ul>

Table 9: Uncertainties at 650 nm for lamp 1

I(j) (A)	$T_\lambda$ final (°C)	Standard uncertainty components (°C)							Combined standard uncertainty (°C)
		$s(T_{Ag})$	$s(\lambda_e)$	$s(R)$	$s(x;y;\theta;\varphi)$	$s(SSE)$	$s[T_\lambda(\lambda)]$	$s[T_\lambda(I)]$	
5.072	<b>962.360</b>	0.020	0.000	0.007	0.028	0.011	0.056	0.026	<b>0.072</b>
5.380	<b>1000.410</b>	0.021	0.003	0.007	0.030	0.011	0.059	0.024	<b>0.075</b>
5.944	<b>1064.516</b>	0.023	0.008	0.008	0.032	0.013	0.065	0.022	<b>0.081</b>
6.141	<b>1085.614</b>	0.024	0.010	0.008	0.034	0.013	0.068	0.022	<b>0.085</b>
6.284	<b>1100.601</b>	0.025	0.012	0.009	0.034	0.013	0.069	0.020	<b>0.086</b>
7.298	<b>1200.671</b>	0.028	0.022	0.020	0.040	0.015	0.080	0.018	<b>0.101</b>
8.398	<b>1300.809</b>	0.032	0.033	0.022	0.044	0.018	0.092	0.018	<b>0.117</b>
9.570	<b>1400.955</b>	0.037	0.045	0.038	0.050	0.020	0.105	0.016	<b>0.138</b>
10.805	<b>1501.042</b>	0.041	0.059	0.043	0.056	0.022	0.120	0.016	<b>0.159</b>
12.099	<b>1601.081</b>	0.046	0.074	0.048	0.064	0.025	0.135	0.016	<b>0.182</b>
13.446	<b>1700.969</b>	0.051	0.090	0.053	0.070	0.028	0.151	0.014	<b>0.205</b>

Table 10 Uncertainties at 950 nm for lamp 1

I(j) (A)	T <sub>λ</sub> final (°C)	Standard uncertainty components (°C)							Combined standard uncertainty (°C)
		s(T <sub>Ag</sub> )	s(λ <sub>e</sub> )	s(R)	s(x; y; θ; φ)	s(SSE)	s[T <sub>λ</sub> (λ)]	s[T <sub>λ</sub> (I)]	
5.072	<b>920.103</b>	0.028	0.004	0.009	0.038	0.006	0.003	0.024	<b>0.054</b>
5.380	<b>955.336</b>	0.030	0.000	0.010	0.040	0.006	0.004	0.022	<b>0.056</b>
5.944	<b>1014.437</b>	0.033	0.006	0.011	0.044	0.007	0.004	0.020	<b>0.060</b>
6.141	<b>1033.829</b>	0.034	0.008	0.011	0.046	0.007	0.005	0.020	<b>0.063</b>
6.284	<b>1047.579</b>	0.034	0.010	0.012	0.046	0.007	0.005	0.020	<b>0.063</b>
7.298	<b>1139.125</b>	0.039	0.021	0.013	0.052	0.008	0.006	0.018	<b>0.073</b>
8.398	<b>1230.088</b>	0.044	0.034	0.030	0.060	0.009	0.007	0.016	<b>0.089</b>
9.570	<b>1320.448</b>	0.050	0.049	0.034	0.068	0.010	0.008	0.014	<b>0.105</b>
10.805	<b>1410.139</b>	0.056	0.064	0.037	0.074	0.012	0.009	0.014	<b>0.120</b>
12.099	<b>1499.205</b>	0.062	0.081	0.041	0.082	0.013	0.011	0.014	<b>0.139</b>
13.446	<b>1587.513</b>	0.068	0.099	0.069	0.092	0.014	0.012	0.012	<b>0.168</b>

## PTB

The uncertainty budget(s) as presented in the participant report is quoted below:

### **Uncertainties-Identification of uncertainty components**

The calibration scheme performed includes three steps (see Ref. 3): At first, two first order working standards (WS) were calibrated with reference to the gold fixed-point blackbody. These two first order WS (C514 and C520) were operated at only one radiance temperature (C514 at 1800 K, C520 at 1337 K).

In a second step, a second order WS (P95) is calibrated with reference to the two first order WS at different radiance temperatures. In the last step, the lamps C860 and C864 are calibrated with reference to the second order WS at nearly the same radiance temperatures.

In the following the contributions to the overall uncertainty are given separately for every calibration step. The uncertainties  $u_i$  are given at a coverage factor  $k=1$ .

a) Calibration of the first order WS with reference to the gold fixed point blackbody

1. Realization of the reference temperature of the gold fixed point. This uncertainty is caused by the impurity of the gold metal inlet (5N, i.e. 0.99999), the emissivity of the cavity ( $0.99996 \pm 0.00001$ ) and the temperature difference  $\Delta T$  across the bottom of the cavity ( $<1$  mK). The realization of the reference temperature  $T_r = 1337.33$  K is within  $\pm 0.01$  K resulting in a standard uncertainty for the radiance temperature of

$$u_2 = \frac{0.01\text{K}}{\sqrt{3}} \left( \frac{T}{T_r} \right)^2$$

2. Long term stability of the interference filters used (includes the mean effective wavelength, the spectral transmission of the interference filter, the spectral responsivity of the detector):  $\pm 0.05$  nm resulting in a standard uncertainty for the radiance temperature of

$$u_3 = T \left( \frac{T}{T_r} - 1 \right) \frac{0.05 \text{ nm}}{\lambda \sqrt{3}}$$

3. Uncertainty in radiance comparison including a lamp (spatial and angular distribution of the spectral radiance, cleaning of the window, alignment, ratio of feed back resistors, non-linearity, SSE)

$$\Delta L/L = 1.5 \times 10^{-3}$$

This results in a standard uncertainty of radiance temperature of (with  $c_2$  being Planck's second radiation constant)

$$u_4 = \frac{1.5 \cdot 10^{-3}}{\sqrt{3}} \frac{\lambda T^2}{c_2}$$

4. Uncertainty due to the measurement of the lamp current. With a relative uncertainty  $u=2.4 \times 10^{-5}$  for the voltage measurement and  $u=1 \times 10^{-5}$  for the standard resistor we obtain a resulting standard uncertainty in radiance temperature (with  $dT/di$  being the slope of the lamp characteristic  $T=T(i)$ )

$$u_5 = i \left( \frac{dT}{di} \right) \cdot \sqrt{(10^{-5})^2 + (2.4 \cdot 10^{-5})^2}$$

5. Short term stability of a vacuum tungsten strip lamp of 0.1 K resulting in a standard uncertainty of radiance temperature

$$u_9 = \frac{0.1\text{K}}{\sqrt{3}}$$

6. Absorption of water vapour (at 950 nm). This may cause a shift in wavelength of 0.065 nm resulting in a standard uncertainty of radiance temperature:

$$u_{10} = T \left( \frac{T}{T_r} - 1 \right) \frac{0.065 \text{ nm}}{950 \text{ nm} \sqrt{3}}$$

b) Calibration of lamp P95 with reference to Lamps C514 and C520

1. When comparing two sources with different radiance temperatures an uncertainty due to poor blocking of the interference filter caused by parasitic transmission at long wavelengths arises. Using "edge filters" as RG780, RG715 and RG9 a rough estimate of the standard uncertainty in radiance temperature can be made, which is presented in Table 3.

Table 3 Standard uncertainties in radiance temperature due to blocking error with reference to a blackbody at 1337 K.

T / K	$u_1 / \text{K}$	T / K	$u_1 / \text{K}$
900	0,16	1500	0,01
1100	0,03	1700	0,02
1300	0,00	1900	0,02

2. Realization of the reference temperature

$$u_2 = u_2(\text{first order WS})(T/T_r)^2$$

3. Long term stability of the interference filter  $u_3$   
 4. Uncertainty in radiance comparison including a lamp  $u_4$   
 5. Measurement of the lamp current  $u_5$

6. Influence of the temperature of the base. The standard deviation for maximum changes of the base temperature  $T_b$  of  $\pm 0.1$  K is (with  $dT_s/dT_B$  being the change in radiance temperature when changing the base temperature by 1 K)

$$u_6 = \frac{dT_s}{dT_B} \frac{0.1\text{K}}{\sqrt{3}}$$

7. Resolution of the IR-pyrometer in terms of the photocurrents equals  $\pm 2 \times 10^{-15} \text{ A}$ . The photocurrent at 650 nm and 1337 K is  $5.4 \times 10^{-10} \text{ A}$ . At 950 nm and 1285 K the photocurrent is  $2.6 \times 10^{-9} \text{ A}$ . The standard deviation for resolution in radiance temperature is then

$$\text{for } 650 \text{ nm} \quad u_7 = \frac{2 \cdot 10^{-15}}{5.4 \cdot 10^{-10}} \cdot \frac{\exp\left(\frac{c_2}{650 \text{ nm} \cdot 1337.33 \text{ K}}\right)}{\exp\left(\frac{c_2}{650 \text{ nm} \cdot T}\right)} \cdot \frac{\left(650 \text{ nm} \frac{T^2}{c_2}\right)}{\sqrt{3}}$$

$$\text{and for } 950 \text{ nm} \quad u_7 = \frac{2 \cdot 10^{-15}}{2.6 \cdot 10^{-10}} \cdot \frac{\exp\left(\frac{c_2}{950 \text{ nm} \cdot 1285 \text{ K}}\right)}{\exp\left(\frac{c_2}{950 \text{ nm} \cdot T}\right)} \cdot \frac{\left(950 \text{ nm} \frac{T^2}{c_2}\right)}{\sqrt{3}}$$

8. Short term stability of the vacuum tungsten strip lamps  $u_9$
9. Absorption of water vapour at 950 nm  $u_{10}$

c) Calibration of lamps C860 and C864 with reference to Lamp P95

1. Realization of the reference temperature  
 $u_2=u_2(\text{second order WS})(T/T_r)^2$
2. Long term stability of the interference filter  $u_3$
3. Uncertainty in radiance comparison including a lamp: in contrast to the first two calibration steps an uncertainty in radiance of  $\Delta L/L=2.0 \times 10^{-3}$  is considered for  $u_4$  as the lamps C860 and C864 have not been investigated as thoroughly as the lamps C514, C520 and P95
4. Measurement of the lamp current  $u_5$
5. Influence of the temperature of the base  $u_6$
6. Resolution of the IR-pyrometer in terms of the photocurrents  $u_7$
7. Short term stability of the vacuum tungsten strip lamps  $u_9$
8. Absorption of water vapour at 950 nm  $u_{10}$

Collecting all the uncertainties mentioned above the final overall uncertainty at the coverage factor  $k=1$  presented in Table 4 is obtained.

Table 4 a)

T (650 nm)/K	Uncertainty ( $k=1$ , 650 nm) / K
1235.15	0.15
1273.15	0.16
1337.15	0.17
1358.15	0.17
1373.15	0.18
1473.15	0.19
1573.15	0.21
1673.15	0.24
1773.15	0.26
1873.15	0.29
1973.15	0.32

Table 4 b)

T (950 nm)/K	Uncertainty ( $k=1$ , 950 nm) / K
1192.63	0.19
1227.82	0.19
1286.82	0.21
1306.18	0.22
1320.09	0.22
1411.67	0.24
1502.63	0.27
1592.85	0.30
1682.42	0.34
1771.34	0.37
1859.75	0.41

Table 4: Overall uncertainty as a function of radiance temperature  
for 650 nm wavelength ( a) and for 950 nm wavelength ( b)

References to Appendix IV

1. *Uncertainty budgets for realisation of scales by radiation thermometry*, Working group 5 of CCT, Joachim Fischer (PTB), Mauro Battuello (IMGC), Mohamed Sadli (BNM-INM), Mark Ballico (CSIRO), Seung Nam Park (KRISS), Peter Saunders (MSL), Yuan Zundong (NIM), B. Carol Johnson (NIST), Eric van der Ham (NMi/VSL), Wang Li (NMC/PSB), Fumihiro Sakuma (NMIJ), Graham Machin (NPL), Nigel Fox (NPL), Sevilay Ugur (UME), Mikhail Matveyev (VNIIM), November 2002.
2. Preston-Thomas, Metrologia 27, 3-10, 107 (1990).
3. Guide to the Expression of Uncertainty in Measurement, Geneva, International Organisation for Standardisation, 101 pp. (1993)

### **Appendix III. Comments by participants on key comparison reference values**

Related to the contents, in Figure 12 to 31 (page 58 through page 77) the difference from KCRV is plotted for each participant. Also the combined uncertainty ( $k=2$ ) is plotted. Observing each figure the following participants have more than two entries that are not in agreement within this combined uncertainty. In order of appearance: NMC, VNIIM, NPL2, NPL3, NRC and INM.

Observing the results more closely, one concludes that these unresolved differences occur at both artifacts for given nominal temperature for NMC (at all temperatures), VNIIM (at 700 °C), NPL2 (temperatures below 1400 °C), NRC (temperatures above 1300 °C). According to the regulation for key comparisons the participants should comment the unresolved differences.

#### **Comments by NMC**

The differences from the KCRV demonstrate a slope from 962 °C to 1700 °C with increment in differences.

We think this is due the drift of the spectral response of the thermometer towards longer wavelength. At the time of the comparison, we did not have capability to measure the spectral response of the thermometer. In fact, the spectral response of the thermometer was measured by NML/CSIRO, now NMIA, a few months before the comparison measurement. Although the past spectral response measurements in about 2 year period showed only slight shift towards the longer wavelength, it was likely that the filters absorbed moisture during transportation which caused the centre wavelength further shifted. When we set up our own spectral response measurement facility about a year later, we tried to measure the shift quantitatively. But unfortunately the thermometer's signal level was significantly reduced and the signal level was too low to be measured by our measurement system.

The reason of the difference at about the Ag temperature remained unknown. As mentioned earlier, the thermometer's signal level was too low to be used so that we could not carry out any meaningful investigation. To solve this problem, we participated APMP KC5 using a new standard radiation thermometer in July 1999, a year later of the CCTKC5. This time we did the spectral response measurement by ourselves just before the comparison measurement. A very good agreement with the average of CCTKC5 linking laboratories, being NMIIJ, KRISS, NIM and NMIA, was obtained. In fact, the differences with the average of the linking laboratories were well within NMC reported measurement uncertainties which were at same level of that reported in the CCT KC5 in the CCT KC5 temperature range. Please see the draft B report of this comparison for details.

#### **Comments by VNIIM**

During the last months of 1999 we investigated our radiation thermometer to determinate a size of source effect (SSE). We have developed the adaptation and have applied a technique of direct SSE measurements with actual distribution of radiance on a diameter of an orifice of the used furnace.

In the correspondence with this SSE measurements we have counted, that the temperature values in a range 960 °C is necessary to reduce about 0,1 - 0,15 K. However when we have studied crucible with a silver we have detected destruction of a graphite internal blackbody, that, apparently, has caused the much greater error in results.

Therefore we ask data in a range of temperatures 960 ... 1000 °C to consider as error and to exclude it from consideration.

Deviations in a range of temperatures 1300 ... 1500 °C, probably, are caused by that for temperatures above 1300 °C we keep a scale on gas filled lamps, which differ on characteristics with the vacuum lamps.

Since then we repeatedly (in 2000-2004) reproduced the Ag fixed point and always received a value of the silver freezing temperature on 0.4 - 0.5 °C above, than during K5 comparison. This fact confirms our suppositions, that the incorrect result was stipulated by destruction of the crucible and we have solid grounds for supposing that it is sufficient to explain the VNIIM results.

## Comments by NPL

It should be noted that all of our results (3 sets of data for loop 2 and one set for loop 1), are in very good agreement with each other with respect to the KCRV. This shows good consistency between the different measurement runs over several years. The NPL2 results below 1400 °C are slightly lower than those of the other NPL sets in loop 2, and, although they agree with the other sets within the combined measurement uncertainties, this difference is sufficient to bring them away from the KCRV by an amount larger than the combined measurement uncertainties.

Our usual procedure for calibrating the lamps was to use a 'bootstrap' method, starting with measurements using the Ag and Au fixed-points and then using a radiance doubling technique to extend the calibration up to 1700 °C. In the case of the NPL2 measurements, however, we calibrated lamps C860 and C864 by comparison with the reserve lamp C840, which had been calibrated the previous year at the start of the circulation but had subsequently not been used. This was done to speed up the process, as the 'bootstrap' technique was time consuming. Check measurements showed that the calibration of C840 had drifted upwards by ~ 0.3 °C at the Ag point, which was within the combined measurement uncertainties. However, this would have meant that the radiance temperatures of lamps C860 and C864 would have appeared lower in comparison by the same amount, and this could explain the results below 1400 °C for this measurement run.

As an additional comment, it should be noted that we calibrated the lamps at ~664.5 nm, some 15 nm away from the reference wavelength. The resulting corrections to the radiance temperature were therefore large (~4.5 °C at 1700 °C) and sensitive to any uncertainties in the data used to produce the polynomial function. Using our own program to calculate the temperature correction leads to values of radiance temperature values that are higher by ~0.1°C at 962 °C and ~0.4 °C at 1700 °C, bringing them closer to the KCRV.

## Comments by NRC

### Introduction

The Comité Consultatif de Thermométrie (CCT) decided at its meeting in 1996 to undertake an international comparison of the local realizations of the International Temperature Scale of 1990 above the freezing point of silver (CCT-K5 comparison) [1]. The National Research Council of Canada (NRC) participated in this comparison and the realization was carried out by the author. Errors were made, which can be broadly categorized into two. The first error was due to the omission of accounting for the out-of-passband residual transmission (blocking) of the interference filter used in the pyrometer for the realization. This can be corrected by retroactive measurement of the response of the pyrometer due to residual transmission. The second error originates from a method of extending the temperature range of the pyrometer for radiance sources higher than 1300°C. Unfamiliarity with this method resulted in some trivial errors and,

more importantly, an erroneous correction for the size-of-source effect for the extended range. All of these can be corrected by proper treatment of the data retroactively. This communication documents the errors and presents the corrections. The methods of measuring the residual response and extending the pyrometer range are basic and may be of interest to other workers.

### **Correction for residual transmission of the interference filter**

Our pyrometer includes an interference filter, a photoelectric detector, aperture stops, converging lenses, and ancillaries (Fig. 1). The matched objective achromatic lenses of 52 mm diameter and 508 mm focal length project an image (1:1) of the target area onto a circular field stop of 0.6 mm diameter. The centre wavelength of the interference filter is 650 nm and the full width at half maximum transmittance is 10 nm. The detector assembly (Hamamatsu HC220-01) comprises a silicon photodiode (Hamamatsu S1227 with a 2.4 mm square active area and a maximum sensitivity at 720 nm), an operational amplifier (Analog Device AD549), and a feedback resistor (1 GΩ). Calibration of the CCT-K5 transfer standard lamps is deduced from the ratio of the response of the pyrometer as it views the lamp to that as it views a Cu-fixed-point blackbody radiator.

Experimental work for the realization was done in the three-month period following 25 November 1997, when the two transfer standards, lamps C860 and C864, arrived at NRC. After completion of the experimental work, analysis of the experimental results began. A complete report was sent to the coordinating institute, NMi Van Swinden Laboratorium (VSL), on 24 September 1998. Up to this time it was assumed that the out-of-passband residual response of the pyrometer, which depends on the spectral sensitivities of the photodiode and the interference filter, was negligible (Fig. 2) [2]. Later, work was done for the establishment of a spectral radiance scale for A. A. Gaertner of our institute. He found that the residual response was not negligible and suggested the use of sharp-cut colored glass filters to measure the residual response [3].

When the pyrometer views the blackbody, the response can be expressed by

$$R_B = F \int s_d(\lambda) \tau_i(\lambda) L(\lambda, T_{Cu}) d\lambda \quad (1)$$

where  $\lambda$  is the wavelength,  $T_{Cu}$  is the freezing temperature of Cu,  $F$  is a geometrical factor of the pyrometer optical system,  $L$  is the spectral radiance of the blackbody,  $s_d$  is the spectral sensitivity of the photodiode, and  $\tau_i$  is the spectral transmittance of the optical components. These optical components include the interference filter and the glass lenses. For the wavelengths that are of concern (near 650 nm) the transmittance of glass is sufficiently constant, and  $\tau_i$  can be considered to be that of the interference filter only.

As is commonly the case, it is necessary to characterize the pyrometer by specifying an effective wavelength. This in turn requires knowledge of the three factors in the integrand in Eq. (1),  $s_d$ ,  $\tau_i$ , and  $L$ . The second factor was partially determined by measurement of the filter transmittance in the wavelength range of 625 nm ( $\lambda_1$ ) to 675 nm ( $\lambda_2$ ) at 0.1 nm intervals. The first factor, however, was not measured to avoid the necessity of dismantling the photodiode from the circuit. For the calculation of the effective wavelength, use of a generic function is sufficient (Fig. 2). We are now in a position to calculate the effective wavelength for an idealized case where the pyrometer responds only to radiation within the wavelength range mentioned previously. Consequently, it is necessary to deduce the idealized response from the measured response, which comprises contributions from radiation outside that range.

The integral in Eq. (1) can be divided into three parts,  $S_{B1}$ ,  $S_{B2}$  and  $S_{B3}$ , covering wavelengths below  $\lambda_1$ , from  $\lambda_1$  to  $\lambda_2$ , and above  $\lambda_2$ , respectively. The second part corresponds to the idealized response mentioned previously. For wavelengths below  $\lambda_1$ ,  $s_d$  and  $s_i$  are zero or negligibly small and  $L$  is relatively small due to the exponential decrease of Planck's function with decreasing

wavelength. Consequently, the first part is negligible compared to the second part and is taken to be zero. The third part, however, may not be negligible for precise temperature measurements because the exponential rise of Planck's function with increasing wavelength may outweigh the diminishing  $s_d$  and  $\tau_i$ . This part can be measured by including a suitable filter in the optical path. An ideal filter is one with a spectral transmittance function equal to a and b for wavelengths below and above  $\lambda_2$ , respectively, where a and b are constants. The response of the pyrometer is now given by

$$R_{BG} = F \int s_d(\lambda) \tau_i(\lambda) \tau_g(\lambda) L(\lambda, T) d\lambda \quad (2)$$

where  $\tau_g(\lambda)$  is the spectral transmittance of the suitable filter.

Equations (1) and (2) can be expressed as

$$R_B = F [S_{B2} + S_{B3}], \quad (3)$$

$$R_{BG} = F [a S_{B2} + b S_{B3}]. \quad (4)$$

From equations (3) and (4) we obtain

$$S_{B2} / S_B = R_B^{-1} (b R_B - R_{BG}) / (b - a), \quad (5)$$

$$\Delta(S_{B2}/S_B) = [(S_{B2}/S_B) (\Delta a - \Delta b) + \Delta b] / (b - a), \quad (6)$$

where  $S_B (= S_{B2} + S_{B3})$  is equal to the integral in Eq. (1) and  $\Delta(S_{B2}/S_B)$  is the uncertainty due to the uncertainties in a and b. The left-hand side of Eq. (5) is the fractional amount of the pyrometer response due to radiation from  $\lambda_1$  to  $\lambda_2$  only. This is the correction factor to be applied to the measured response to account for the residual transmission for wavelengths above  $\lambda_2$ . It can be calculated from the right-hand side of the equation, where the factors, a, b,  $R_B$ , and  $R_{BG}$  can be obtained by measurement. Eq. (6) indicates that b should be much larger than a to reduce the uncertainty.

The sharp-cut colored glass filter (Schott) RG830 is a suitable candidate for approximation of the ideal filter. Its spectral transmittance is very small ( $< 10^{-6}$ ) for  $\lambda < \lambda_2$  and is fairly constant ( $0.9061 \pm 0.0005$ ) from 940 nm to 1300 nm. In the wavelength region from  $\lambda_2$  to 940 nm, the transmittance varies. Under the assumption that the first appreciable sideband of our interference filter occurs at 970 nm [3], the variation in that wavelength region is inconsequential. The contribution to the response of the pyrometer due to radiation from  $\lambda_2$  to 940 nm is assumed to be negligible and the filter transmittance may be arbitrarily considered to be constant (0.9061) for  $\lambda > \lambda_2$ , as in the derivation of Eq. (5).

When the pyrometer views the lamp, the response can be expressed as

$$R_L = F \int s_d(\lambda) \tau_i(\lambda) \varepsilon(\lambda, T) L(\lambda, T) d\lambda \quad (7)$$

where  $\varepsilon$  is the spectral emissivity of tungsten and T is the filament temperature. Consideration similar to that for the blackbody source yields

$$S_{L2} / S_L = R_L^{-1} (b R_L - R_{LG}) / (b - a), \quad (8)$$

where  $S_L$  is equal to the integral in Eq. (7),  $S_{L2}$  is the component of  $S_L$  due to radiation from  $\lambda_1$  to  $\lambda_2$ , and  $R_{LG}$  and  $R_L$  are the responses of the pyrometer with and without the glass filter.

Note that the correlation between the correction factors,  $S_{B2}/S_B$  and  $S_{L2}/S_L$ , is not obvious. If the emissivity of tungsten is independent of wavelength, however, the term  $\varepsilon(\lambda, T)$  in Eq. (7) becomes a constant for a particular temperature and can be lumped into the geometrical factor F. As a result, Eqs. (1) and (7) are of the same form. It follows that both correction factors are numerically the same at the same temperature (e.g.  $T = T_{Cu}$ ).

The radiance temperature of the lamp is deduced from the radiance ratio  $R_L / R_B$  where  $R_L$  and  $R_B$  are to be corrected by multiplying them by the factors  $(S_{L2} / S_L)$  and  $(S_{B2} / S_B)$ , respectively, to account for the residual transmission. Using the RG830 filter and the same copper blackbody radiator used for the calibration of lamps C860 and C864, we measured  $R_{BG}$  and  $R_B$  and evaluated the right-hand side of Eq. (5) with a and b equal to  $10^{-6}$  and 0.9061, respectively. Lamps C860 and C864 were, of course, no longer in our possession. We used a high-stability tungsten strip lamp of our own (644C) for the measurement of  $R_L$  and  $R_{LG}$  and evaluated the right-hand side of Eq. (8). Numerical results, which show the corrections (corrected - uncorrected), are shown in Table 1. The left-most column indicates true temperature for the blackbody and the radiance temperature for the lamp.

**Table 1:** Corrections (corrected - uncorrected) due to the residual transmission of the interference filter

Temperature / °C	Radiation source		Correction	
	Blackbody	Tungsten lamp	Correction factor $S_{L2} / S_L$	Fraction $(S_{L2}/S_L)/(S_{B2}/S_B) - 1$
962		0.994 81	-0.000 18	-0.012
1000		0.995 68	0.000 70	0.051
1064		0.996 77	0.001 79	0.145
1084.62	0.994 99	0.997 04	0.002 06	0.172
1100		0.997 22	0.002 24	0.191
1200		0.998 11	0.003 14	0.307
1300		0.998 65	0.003 68	0.411
1400		0.998 99	0.004 02	0.508
1500		0.999 22	0.004 24	0.602
1600		0.999 38	0.004 41	0.699
1700		0.999 50	0.004 53	0.797

#### Correction for the SSE for the higher temperature range

At the highest calibration point of the lamp (1700°C), the spectral radiance of the lamp at 650 nm is approximately 160 times larger than that of the copper blackbody. Since the response for the blackbody is 0.67 V, the response for the lamp should be 107 V. The maximum response of the pyrometer, however, is limited to 10.7 V. Our photoelectric detector has a fixed feedback resistor and therefore it is not possible to reduce the gain by switching to a resistor of lower value. We are left with the option of reducing the radiant flux incident on the photodiode.

The reduction can be achieved by attenuating the incoming flux with a suitable filter (e.g. a neutral density filter). It was decided, however, to explore a method of reducing the size of the entrance aperture (A, Fig. 1). For temperatures up to 1300°C the radiant flux needs no reduction and an iris diaphragm with an aperture of approximately 48 mm dia. was used. Starting from the next higher calibration point at 1400°C, reduction was necessary and the iris diaphragm was replaced by a home-made aperture stop comprising a brass plate (120 mm x 120 mm x 1.8 mm thick) with a centre hole of approximately 13 mm diameter and a circular bevelled edge.

It is well known that the pyrometer response is dependent on the size of the radiant source. Precise comparison of measurements of two sources of different sizes requires that each measurement be reduced to correspond to a common source of a specific size. In our case, the common source was chosen to be a circular one of 0.6 mm diameter. This is the minimum target that provides an image completely filling the field stop. The size-of-source effect (SSE) is due to diffraction and to scattering from lens imperfections (including surface dust) and the aperture edge. Therefore, replacement of the large aperture with the small one changes the SSE. We used the method of Ohtsuka and Bedford to measure the SSE and expressed it as  $\Delta R / R$  where  $R$  is the total response of the pyrometer and  $\Delta R$  is the portion due to radiation outside the target [4]. Curve 1 in Fig. 3 shows the SSE for circular sources of different diameters. Curve 2 is for rectangular sources of 40 mm height and different widths. For both curves 1 and 2, the aperture was the large one. Curve 3 is similar to curve 2 except that the aperture was the small one.

Use of the large and small apertures for temperatures up to and above 1300°C results, respectively, in radiance ratios  $R_{L48} / R_{B48}$  and  $R_{L13} / R_{B48}$  where the subscripts 48 and 13 denote the use of the large and small apertures, respectively. Our furnace used for the measurement of Cu freezing points provides a circular opening of 44 mm diameter. It follows that the fractional correction for the SSE for  $R_{B48}$  is 0.0059 (point U). The width of the lamp filament is 1.5 mm and the correction for  $R_{L48}$  is 0.0011 (point V). The fractional correction for the ratio  $R_{L48}/R_{B48}$ , which was used to deduce lamp temperatures up to 1300°C, is equal to 0.0048.

To find the SSE correction for the ratio  $R_{L13} / R_{B48}$  used to deduce temperatures above 1300°C, we introduce the expressions:

$$R_{L13} / R_{B48} = R_{L13} R_{B13}^{-1} \beta_0^{-1}, \quad (9)$$

$$\beta_0 = R_{B48} / R_{B13} \quad (10)$$

where  $R_{B13}$  is the response of the pyrometer viewing the blackbody with the small aperture.

The ratio  $\beta_0$  is related to the ratio of the radiant flux passing through the large aperture and reaching the photodiode to that passing through the small aperture. It is not exactly equal to the one given by the areas of the two apertures because the latter ratio does not account for undesirable effects such as scattering from the edge of the aperture. The size of the irradiated area on the off-focus photodiode is dependent on the aperture in place. Consequently, the measured  $\beta_0$  depends on the spatial distribution of the surface sensitivity of the photodiode. It also depends on the spatial distribution of the incoming flux from the radiation source. As an example, if the distribution changes from Lambertian to non-Lambertian, the measured  $\beta_0$  will change.

The solid angle originating from the radiation source and subtended by the nearby objective lens is small ( $\sim 0.008$ ). For such a small angle, the spatial distributions of flux from the blackbody and the lamp are closely the same. The latter may replace the former as the radiation source. It follows that  $R_{B48} / R_{B13} = R_{L48}(T_{Cu}) / R_{L13}(T_{Cu})$  where  $R_{L48}(T_{Cu})$  and  $R_{L13}(T_{Cu})$  are the responses of the pyrometer when it views the lamp at a radiance temperature of 1357.77 K ( $T_{Cu}$ ) with the large and small apertures, respectively. Furthermore, both  $R_{L48}(T_{Cu}) / R_{L13}(T_{Cu})$  and  $R_{L48}(T) / R_{L13}(T)$ , where  $R_{L48}(T)$  and  $R_{L13}(T)$  are the responses at any lamp temperature, express the ratio of the fluxes passing through the large and small apertures and are approximately equal (see later discussions). The last equality becomes  $R_{B48} / R_{B13} = R_{L48}(T) / R_{L13}(T)$ , which readily yields  $R_{L13}(T) / R_{B13} = R_{L48}(T) / R_{B48}$ . Eqs. (9) and (10) may be rewritten as

$$R_{L13} / R_{B48} = R_{L48} R_{B48}^{-1} \beta_0^{-1}, \quad (11)$$

$$\beta_0 = R_{L48}(T_{Cu}) / R_{L13}(T_{Cu}). \quad (12)$$

We note that in practice the ratio  $R_{L48}(T) / R_{L13}(T)$  is meaningful only for temperatures below  $\sim 1400^{\circ}\text{C}$  due to the limitation of  $R_{L48}(T)$  to 10.7 V. The SSE, however, should be fairly independent of lamp temperature and the SSE which is valid for  $T$  below  $1400^{\circ}\text{C}$  should remain sufficiently valid for temperatures above.

In Eq. (11),  $\beta_0$  is simply a number. Determination of the SSE correction for the ratio on the left-hand side of the expression is reduced to that for the ratio  $R_{L48} / R_{B48}$  on the right-hand side. It follows that the fractional correction for the SSE is the same as in the case of the large aperture (0.0048). In the report to VSL an erroneous correction (0.0019, based on points V and W in Fig. 3) was applied to temperatures above  $1300^{\circ}\text{C}$ . The error in temperature (corrected - uncorrected) due to this error amounts to 0.26 K at  $1400^{\circ}\text{C}$  and 0.38 K at  $1700^{\circ}\text{C}$ .

Straightforward determination of  $\beta_0$  based on the measurements of  $R_{B48}$  and  $R_{B13}$  is not preferable because  $R_{B13}$  is small ( $\sim 0.05$  V) and its uncertainty is relatively large. More accurate determination of  $\beta_0$  is desirable.

Equation (12) suggests that  $\beta_0$  may be determined more accurately from a function of  $\beta$  versus  $R_{L48}(T)$  where  $\beta = R_{L48}(T) / R_{L13}(T)$ . Some of the values of  $\beta$  measured periodically over several months are plotted in Fig. 4. Those values at  $R_{L48}$  approximately equal to 6.8 V indicate that  $\beta$  progressively decreased as time passed. This is because the small aperture stop was machined and painted black one day before it was used (22 February). The painting was a mistake. As the paint dried, the area of the aperture increased, resulting in a decreasing  $\beta$ . Measurements within a specific day (e.g. 25 June) also indicate that  $\beta$  is not constant. Lamps C860 and C864 were calibrated in the period of 23-26 February. Due to the change of  $\beta$  with time, it was necessary to estimate  $\beta_0$  for that period. Based on the measurements obtained on 23-24 February and 25 June, the estimate was 13.565. Preliminary calculations, however, were based on the value of  $\beta$  obtained on 23 February (13.5523, point P). They were not (but should have been) repeated with the proper estimate for  $\beta_0$ . The error due to the incorrect  $\beta_0$  is 0.12 K at  $1400^{\circ}\text{C}$  and 0.16 K at  $1700^{\circ}\text{C}$ .

The change of  $\beta$  with  $R_{L48}$ , as shown in the curve in Fig. 4, is of interest. It is reasonable to assume that, as the temperature of the lamp varies, the normalized spatial distribution of flux and the percentage contribution to the total response due to undesirable effects (e.g. SSE and those due to scatter, inter-reflection and background stray light) remains unchanged. Under these assumptions the changing  $\beta$  can be interpreted as a measure of the nonlinearity of the pyrometer. Our result shows degradation of response with increasing irradiance and agrees qualitatively with that shown in Fig. 3 of Liu, et al [5], where the non-linearity for temperatures up to  $1100^{\circ}\text{C}$  with the single-light-source double-aperture method is shown. Both results disagree with those of Jung [6] in his Fig. 4 and Duan et al [7] in their Fig. 4. Results of Jung and Duan et al, obtained with the method of superposition of two light sources, show enhancement of response with increasing irradiance.

In the curve in Fig. 4,  $\beta$  changes by a total fractional amount of  $15 \times 10^{-4}$ . This is unexpectedly large. The maximum photocurrent in our case is small ( $< 10$  nA) and the response of the silicon diode itself is expected to be linear [8,9]. In an attempt to determine the possible causes for the large change, the distance between the photodiode and the nearby converging lens was varied to prevent undue concentration of incident flux on the photodiode. The distance between the radiation source and the nearby objective lens was varied to investigate the dependence on focussing. The matched objective lenses were cleaned to eliminate excessive residual film. The shutter was placed at various positions along the optical path to look for unaccounted stray light. Measurements of  $\beta$  were repeated without the interference filter. They were also repeated after replacement of the lamp by a cavity radiator to ensure sufficiently diffuse

radiation at various temperatures. The detector assembly was replaced by a home-made one which employs a different silicon photodiode (Hamamatsu S1336-5BQ) and a series of selectable feedback resistors. The nonlinearities of a similar operational amplifier (AD549LH) and the digital voltmeter (Keithley K182) used for measuring the pyrometer response were studied [10]. Results are inconclusive. Perhaps there is no single major cause for the nonlinearity, as commented by Jung [5].

In summary, we have accounted for the known errors in the realization of the ITS-90 above 981.78°C at NRC for the CCT-K5 comparison. Errors due to the unaccounted residual transmission outside the selected passband of the interference filter are corrected by the use of a suitable sharp-cut colored glass filter to measure the contribution due to the residual transmission. The method provides nearly direct measurement of a small part in a large signal, circumventing the necessity of the precise measurement of the blocking of the interference filter. Errors due to an erroneous correction for the size-of-source effect for temperature measurements above 1300°C, obtained by reducing the entrance aperture of the pyrometer, are corrected through the derivation of the proper correction. The method of extending the temperature range of the pyrometer by reducing the aperture is simple and practical, providing an addition to other methods.

## References

1. Bloembergen, P., *Protocol to the comparison of local realizations of the ITS-90 between the silver point and 1700°C using vacuum tungsten-strip lamps as transfer standards*, June 1997.
2. The author thanks Dr. A. A. Gaertner and Dr. L. P. Boivin for supplying data for curve 1 in Fig. 2, Dr. J. C. Zwinkels and M. Noel for curve 2, and Dr. A. A. Gaertner and M. Noel for curve 3.
3. Schreiber, E., *Fast determination of pyrometer interference filter blocking*, Temperature – Its Measurement and Control in Science and Industry, Vol. 6, Edit. J. F. Schooley, American Institute of Physics, New York, 1992.
4. Ohtsuka, M., Bedford, R. E., *Measurement of size-of-source effects in an optical pyrometer*, Measurement, **7**, 1989, 2-6.
5. Liu, K., Yuan, Z., Duan, Y., Zhao, Q., *Nonlinearity measurement for the d.c. photoelectric pyrometer*, Proceedings of TEMPBEIJING'97, 1997, 111-116.
6. Jung, H. J., *Spectral nonlinearity characteristics of low noise silicon detectors and their application to accurate measurements of radiant flux ratios*, Metrologia **15**, 1979, 173-181.
7. Duan, Y., Yuan, Z., Wu, J., Zhao, Q., *A new non-linearity measurement system for pyrometers at NIM*, Proceedings of TEMPMEKO'99, 1999, 549-554.
8. Boivin, L.P., *Automated absolute and relative spectral linearity measurements on photovoltaic detectors*, Metrologia **30**, 1993, 355-360.
9. Kübarsepp, T., Haapalinna, A., Kärha, P., and Ikonen, E., *Nonlinearity measurements of silicon photodetectors*, Applied Optics, **37**, 1998, 2716-2722
10. The author thanks D. J. Woods for the measurements of the linearities of the operational amplifier and the digital voltmeter.

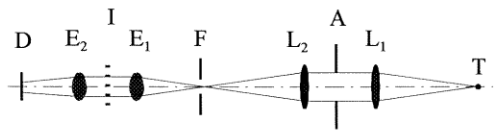


Fig. 1. Schematic diagram of the pyrometer. T, target field; L1, L2, E1, and E2, lenses; A, aperture stop; F, field stop; I, interference filter; D, silicone photodiode.

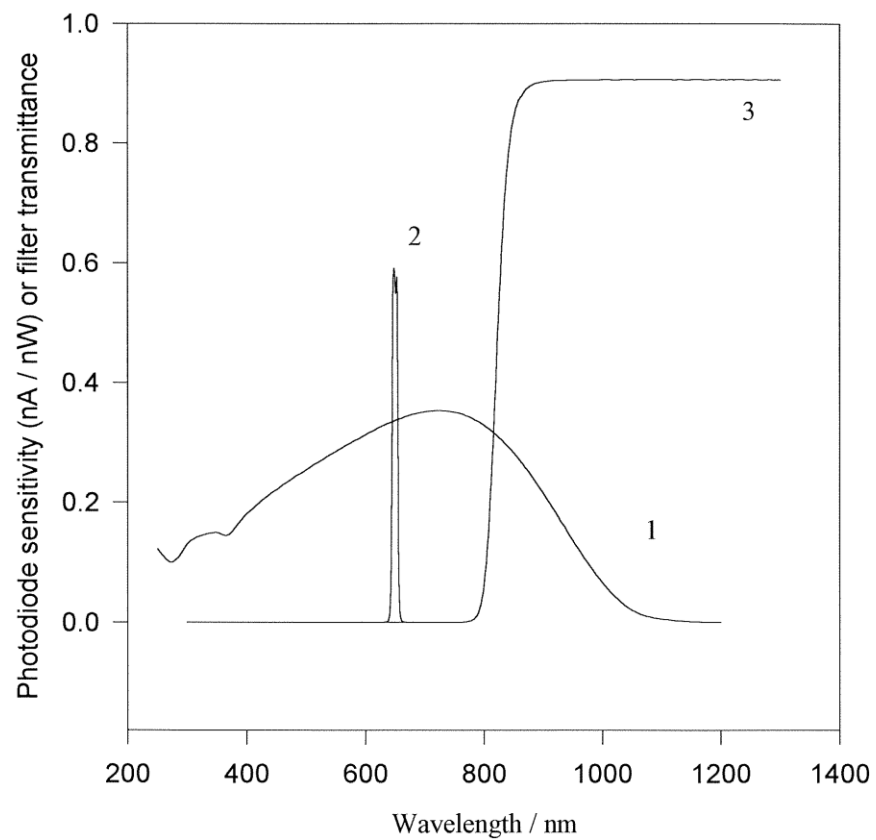


Fig. 2. Curve 1: generic spectral sensitivity for the photodiode (Hamamatsu S1227). Curves 2 and 3: spectral transmittances for the interference filter and the RG830 glass filter, respectively.

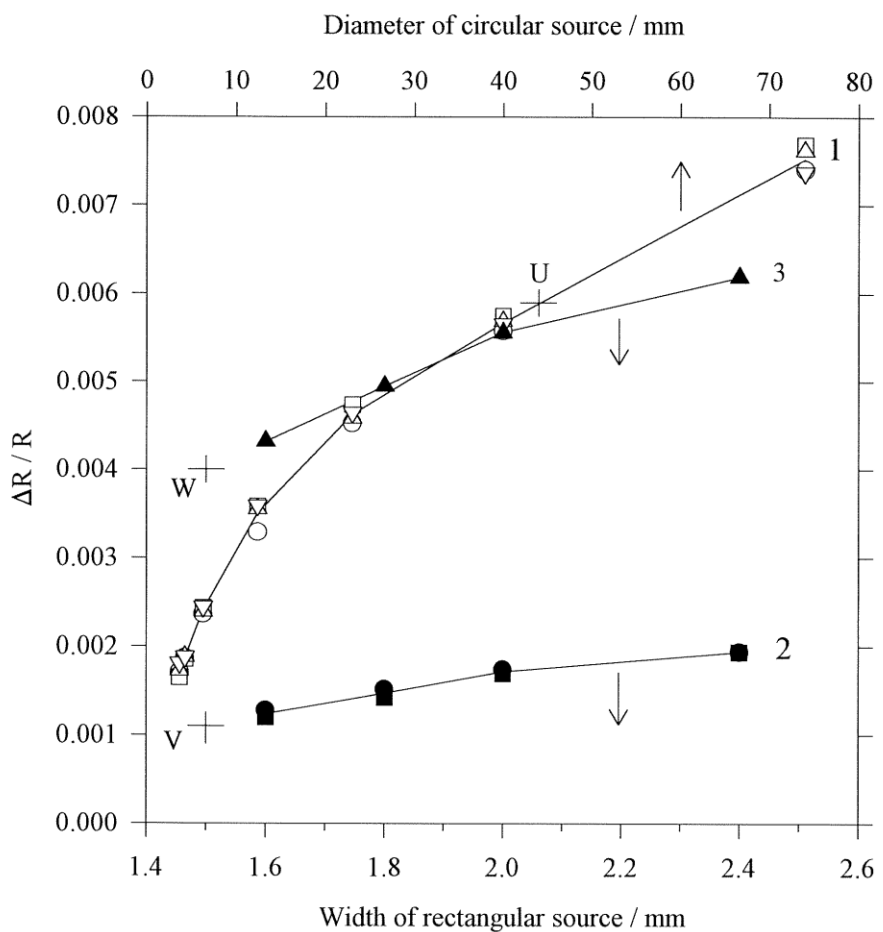


Fig. 3. Size-of-source effect (SSE) expressed as  $\Delta R / R$  where  $R$  is the total response of the pyrometer and  $\Delta R$  is part of the response due to radiation outside the target field. Curve 1, circular source with an entrance aperture of 48 mm dia. Curves 2 and 3, rectangular source of 40 mm height with the 48 mm aperture and a smaller 13 mm aperture, respectively. Points U, V, and W indicate the SSE for the blackbody radiator, the lamp with the large aperture, and the lamp with the small aperture, respectively.

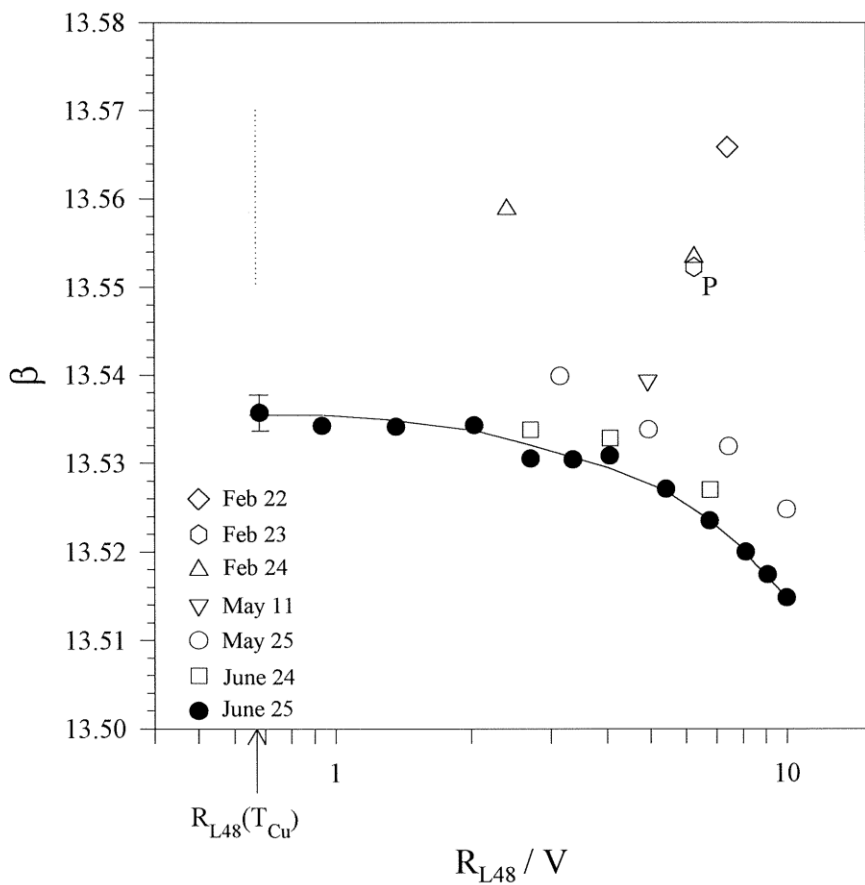


Fig. 4. Measurements of the radiance ratio  $\beta = R_{L48} / R_{L13}$  where  $R_{L48}$  is the response of the pyrometer viewing a tungsten strip lamp with an entrance aperture of  $\sim 48$  mm dia. and  $R_{L13}$  is that with an aperture of  $\sim 13$  mm dia.  $R_{L48}(T_{Cu})$  denotes the response for a lamp temperature of  $1084.62^\circ\text{C}$ . Preliminary calculations were based on the value of  $\beta$  for point P.

## **Comments by INM**

(April 3<sup>rd</sup> 2001)

We have been investigating any possible cause able to explain the difference between 860 and 864 lamps results. Lamps have been measured on the same bench at the same time. Electrical equipment was the sole difference. The current in the lamps is measured as a voltage drop in calibrated resistors. A change in the value of one of these resistors (used in 860 lamp electrical circuit) had been previously observed but accepted as a reasonable drift. But it was actually the beginning of a large and uncontrolled instability confirmed later. Consequently, temperatures given for the 860 lamp do not represent the best measurements of our institute.

## ***Appendix IV. Instrumentation and experimental details***

In this appendix the instrumentation as used by each participant is given in more detail. After the intercomparison participants were asked to describe their facility. Their reflections are presented below.

Participant	Page
CENAM	137
CSIRO	147
IMGC	162
INM	179
KRISS	194
NIST	218
NMC	235
NPL	246
PTB	321
VNIIM	328
VSL	330
NRC	Scanned from paper
NRLM	Scanned from paper
NIM	Scanned from paper